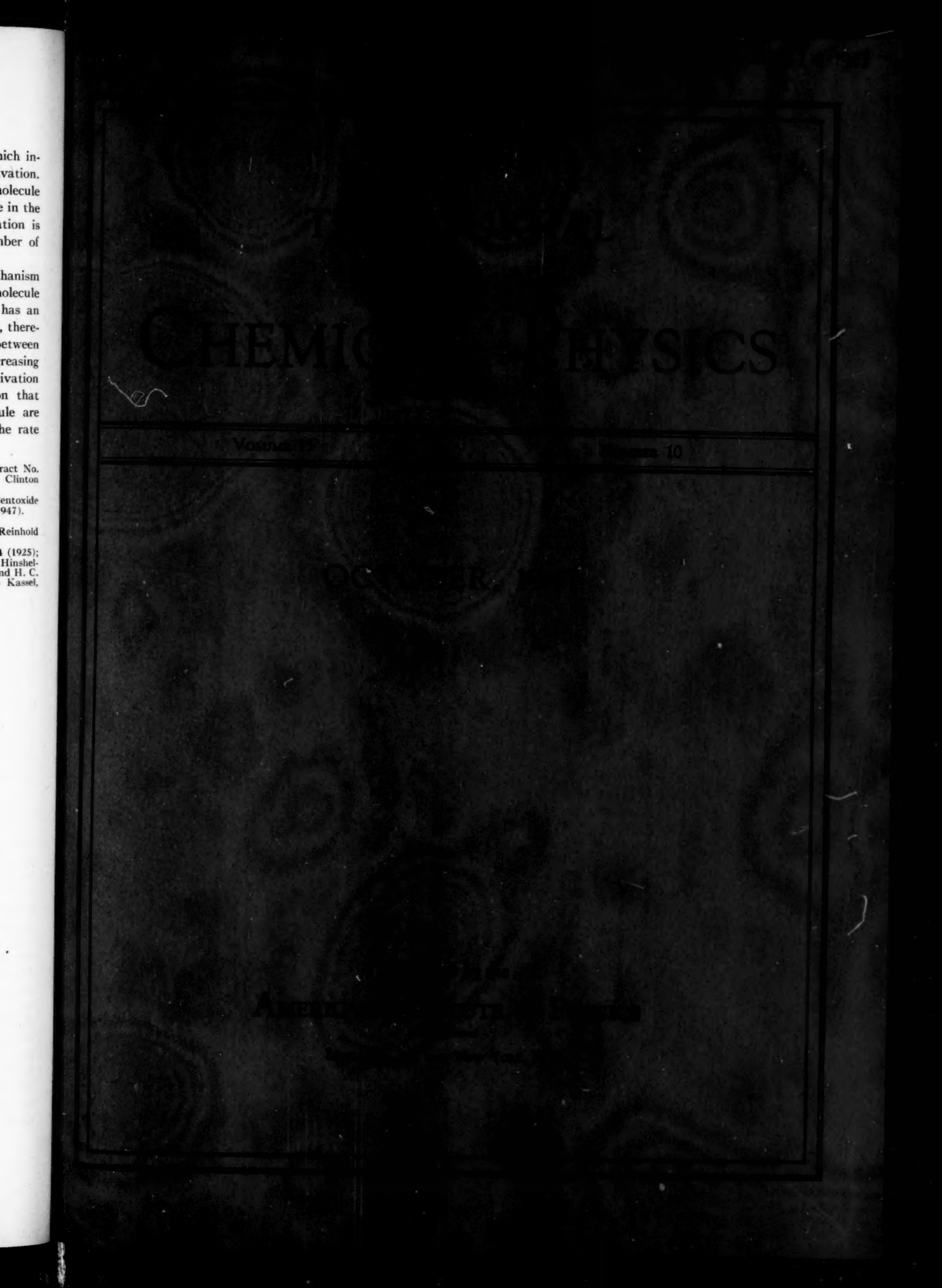

Costello

K. J. McCallum
A. L. Patterson
Hester Sponer
George Uhlenbeck
Basino H. [illegible]

C. W. Wieland
E. Bright Wilson, Jr.

---

dated exponents. The solidus (/) should be used wherever possible for fractions.

All illustrations should accompany manuscript and should always be referred to in the text. Line drawings must be made with India ink on white paper or on tracing cloth. Coordinate paper is not desirable, but if used must be blue-lined with all coordinates to be reproduced drawn with India ink. Lettering should be of sufficient size to be legible after reduction.

Proof and all correspondence concerning papers in the process of publication should be addressed to the Publications Manager, American Institute of Physics, 57 East 55 Street, New York 22, New York.

Subscription Rates

The United States and Possessions, Canada and Mexico $10.00
Elsewhere 11.00

Back Numbers

Complete set: Vol. 1, 1933—Vol. 14, 1946 (except Vol. 1, No. 1) $140.00
Yearly rate: $11.00.
Single copies: $1.00 each.

Subscriptions and orders for single copies should be addressed to Prince and Lemon Streets, Lancaster, Pennsylvania, or to the American Institute of Physics, 57 East 55 Street, New York 22, New York.

Changes of address should be sent to the Business Manager, American Institute of Physics.

Published monthly at Prince and Lemon Streets, Lancaster, Pennsylvania.

Entered as second class matter at the Post Office at Lancaster, Pa., under the Act of August 24, 1912. Acceptance for mailing at the special rate of postage provided for in section 1103, Act of October 3, 1917, embodied in paragraph 4, Section 538, P. L. & R. Not authorized

THE JOURNAL
OF
CHEMICAL PHYSICS

VOLUME 15, NUMBER 10 OCTOBER, 1947

Kinetics of the Photolysis of Methyl Iodide and the Hydrogen Halides*

I. Photolysis of Hydrogen Iodide in the Presence of Iodine, Hydrogen Bromide and Hydrogen Chloride

RUSSELL R. WILLIAMS, JR.** AND RICHARD A. OGG, JR.
Department of Chemistry, Stanford University, Stanford University, California

(Received March 28, 1947)

The photodissociation of hydrogen iodide by light of λ2537A has been utilized as a source of hydrogen atoms for a study of their subsequent reactions with iodine and the hydrogen halides. The observed rate of hydrogen formation has been used to evaluate the ratio of rate constants for the following reactions:

$$H+HX\rightarrow H_2+X$$
$$H+I_2\rightarrow HI+I$$

where X represents Cl, Br or I.

INTRODUCTION

HYDROGEN iodide absorbs ultra-violet radiation continuously and with increasing efficiency toward shorter wave-lengths below λ3000A. Absorption of radiation dissociates the molecule into a hydrogen atom and an iodine atom.[1] The photolysis has been investigated by several workers[2,3] and the mechanism of the reaction is analogous to the well known photolysis of hydrogen bromide.[4,5] The accepted mechanism and appropriate rate constants are given as follows:

$$HI+h\nu\rightarrow H+I \quad E_{abs.}$$
$$H+HI\rightarrow H_2+I \quad k_1$$
$$H+I_2\rightarrow HI+I \quad k_2$$
$$2I+M\rightarrow I_2+M$$

The last reaction is assumed to proceed rapidly enough, in comparison with other possible reactions of iodine atoms, so that the concentration of molecular iodine is equal to the concentration of molecular hydrogen. By use of the "steady state" treatment the following differential rate expression is obtained:

$$\frac{d(H_2)}{dt}=\frac{E_{abs.}}{1+k_2(I_2)/k_1(HI)}. \quad (1)$$

Integration of this expression gives the following equation, with the indicated substitutions performed:

$$X+\frac{k_2}{k_1}\left[\frac{a+2b}{4}\ln\frac{a}{a-2X}-\frac{X}{2}\right]=E_{abs.}t \quad (2)$$

* Taken from a thesis presented in partial fulfillment of the requirements for the degree of Doctor of Philosophy.
** Present address: Department of Chemistry, University of Notre Dame.
[1] K. F. Bonhoeffer and P. Harteck, *Grundlagen der Photochemie* (Steinkopf, Dresden and Leipzig, 1933).
[2] E. Warburg, Sitz. Preuss. Akad. Wiss., Physik.-Math. Klasse, 300 (1918).
[3] K. F. Bonhoeffer and L. Farkas, Zeits. f. Physik. Chemie **132**, 235 (1928).
[4] G. K. Rollefson and M. Burton, *Photochemistry* (Prentice-Hall, New York, 1939).
[5] W. A. Noyes and P. A. Leighton, *Photochemistry of Gases* (Reinhold, New York, 1941).

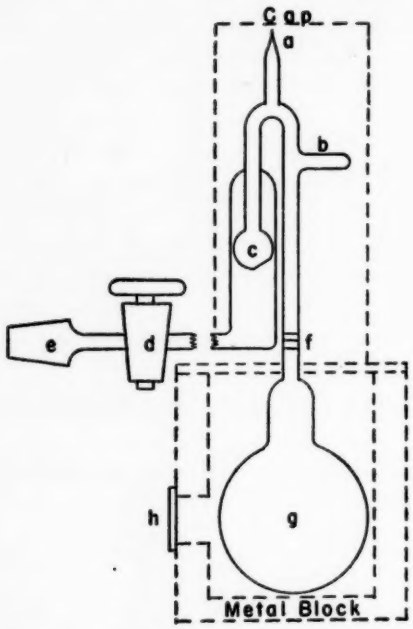

FIG. 1. Reaction system. (a) Capillary seal-off. (b) Sidearm. (c) Click gauge. (d) Stopcock. (e) Ground joint. (f) Graded seal. (g) Silica bulb. (h) Silica window.

where X = change in (H_2) in time interval $t = \Delta(H_2)$, $a = (HI)$ at beginning of time interval $t = (HI)_0$, and $b = (I_2)$ at beginning of time interval $t = (I_2)_0$. The measurable quantities in this equation are X, a, $E_{abs.}$, and t, leaving the ratio of the rate constants, k_2/k_1, to be evaluated. This reaction was reinvestigated[6] in order that it might be used as an actinometer in other studies.

The effects of added hydrogen bromide or hydrogen chloride have also been studied under conditions where they do not themselves absorb light.[1] They add the following reactions to the mechanism given for hydrogen iodide:

$$H+HBr \rightarrow H_2+Br \quad k_3$$
$$Br+HI \rightarrow HBr+I$$

or, in the case of hydrogen chloride:

$$H+HCl \rightarrow H_2+Cl \quad k_5$$
$$Cl+HI \rightarrow HCl+I$$

The second reaction in each case is assumed to take place at virtually every collision, since it is highly exothermic and since the concentration of hydrogen iodide is quite large. Therefore, we treat the concentration of the added hydrogen halide as remaining constant during the reaction and assume that no appreciable concentration of molecular bromine or chlorine is built up.

The differential rate expression is modified as follows:

$$\frac{d(H_2)}{dt} = \frac{E_{abs.}}{1+k_2(I_2)/[k_1(HI)+k_3(HBr)]}. \quad (3)$$

A similar expression holds for the case of added hydrogen chloride, and $k_3(HBr)$ or $k_5(HCl)$ are constant additive factors for a given experiment. The integrated rate expression is similarly modified, although not so simply.

Experimentally, the mixtures were treated as pure hydrogen iodide, and from the values of $E_{abs.}$, t, and $\Delta(H_2)$ an "effective $(HI)_0$" was found by trial in Eq. 2. This effective $(HI)_0$ represents the actual $(HI)_0$ plus whatever contribution is made to the rate by HBr or HCl molecules and in the case of HBr may be represented as follows:

$$\text{effective } (HI)_0 = (HI)_0 + \frac{k_3}{k_1}(HBr). \quad (4)$$

A similar expression holds for the case of added hydrogen chloride. Iodine was added initially to furnish the basis for comparison of pure hydrogen iodide with the mixtures. The quantities obtained, then, are relative reaction rate constants for the reactions of hydrogen atoms with iodine and various hydrogen halide molecules.

EXPERIMENTAL DETAILS

Hydrogen iodide, hydrogen bromide and hydrogen chloride were all prepared in essentially the same way, with minor variations according to the nature of the individual substances. The method consisted simply of dropping a concentrated solution of phosphoric acid onto the potassium or sodium salt of the halogen contained in a distilling flask. This vessel was connected by glass-to-glass seals to successive traps cooled in ice water, dry ice, and liquid air. Heat applied to the distilling flask caused the hydrogen halide to condense in the two coldest traps. After most of the product had distilled into the liquid air trap, this section of the system was sealed off, together with a fourth trap and stopcock, as yet unused. The fourth trap was used for a final

[6] R. A. Ogg, Jr. and R. R. Williams, Jr., J. Chem. Phys. 11, 214 (1943).

distillation under vacuum from a dry ice bath to liquid air. The products were always water white and were kept in small reservoirs at dry ice temperatures. Some discoloration in the grease of the stopcocks over these reservoirs was noticed, but the samples themselves remained colorless for long periods of time.

The iodine used was Baker's reagent grade, resublimed.

The reactions and actinometer runs were performed in a spherical flask of fused silica about sixty millimeters in diameter, with filling and pressure measuring devices attached through a graded seal to Pyrex tubing (see Fig. 1). Reactants were introduced through a capillary seal-off at a, and their pressures measured through the click gauge *c*. Progress of the reaction was determined at various times by measuring, through the click gauge, the pressure of gases not condensible in liquid air (hydrogen). The cold bath was applied at side-arm *b*, so that the effective temperature of the main body of gas was that of the surrounding air. Pressure measurements were reproducible within 0.05 millimeters of mercury. Frequently some iodine vapor, in equilibrium with solid iodine at room temperature, would remain in the warm part of the system when a minimum pressure had been reached. This was due to the low vapor pressure (0.2–0.3 millimeters of mercury) of iodine at room temperature, and the consequent slowness of its transfer to the cold trap. This vapor pressure was subtracted from the total pressure and the pressure of non-condensable gas corrected to 25°C.

Analysis for iodine was made, if necessary, at the end of a series of exposures only, since this necessitated opening the system. The seal-off constriction was broken and air admitted slowly while the reactants were cooled in liquid air. After reaching atmospheric pressure, aqueous potassium iodide was added to dissolve the iodine. The dissolved iodine was titrated in the reaction flask, using standard sodium thiosulfate solution. In this way the hydrogen analyses could be checked, or, if iodine was added initially, subtraction of the quantity of iodine produced during the experiment gave the initial iodine concentration.

A metal block thermostat was used to maintain the reaction cell at the desired temperatures. The general outline of this thermostat is indicated by the broken lines in Fig. 1. A heated cap in the indicated position kept the reactants from condensing in the upper portion of the reaction vessel, while the stopcock remained outside the heated zone. Diffusion of the reactants to this cold portion was prevented by the glass membrane of the click gauge. Cap and metal block were wound with resistance wire, and the temperature controlled by a thermoregulator and appropriate resistances. Temperature control, as measured by a thermometer inserted in the metal block, was good to $\pm 0.5°$ variation from the average temperature.

Light was admitted to the reaction vessel through a hole twenty-three millimeters in diameter in the metal block, covered with a fused-silica plate. A crystal-quartz lens focussed the light from the illuminating lamp in such a manner as to give a nearly cylindrical beam of light within the reaction cell. This was necessary in order to insure a thick absorbing layer of gas.

Ultra-violet radiation of λ2537A was supplied by a "Life-Lite" mercury resonance lamp in conjunction with a "Sola" constant-voltage transformer. This lamp contains argon gas at a low pressure and liquid mercury in equilibrium with its vapor. The operating temperature is only a little above room temperature and therefore its intensity depends markedly upon such factors as room temperature and air circulation. These variations were a serious drawback in certain phases of the work, as will be explained later.

TABLE I. Photolysis of hydrogen iodide.

Exposure	Temp. °C	$(HI)_0$* mm Hg	$(I_2)_0$* mm Hg	$E_{abs.}$**	Time hrs.	$\Delta(H_2)$* mm Hg	k_2/k_1
17a	189.0	166.40	12.20	0.930	6.00	4.30	3.4
17b	189.0			0.930	6.00	3.95	3.5
17c	189.0			0.930	6.00	3.75	3.3
18a	189.0	189.40	11.23	0.920	6.00	4.30	3.9
18b	189.0			0.920	6.00	4.10	3.5
22a	189.0	202.80	6.55	0.915	5.12	4.10	3.3
22b	189.0			0.915	5.28	3.95	3.4
22c	189.0			0.915	5.13	3.70	3.0
24a	102.0	195.70	10.15	0.915	5.33	3.90	3.9
24b	102.0			0.915	5.38	3.65	3.9
24c	102.0			0.915	5.88	3.75	3.9
27a	102.0	174.00	8.45	0.860	5.13	3.85	2.4
27b	102.0			0.860	6.13	3.95	3.8
27c	102.0			0.860	7.08	4.35	3.3

* All pressures of reactants were measured at room temperature and corrected to 25°C.

** $E_{abs.}$ was measured in an independent run with no iodine added initially and is given in millimeters of hydrogen per hour for the system used.

TABLE II. Photolysis of hydrogen halide mixtures.

a. Hydrogen iodide and hydrogen chloride

Exposure	Temp. °C	$(HI)_0$* mm Hg	$(HCl)_0$* mm Hg	$(I_2)_0$* mm Hg	$E_{abs.}$**	Time hrs.	(H_2)* mm Hg	Eff. $(HI)_0$* mm Hg	k_1/k_2
15	102.0	173.00	417.00	11.70	0.895	10.63	7.20	175	
16	102.0	163.50	292.50	10.35	0.895	10.92	7.40	165	
17	102.0	142.30	272.70	10.40	0.895	12.33	7.80	140	
19	154.5	185.00	420.00	13.15	1.170	10.53	9.50	220	12
20	154.5	139.50	439.50	10.20	1.170	11.40	9.70	155	30
9	189.0	136.30	274.20	0.00	0.932	7.67	6.71	190	5.1
10	189.0	129.50	270.00	9.35	0.932	6.72	5.00	170	6.6
11	189.0	148.50	283.50	11.20	0.927	8.70	6.20	180	6.8

b. Hydrogen iodide and hydrogen bromide

Exposure	Temp. °C	$(HI)_0$* mm Hg	$(HBr)_0$* mm Hg	$(I_2)_0$* mm Hg	$E_{abs.}$**	Time hrs.	(H_2)* mm Hg	Eff. $(HI)_0$* mm Hg	k_1/k_2
15	102.0	159.25	120.25	10.50	0.865	11.87	8.20	210	2.4
16	102.0	162.00	173.00	12.05	0.865	10.98	8.15	220	3.0
17	154.5	152.30	156.70	11.00	0.865	11.42	8.10	240	1.8
19	154.5	140.50	240.50	12.75	1.130	9.93	9.15	275	1.8
20	154.5	182.70	180.80	11.00	1.130	11.12	10.35	270	2.0
11	189.0	158.90	75.60	13.72	0.925	6.83	4.85	190	2.4
12	189.0	159.30	167.30	11.37	0.955	6.80	5.50	260	1.7
13	189.0	160.60	121.30	11.85	0.920	8.00	6.10	250	1.4

* All pressures of reactants were measured at room temperature and corrected to 25°C.

** $E_{abs.}$ was measured in an independent run with no iodine added initially and is given in millimeters of hydrogen per hour for the system used.

Protection of the lamp from drafts and undue temperature changes helped to minimize this difficulty, but it still gave an uncertainty of up to five percent in the actinometer values. Approximately ninety percent of the radiant energy of this lamp is furnished at λ2537A, and therefore it can be considered essentially a monochromatic source. The position of the reaction cell was reproducible, and therefore reflection losses were constant and required no correction factor.

Our experimental procedures were such as to permit mercury in the reaction system to the extent of its vapor pressure at room temperature, as a *maximum*. While this may seem undesirable, due to the high absorption coefficient of mercury for the radiation used, this contamination should disappear in the earliest stages of the reaction, through reactions with iodine atoms, if not hydrogen iodide and iodine. The removal of iodine atoms by silver foil, an analagous reaction, is well known.[7]

[7] W. West and L. Schlesinger, J. Am. Chem. Soc. 60, 961 (1938).

EXPERIMENTAL RESULTS

Hydrogen Iodide

Earlier experiments performed with somewhat lower pressures of hydrogen iodide than those reported below were inaccurate due to incomplete absorption of the incident radiation, and gave a spuriously high value of k_2/k_1.[6] It was later found that a pressure of 150 mm of hydrogen iodide was sufficient for complete absorption. When such quantities of reactant are used, and only a few millimeters pressure of hydrogen produced, the value of $E_{abs.}$ obtained by use of Eq. (2) is very insensitive to errors in k_2/k_1. This is due to the fact that the ratio $(I_2)/(HI)$ is very small at all times during the run, and consequently there is very little retardation. Using only an approximate value of k_2/k_1 it is possible, therefore, to get a good value of $E_{abs.}$. This was done in the second determination of k_2/k_1.

In these experiments an actinometer run, to get $E_{abs.}$ in the manner indicated above, was followed by runs with iodine added initially. Using the value of $E_{abs.}$ previously obtained, an accurate value of k_2/k_1 was obtained in these runs by virtue of the fact that there was sufficient iodine to cause considerable retardation. It was necessary, however, to keep the iodine concentration as low as about one-tenth the concentration of hydrogen iodide lest it compete in absorption of ultra-violet light.[8]

Table I presents the data obtained on the photolysis of hydrogen iodide with iodine initially added. An interval method was used, employing successive exposures and measurements with the same initial mixture. These showed that there was no variation of the ratio of rate constants over a range of concentrations of the reactants. The extreme cases are experiments $17c((HI)=142$ mm, $(I_2)=24$ mm) and $22a((HI)=202$ mm, $(I_2)=6$ mm).

The best value of k_2/k_1 obtained from these measurements is taken as 3.5 ± 0.3. This ratio of constants is apparently independent of temperature.

Hydrogen Halide Mixtures

The absorption coefficients of hydrogen bromide and hydrogen chloride at λ2537A are such

[8] A. Coehn and Stuckardt, Zeits. f. physik. Chemie 91, 722 (1916).

that considerable amounts of these gases may be added to hydrogen iodide without appreciable change in the primary absorption process. Since pressures of hydrogen iodide above 150 mm are needed to insure complete light absorption, the effect of added HX on the observed rate of reaction is sometimes rather small, and the light intensity difficulties mentioned previously become rather serious. Consequently, the results of this section of the work can only be regarded as good approximations.

The data for hydrogen halide mixtures is given in Table II, with the value of the effective $(HI)_0$ calculated as indicated in the Introduction. Also given are the ratios of constants k_1/k_3 and k_1/k_5, which are seen to be the relative effectiveness of two halides in reacting with hydrogen atoms. The $E_{abs.}$ given for each run is the result of an independent hydrogen iodide actinometer run, with no iodine initially added, which immediately preceeded or followed the experiment in question.

The value of k_1/k_5 for hydrogen iodide-hydrogen chloride mixtures is seen to be strongly temperature dependent. The mixtures studied at the lowest temperature (Nos. 15, 16, and 17) were experimentally indistinguishable from pure hydrogen iodide. At 154.5°C the precision is obviously poor, but for purposes of approximate calculation we have taken the value 12 for k_1/k_5 since it represents the greatest difference in the effective and actual $(HI)_0$. Combining this with the values for 189.0°C, we see that k_1/k_5 may be approximately given as:

$$2\times10^{-3}\exp(7500/RT).$$

The value of k_1/k_3 for hydrogen iodide-hydrogen bromide mixtures is much less dependent on temperature. Figure 2 is a plot of $\log k_1/k_3$ against $1/T$. The slope and intercept of the indicated line correspond to

$$k_1/k_3=0.54\exp(1000/RT).$$

DISCUSSION

Subsequent work[9] has indicated that the rate constants evaluated here probably refer to high velocity hydrogen atoms produced in the primary process:

$$HI+h\nu(\lambda 2537A)\rightarrow H(^2S_{\frac{1}{2}})+I'(^2P_{\frac{1}{2}})$$

which is exothermic by some 20 kilocalories per mole. In the absence of inert molecules to slow down the hydrogen atoms, the reaction rates observed are probably those of thermally "hot" hydrogen atoms. Thus the effective temperature may be much higher than the reported values and activation energy effects may be quite unpredictable or too small to be observed.

The ratios of rate constants obtained in this work may be summarized in terms of the following equations:

$H+HI\rightarrow H_2+I$	k_1
$H+I_2\rightarrow HI+I$	k_2
$H+HBr\rightarrow H_2+Br$	k_3
$H+Br_2\rightarrow HBr+Br$	k_4
$H+HCl\rightarrow H_2+Cl$	k_5
$H+Cl_2\rightarrow HCl+Cl$	k_6

The value of k_2/k_1 was found in this work to be 3.5 ± 0.3 and was independent of temperature. This may be compared to a value of 7.0 ± 0.4 at 155°C obtained in the presence of a deactivating agent.[9] The difference may be due to a small difference in activation energies of the first two reactions. The value 3.5, then, probably is the ratio of frequency factors. Both values are in marked disagreement with the value obtained by Bonhoeffer and Farkas,[3] who report that fifteen

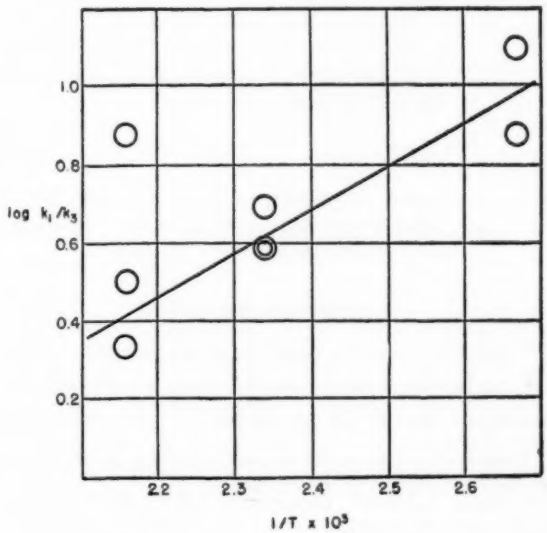

FIG. 2. $\log k_1/k_3$ as a function of $1/T$.

[9] R. A. Ogg, Jr. and R. R. Williams, Jr., J. Chem. Phys. 13, 586 (1945).

percent of iodine "completely inhibits" the photolysis of hydrogen iodide. On this observation they base their estimate of k_2/k_1 as greater than 100. Their experiments were conducted at extremely low gas pressures, and the secondary reactions probably occurred principally on the walls of the vessel. The value reported in this work certainly corresponds to the true homogeneous reactions.

The value of k_4/k_3 has been accurately determined by other workers[10] as 8.4 and is also independent of temperature. The value of k_6/k_5 has been estimated to be greater than 100.[11] The new values for k_2/k_1 therefore fall into a more logical sequence with the other halogens and hydrogen halides.

The value of k_1/k_3 obtained in this work was $0.54\exp(1000/RT)$. In view of the "hot atom" hypothesis proposed above, this representation of the data can be regarded only as tentative, until further experiments with deactivating agent present have been performed. However, the activation energy given is not in conflict with other information, such as an estimate by Morris and Pease[11] that reaction 3 has an activation energy of about 1 Kilocalorie/mole. This would give reactions 1 and 2 small and nearly equal activation energies.

Note: The ratio of rate constants k_1/k_5 obtained in this work corresponds to the form

$$0.002\exp(7500/RT).$$

The approximate nature of this portion of the work and the extremely small ratio of frequency factors obtained leave this result open to grave doubt. Further experiments in the presence of a deactivating agent have given significantly different results, which may contribute to a better understanding of this value.

[10] M. Bodenstein and G. Jung, Zeits. f. physik. Chemie **121**, 127 (1926).
[11] J. C. Morris and R. N. Pease, J. Chem. Phys. **3**, 796 (1935).

THE JOURNAL OF CHEMICAL PHYSICS VOLUME 15, NUMBER 10 OCTOBER, 1947

Kinetics of the Photolysis of Methyl Iodide and the Hydrogen Halides*

II. Photolysis of Methyl Iodide in the Presence of Iodine and the Hydrogen Halides

RUSSELL R. WILLIAMS, JR.** AND RICHARD A. OGG, JR.
Department of Chemistry, Stanford University, Stanford University, California
(Received March 28, 1947)

The photodissociation of methyl iodide by light of λ2537A has been utilized as a source of methyl radicals for a study of their subsequent reactions with iodine and the hydrogen halides. The observed rate of methane formation has been used to evaluate the ratio of rate constants for the following reactions:

$$CH_3+HX\rightarrow CH_4+X$$
$$CH_3+I_2\rightarrow CH_3I+I$$

where X represents Cl, Br or I. The reaction with hydrogen chloride has been found to be complicated by the unequal yield of methane and iodine, and possible explanations of this phenomenon have been considered.

INTRODUCTION

GASEOUS methyl iodide absorbs ultra-violet radiation below λ3650A with an absorption maximum occurring at λ2632A.[1] The reactions resulting when pure methyl iodide vapor is irradiated with light of λ2537A have been carefully studied[2] with the conclusion that the primary process of light absorption results in the formation of a methyl radical and an iodine atom. The very low quantum yield obtained with pure

* Presented in partial fulfillment of the requirements for the degree of Doctor of Philosophy.
** Present address: Department of Chemistry, University of Notre Dame.
[1] G. K. Rollefson and M. Burton, *Photochemistry* (Prentice-Hall, New York), 1939.
[2] W. West and L. Schlesinger, J. Am. Chem. Soc. 60, 961 (1938).

methyl iodide indicates that reactions of the type

$$CH_3+CH_3I\rightarrow C_2H_6+I$$

are very slow. Therefore, in the fast photolysis with hydrogen halides, the important reactions will be

$$\begin{aligned} CH_3I+h\nu &\rightarrow CH_3+I \quad E_{abs.}\\ CH_3+HI &\rightarrow CH_4+I \quad k_1\\ CH_3+I_2 &\rightarrow CH_3I+I \quad k_2\\ 2I+M &\rightarrow I_2+M \end{aligned}$$

neglecting, of course, atom-radical reactions. The rate of the last reaction is assumed to be such that the rate of formation of molecular iodine is substantially equal to the rate of formation of methane.

The photolysis of methyl iodide thus furnishes us with a convenient source of methyl radicals for the study of their relative rates of reaction with hydrogen halides and iodine.[3]

By application of the "steady state" treatment it is possible to derive the following differential rate expression:

$$\frac{d(CH_4)}{dt}=\frac{E_{abs.}}{1+k_2(I_2)/k_1(HI)}. \qquad (1)$$

After integrating and performing the indicated substitutions we have:

$$X+k_2/k_1\left[(a+b)\ln\frac{a}{a-X}-X\right]=E_{abs.}\cdot t \qquad (2)$$

where X = change in (CH_4) in time interval $t=\Delta(CH_4)$, $a=(HI)$ at beginning of time interval $t=(HI)_0$, and $b=(I_2)$ at beginning of time interval $t=(I_2)_0$.

The photochemical reaction of methyl iodide and hydrogen iodide has been studied[4] in a roughly quantitative fashion, using mixtures varying from fifty to zero percent hydrogen iodide. It was found that the quantum efficiency of iodine production stayed near two until concentrations of hydrogen iodide as low as ten percent of the total were reached. The work suffers somewhat in that the light source used gave a variety of wave-lengths in the absorbing region, and contrary to the opinion of the investigators, the absorption characteristics of the two vapors are somewhat dissimilar. Methyl iodide, as previously mentioned, shows an absorption maximum at λ2632A while the absorption of hydrogen iodide increases continuously toward shorter wave-lengths in this region.[5] The work indicates that the primary process in this reaction, as well as in the photolysis of methyl iodide, is the dissociation of the methyl iodide molecule into a methyl radical and an iodine atom.

The present work is designed to give more quantitative information about the photochemical reactions of methyl iodide and hydrogen halides, and in particular about the reaction rates of the methyl radicals produced in the course of the reaction.

The photochemical reaction of methyl iodide and hydrogen bromide has also been studied[6] to gain information about the relative rates of the following two reactions:

$$\begin{aligned} CH_3+HBr &\rightarrow CH_4+Br \quad k_3\\ CH_3+I_2 &\rightarrow CH_3I+I \quad k_2 \end{aligned}$$

The present work was continued to check and extend this work. Also, further extension to the reaction involving hydrogen chloride seemed feasible, and was accordingly carried out. The appropriate modifications in the rate expressions will be noted in the section on Experimental Results.

The analogy of these studies to those reported in the first paper of this series[7] is clear, the difference being that in the former cases the reactant of interest is the hydrogen atom, and in the present case it is the methyl radical.

EXPERIMENTAL DETAILS

Methyl iodide was prepared according to the method outlined in *Organic Syntheses*.[8] This method consists of the addition of dimethyl sulfate to a heated solution of potassium iodide and calcium carbonate. The product distills into an ice-cold receiving flask. This product was

[3] E. W. R. Steacie and D. J. LeRoy, Chem. Reviews **31**, 227 (1942).
[4] T. Iredale and D. Stephen, Trans. Faraday Soc. **33**, 800 (1937).
[5] K. F. Bonhoeffer and P. Harteck, *Grundlagen der Photochemie* (Steinkopf, Dresden and Leipzig, 1933).
[6] H. C. Andersen and G. B. Kistiakowsky, J. Chem. Phys. **11**, 6 (1943).
[7] R. R. Williams, Jr. and R. A. Ogg, Jr., J. Chem. Phys **15**, 691 (1947).
[8] *Organic Syntheses*, Vol. 18, R. Fuson, Ed., John Wiley & Sons, New York, 1938.

TABLE I. Photolysis of methyl iodide and hydrogen iodide.

Exposure	Temp. °C	$(CH_3I)_0$* mm Hg	$(HI)_0$* mm Hg	$E_{abs.}$**	Time hrs.	$\Delta(CH_4)$* mm Hg	k_2/k_1
35a	82.5	181.60	27.70	1.19	3.00	2.35	12.3
35b	82.5			1.19	4.25	1.85	12.8
36a	82.5	190.10	7.90	1.06	7.92	2.50	11.8
39a	154.5	198.95	27.75	1.06	3.13	2.25	10.7
39b	154.5			1.06	5.92	2.50	10.5
40a	154.5	196.40	26.90	1.14	2.53	2.05	10.5
38a	192.0	196.25	27.75	1.06	3.72	3.00	5.5
38b	192.0			1.06	5.50	2.75	6.0
38c	192.0			0.00	7.5	-0.20	

* Concentrations of all reactants and products measured in millimeters of mercury and corrected to 25°C.
** $E_{abs.}$ measured in millimeters of hydrogen (or methane) per hour for the system used.

washed, dried with anhydrous sodium sulfate and redistilled over a crystal of potassium iodide. The fraction distilling between 42.3° and 42.8°C was collected and kept under vacuum at 0°C where it remained waterwhite for nine months.

The apparatus used was that described in the first paper of this series.[7] All details of filling, illumination, and analysis are the same.

EXPERIMENTAL RESULTS

Methyl Iodide

A single experiment was conducted to check the low quantum efficiency of methyl iodide decomposition reported by West and Schlesinger.[2] They report a quantum efficiency of approximately 0.001, with 80 percent of the hydrocarbon products being methane. The experiment reported here consisted in exposing methyl iodide at a pressure of 186.70 mm to radiation of λ2537A in the reaction system previously described. The exposure lasted 4.00 hours at a temperature of 159.8°C, and 8.12 hours at 21°C, during which time less than one-tenth of a millimeter of non-condensible gas was formed. The $E_{abs.}$ for this system was equivalent to 1.20 mm of methane per hour. This work confirms the low quantum efficiency reported and shows that direct decomposition of methyl iodide will not interfere with the reactions involving the hydrogen halides.

Methyl Iodide and Hydrogen Iodide

The relative absorption coefficients of methyl iodide and hydrogen iodide are such that the concentration of hydrogen iodide must be less than about one-sixth the concentration of methyl iodide, if practically all of the light is to be absorbed by methyl iodide. If the hydrogen iodide concentration increases above this amount, it absorbs radiation and decomposes into hydrogen and iodine. Analyses were made, as indicated,[7] by measuring the pressure of non-condensable gas, and therefore the products hydrogen and methane are indistinguishable as far as the pressure measurements are concerned. The assumption that the products of this reaction are methane and iodine only may be justified by the following observations: Comparison of the amounts of non-condensible gas, as determined by pressure measurements, and of iodine, as determined by titration, shows that they are formed in equal amounts. This rules out of consideration any higher hydrocarbons, since they would be condensed by liquid air. The non-condensible product must then be methane or hydrogen. In early experiments liquid nitrogen was used as the condensing agent, and it was found that pressures of non-condensible gas in excess of approximately fifteen millimeters were never reached regardless of the length of exposure. This is attributed to the fact that this pressure is approximately the vapor pressure of liquid methane at the normal boiling point of liquid nitrogen (n.b.p. = −196°C).[9] Later measurements used liquid oxygen (n.b.p. = −183°C) as a cooling agent and this difficulty was not encountered. The time of diffusion of a given amount of iodine from the main bulb to the cold side-arm was three or four times as long for these experiments as in the case of the hydrogen-halide experiments,[7] where the non-condensible product is known to be hydrogen. The diffusion coefficients for bromine through hydrogen and methane at 20°C are, respectively, 0.562 and 0.1558 cm^2/sec.[10] Comparison with the observed rates shows the approximate analogy. These three types of observations support the assumption of the simple mechanism given in the Introduction involving the production of methane as the principal non-condensible product.

It is apparent from the introductory discussion

[9] Landolt-Bornstein, *Physikalische-Chemische Tabellen* (Erganzungsband I), Julius Springer, Berlin, 1935), p. 730.
[10] Landolt-Bornstein, *Physikalische-Chemische Tabellen* (Erganzungsband III), (Julius Springer, Berlin, 1935) p. 240.

that the concentration of methyl iodide should not affect the rate of the reaction as long as it is present in sufficient quantity to absorb practically all of the incident radiation.

Table I gives the data for several representative experiments with methyl iodide and hydrogen iodide. The values of $E_{abs.}$ were obtained by independent actinometer runs using pure hydrogen iodide.[7] Precise control of light intensity is not as important in these experiments as in the case of hydrogen-halide mixtures, since the retardation is quite considerable. The various exposures and measurements show that the ratio of rate constants k_2/k_1 does not vary with variations in the HI pressure from 5 mm to 27 mm (Exps. 35 and 36) and in the I_2 pressure from 0 to 5 mm.

The experiments show that the value of the ratio of rate constants k_2/k_1 is slightly dependent on temperature. This dependence is barely large enough to be detectable. Figure 1 contains a plot of $\log k_2/k_1$ against $1/T$. The points corresponding to 192.0°C definitely do not fall on a straight line with those at the lower temperatures. Exposure No. 38c shows that a slow thermal reaction takes place at this higher temperature, which probably accounts for the increased rate. This thermal reaction is known from other sources.[11] No such thermal reaction was detected at the lower temperatures. The slope and intercept of the indicated line correspond to

$$k_2/k_1 = 4.4 \exp(750/RT).$$

Several experiments were performed with methyl iodide and hydrogen iodide in which the reactants were illuminated simultaneously with ultraviolet and visible light. This procedure was designed to examine the possibility that the iodine atoms produced when iodine vapor absorbs green light might have an appreciable effect on the course of the reaction, namely, to combine with methyl radicals and thus lower the rate of methane production. The source of visible light was a 1000-watt tungsten filament lamp, focussed on the cell by means of a water lens. No retardation was found and, in fact, a slight acceleration was noted. This was later traced to a heating of the ultra-violet source by the tungsten lamp. As has been previously mentioned,[7] the ultra-violet source is quite sensitive to the temperature of its environment.

[11] R. A. Ogg, Jr., J. Am. Chem. Soc. **56**, 526 (1934).

Methyl Iodide and Hydrogen Bromide

When hydrogen bromide is added to methyl iodide and the mixture illuminated with light of λ2537A, a reaction analogous to that described in the previous section takes place. The low absorption coefficient of hydrogen bromide at this wave-length[5] makes possible the use of higher concentrations than is the case with hydrogen iodide. The mechanism given for methyl iodide and hydrogen iodide is modified to the following form:

$$\begin{aligned} CH_3I + h\nu &\rightarrow CH_3 + I & E_{abs.} \\ CH_3 + HBr &\rightarrow CH_4 + Br & k_3 \\ CH_3 + I_2 &\rightarrow CH_3I + I & k_2 \\ Br + CH_3I &\rightarrow CH_3Br + I & \\ 2I + M &\rightarrow I_2 + M & \end{aligned}$$

The fourth reaction is assumed to be rapid enough so that no appreciable concentration of molecular bromine is built up. As in previous cases, the last reaction is assumed to be rapid enough so that the rate of formation of molecular iodine is equal to the rate of formation of methane.

The differential and integrated rate expressions are entirely analogous to those previously given, with (HBr) substituted for (HI). If $E_{abs.}$ is

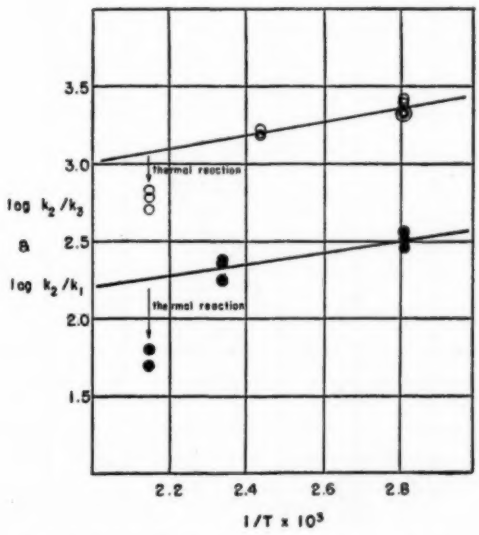

FIG. 1. $\log k_2/k_3$ (upper points) and $\log k_2/k_1$ (lower points) as functions of $1/T$.

TABLE II. Photolysis of methyl iodide and hydrogen bromide.

Exposure	Temp. °C	$(CH_3I)_0$* mm Hg	$(HBr)_0$* mm Hg	$E_{abs.}$**	Time hr.	$\Delta(CH_4)$* mm Hg	k_2/k_3
6a	82.5	186.95	35.75	1.19	4.05	2.30	28
6b	82.5			1.19	5.87	1.85	30
6c	82.5			1.19	7.42	1.60	28
7a	82.5	193.30	59.40	1.06	3.00	2.10	31
7b	82.5			1.06	6.13	2.30	28
7c	137.5			1.06	5.17	1.60	24
8a	137.5	127.50	40.70	1.19	4.65	2.90	24
8b	137.5			1.19	6.07	2.00	25
9a	192.0	192.00	60.00	1.06	3.38	2.70	15
9b	192.0			1.06	5.08	2.50	16
10a	192.0	190.40	57.10	1.14	4.08	3.20	16
10b	192.0			1.14	5.07	2.35	17
11a	192.0	189.50	55.00	1.14	3.25	2.55	17
11b	192.0			0.00	12	0.30	

* Concentrations of reactants and products were measured in millimeters of mercury and corrected to 25°C.
** $E_{abs.}$ is measured in millimeters of hydrogen (or methane) per hour for the system used.

determined by independent actinometer runs of the type described previously,[7] then the value of k_2/k_3 can be obtained by observations of the rate of the reaction such as those given in Table II.

The amounts of methane and iodine formed were compared and found to be equal, confirming the assumption that no appreciable quantities of complicated products are formed. Other workers[6] have analyzed the gaseous products of this reaction and found them to contain at least 94 percent methane.

From the values of k_2/k_3 given in Table II it appears that this reaction is somewhat slower than the photoreaction of methyl iodide and hydrogen iodide. Also, the ratio of rate constants k_2/k_3 has a small temperature coefficient. Figure 1 contains a plot of $\log k_2/k_3$ against $1/T$. It is obvious that the points obtained do not lie on a straight line. This can be explained by noting exposure 11b, in which $E_{abs.}=0$. This experiment was made to test for a thermal reaction which might be contributing to the observed rate. The amount of thermal reaction noted in this experiment is approximately enough to account for the deviation of the points at 192.0°C from the straight line corresponding to the values at lower temperatures. This result is entirely analogous to that obtained with methyl iodide and hydrogen iodide.

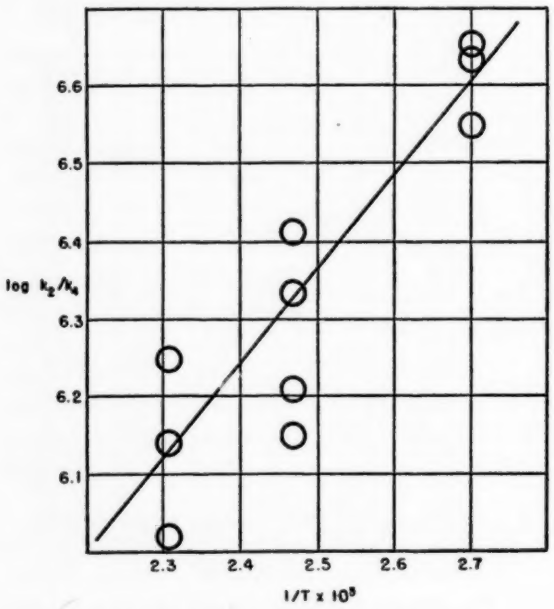

FIG. 2. Logk_2/k_4 as a function of $1/T$.

The slope and intercept of the indicated line in Fig. 1 correspond to

$$k_2/k_3 = 7.5 \exp(950/RT).$$

Methyl Iodide and Hydrogen Chloride

The photochemical reaction between methyl iodide and hydrogen chloride is initiated in the same way as those described in the previous sections. It differs from them in two important respects, however. The reaction is much slower than those involving hydrogen iodide and hydrogen bromide, and the products, methane and iodine, are not formed in equal quantities. This second fact indicates a more complicated mechanism. One possible way in which the inequality in products may be explained is the mechanism given below. A rate expression based on these assumptions will be formulated in order to facilitate treatment of the data. The proposed reactions and their corresponding rate constants are given as follows:

$$CH_3I + h\nu \rightarrow CH_3 + I \qquad E_{abs.}$$
$$CH_3 + HCl \rightarrow CH_4 + Cl \qquad k_4$$
$$CH_3 + I_2 \rightarrow CH_3I + I \qquad k_2$$
$$CH_3I + Cl \rightarrow CH_3Cl + I \qquad k_5$$

competing with

$$CH_3I + Cl \rightarrow CH_2I + HCl \qquad k_6$$

followed by

$$CH_2I + I_2 \rightarrow CH_2I_2 + I$$
$$2I + M \rightarrow I_2 + M$$

The entrance of the complicating steps represented by the fourth through sixth equations above has the effect of accelerating the total reaction, since hydrogen chloride is regenerated, and the concentration of iodine is less than would otherwise be the case.

A rate expression similar to those used in the preceeding sections can be derived if certain approximations are made. A factor R, the ratio of methane to iodine produced in a given experiment, and assumed to be independent of time during the run, is introduced. At any time therefore:

$$(I_2)=(CH_4)/R.$$

Also, a large concentration of hydrogen chloride is necessary to obtain a reasonable rate of reaction, and since very little is consumed in a given experiment, it is taken as remaining constant. The differential rate expression proposed for the photo-reaction of methyl iodide with hydrogen chloride is therefore as follows:

$$\frac{d(CH_4)}{dt}=\frac{E_{\text{abs.}}}{1+k_2(CH_4)/k_4R(HCl)_0}. \quad (3)$$

Integration of this relation gives the following formula for the ratio of rate constants k_2/k_4:

$$\frac{k_2}{k_4}=\frac{2Ra}{x^2}(E_{\text{abs.}}\cdot t-x) \quad (4)$$

where x=change in (CH_4) in time interval $t=\Delta(CH_4)$, and a=initial concentration of hydrogen chloride=$(HCl)_0$.

The ratio of products, R, varies with temperature, and, to a smaller and more doubtful extent, with the concentration of hydrogen chloride. Neglecting, as a first approximation, the variation with hydrogen-chloride concentration, we see that the ratio R is related to the ratio of rate constants k_6/k_5 in the following manner:

$$R-1=k_6/k_5. \quad (5)$$

Table III contains the data obtained for the photo-reaction of methyl iodide and hydrogen chloride. The ratio of rate constants k_2/k_4 appears to be large and temperature dependent. Figure 2 contains a plot of $\log k_2/k_4$ against $1/T$. The scattering of points is quite large, and only a rough estimate of the slope of a line drawn through the points may be made. The slope and intercept of the indicated line correspond to

$$k_2/k_4=28.7\ \exp.(2400/RT).$$

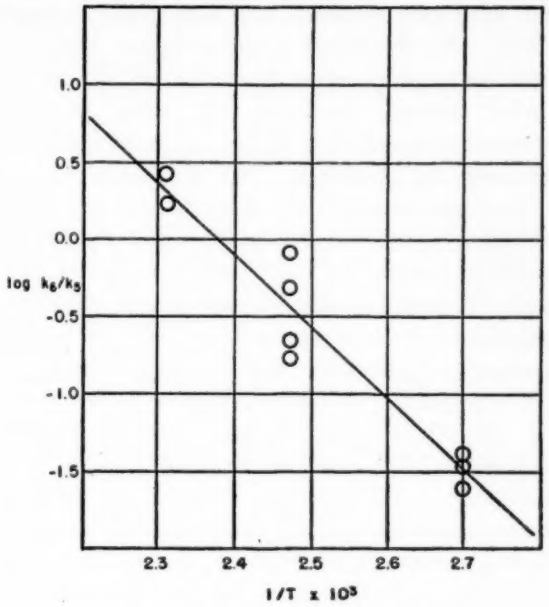

FIG. 3. Logk_6/k_5 as a function of $1/T$.

Figure 3 contains a plot of k_6/k_5, as obtained by use of Eq. (5), against $1/T$. The slope and intercept of the line correspond to:

$$k_6/k_5=6\times10^4\exp(-9000/RT).$$

DISCUSSION

Considerable evidence supports the belief that the simple mechanisms given for the photo-reactions of methyl iodide with hydrogen iodide

TABLE III. Photolysis of methyl iodide and hydrogen chloride.

Exposure	Temp. °C	$(CH_3I)_0$* mm Hg	$(HCl)_0$* mm Hg	$E_{\text{abs.}}$**	Time hr.	$(CH_4)f$* mm Hg	$\frac{(CH_4)}{(I_2)}$	k_2/k_4
4	97.7	126.70	279.30	1.25	14.05	3.70	1.25	700
5	97.7	70.30	406.50	1.25	8.00	3.00	1.23	780
8	97.7	118.30	406.00	1.25	8.58	3.15	1.20	760
9	131.5	121.80	391.70	1.20	8.12	3.50	1.52	610
10	131.5	183.50	275.50	1.15	14.25	4.50	1.73	560
11	131.5	61.80	390.20	1.20	12.11	4.80	1.46	470
12	131.5	126.30	280.00	1.15	26.25	7.05	1.92	500
1	159.8	191.95	74.55	1.25	10.08	2.90		410
2	159.8	128.50	273.30	1.20	17.00	6.50	2.27	460
3	159.8	128.80	200.00	1.25	7.88	3.45	2.55	520

* All pressures of reactants were measured at room temperature and corrected to 25°C.

** $E_{\text{abs.}}$ is measured in millimeters of hydrogen (or methane) per hour for the system used.

and hydrogen bromide are essentially correct. Abnormally increased rates at higher temperatures are to be expected from a knowledge of the similar thermal reactions. The value of k_2/k_3 reported here is in fair agreement with the value obtained by Andersen and Kistiakowsky[6] at 60°C. Their observation of up to six percent of hydrogen in the non-condensible gas products is probably due to the fact that they used a light source having a rather broad range of wavelengths, since the absorption coefficient of hydrogen bromide increases rapidly below λ2500A.

The primary process in this case, as well as in the photolysis of hydrogen iodide,[7] is highly exothermic, although not as great a fraction of this energy will be given to the methyl radical as was the case with the hydrogen atom. In addition, the large amounts of methyl iodide present in the photolysis with hydrogen iodide and hydrogen bromide will serve to deactivate the "hot" methyl radicals.[12] This is confirmed by experiments which show that addition of an inert gas has little effect on the rates of these reactions.[13]

In the photolysis of methyl iodide and hydrogen chloride, the large amounts of hydrogen chloride used have made the reactions of "hot" methyl radicals important, as shown by experiments with inert gas in which the ratio k_2/k_4 increases by several hundred fold.[13] It must be assumed, therefore, that the values reported here refer to the reactions of high velocity methyl radicals. The ratio k_6/k_5, obtained from the ratio of products, showed an abnormally large frequency factor, which is ordinarily observed only when a chain process is involved. A chain such as the following is conceivable:

$$CH_3I+Cl\rightarrow CH_2I+HCl$$
$$CH_2I+CH_3I\rightarrow CH_3+CH_2I_2$$
CH_3 follows usual steps.

This would result in an increase of the methane yield without producing iodine, but since the amount of methane is never greater than two or three times that of the iodine, the chain cannot be very long.

The values of the ratio of rate constants for the reactions of methyl radicals with hydrogen halides and halogens are summarized below:

$$CH_3+HI\xrightarrow{k_1}$$
$$vs.\qquad \frac{k_2}{k_1}=4.4\exp(750/RT),$$
$$CH_3+I_2\xrightarrow{k_2}$$

$$CH_3+HBr\xrightarrow{k_3}$$
$$vs.\qquad \frac{k_2}{k_3}=7.5\exp(950/RT),$$
$$CH_3+I_2\xrightarrow{k_2}$$

$$CH_3^*+HCl\xrightarrow{k_4}$$
$$vs.\qquad \frac{k_2}{k_4}=28.7\exp(2400/RT).$$
$$CH_3^*+I_2\xrightarrow{k_2}$$

[12] R. A. Ogg, Jr. and R. R. Williams, Jr., J. Chem. Phys. **13**, 586 (1945).
[13] R. A. Ogg, Jr., unpublished work.

* "hot" methyl radicals.

THE JOURNAL OF CHEMICAL PHYSICS VOLUME 15, NUMBER 10 OCTOBER, 1947

Short-Lived Isomeric States of Se^{83} and Ge^{77}

JAMES R. ARNOLD* AND NATHAN SUGARMAN
Argonne National Laboratory and Institute for Nuclear Studies, University of Chicago, Chicago, Illinois
(Received June 5, 1947)

Extractions of Br from neutron irradiated $SeO_3^=$ solutions and of As from irradiated $GeS_3^=$ solutions revealed the presence of short-lived isotopes of Se^{83} and Ge^{77} decaying by β^--emission to 2.4-hr. Br^{83} and 40-hr. As^{77}, respectively. Direct observation of the radiations from a short-lived Se, effected by measuring the activity of Se irradiated for 20 sec. through Al absorbers, led to a half-life determination of 67 ± 3 sec. and a β-energy of 3.4 Mev. A γ-ray was also observed. Similarly, a short-lived Ge activity was found by irradiating GeS_2 with neutrons for 20 sec. and measuring the activity through Al absorbers. The half-life was determined to be 59 ± 2 sec. and the β-energy, 2.8 Mev. The agreement between the cross sections for formation of the 67-sec. Se and the 2.4-hr. Br^{83} from the short-lived Se^{83} makes it probable that the 67-sec. Se is genetically related to the 2.4-hr. Br^{83}. In a like manner it was shown that the 59-sec. Ge is probably identical with the short-lived Ge^{77}.

The presence of the 67-sec. Se^{83} activity decaying by β^--emission to 2.4-hr. Br^{83} and the 59-sec. Ge^{77} activity decaying to 40-hr. As^{77} resolves the difficulty of the apparently high "independent" yields of Br^{83} and As^{77} in fission.

A new Se activity of 17.5 ± 0.3 sec. half-life was also found. It appears to decay by emission of γ-radiation of $\sim$150 Kev. The cross section for formation of this activity by neutron activation of Se is $\sim$0.6 barn.

1. INTRODUCTION

THE status of the problem of the distribution of the fission products as a function of mass number is considerably more advanced than that of an allied problem, the distribution in nuclear charge for the primary fission products of a given mass. The publication of the Plutonium Project *Table of Nuclei Formed in Fission*[1] summarizes the yield data of the fission products of U^{235}. Among the data given are the fission yields of the three "shielded nuclei," i.e. radioactive nuclei having isobaric stable nuclei of lower charge, Br^{82}, Rb^{86}, and $Cs^{(136)}$, which bear on the charge-distribution problem. Glendenin, Coryell, and Edwards[2] have summarized the data presently available and discussed them in terms of several possible theories. They found that the experimentally determined fractional yields of particular chain members (especially the "shielded nuclei") lay on a smooth curve of yield *versus* charge displacement from the most probable charge. For a given mass, the most probable charge was found by assuming equal charge displacements of the primary fragments of complementary chains from the stability curve of nuclei. More recently Present[3] examined the problem theoretically on the basis of a non-uniform charge distribution in the nucleus and found that the experimental data on independent fractional yields approximated a smooth (error) curve when plotted with the aid of the theoretical results.

From a consideration of the ratio of neutrons to protons for nuclei in the heavy and intermediate mass regions, it is clear that the average fission fragment will be several charges removed from stability, that is, it will emit several successive β^--particles before becoming a stable nucleus. Moreover, from the very low yields of the "shielded nuclei," it may be inferred that the distribution of nuclear charge for a given mass number must fall off sharply from the maximum value, at least on the high charge side. It may be concluded then, that direct formation of a large fraction of the chain yield on a nucleus near stability is likely to be uncommon. Two apparent discrepancies have been found, however; namely 40-hr. As^{77}[1,4] and 2.4-hr. Br^{83}.[1,5] In each of these cases the fission yield of

* Now at the Department of Chemistry, Harvard University, Cambridge, Mass.

[1] Issued by the Plutonium Project, J. Am. Chem. Soc. 68, 2411 (1946); Rev. Mod. Phys. 18, 441 (1946).

[2] L. E. Glendenin, C. D. Coryell, and R. R. Edwards, Clinton Laboratory Memo CL-LEG No. 1, July 25, 1946.

[3] R. D. Present, Clinton Laboratory unclassified report Mon P-235, January 13, 1947 (recently published in Phys. Rev. 72, 7 (1947)).

[4] E. P. Steinberg and D. W. Engelkemeir, Metallurgical Laboratory Report, CC-2310, January 1, 1945; Plutonium Project Record Vol. 9B, 7.2.1 (1946).

[5] L. E. Glendenin, Clinton Laboratory Reports CN-2839, June, 1945, Mon N-15, September, 1945; Plutonium Project Record Vol. 9B, 7.3.1 (1946).

the nucleus was found to be considerably higher than that of its immediate precursor, 12-hr. Ge^{77} and 25-min. Se^{83}, respectively. A possible interpretation might be that these two nuclei are formed in relatively high yields as primary fission fragments.

However, since such a conclusion conflicts with the simple considerations given above, Glendenin and co-workers[2] proposed the following possible mechanism to account for the observed yields. They suggested that Ge^{77} and Se^{83} have short-lived isomeric states, which decay by β^--emission to As^{77} and Br^{83}, and that these isomeric states are formed in relatively high yield in fission, thus leading to a high yield of apparently "independently" formed As^{77} and Br^{83}. They suggested also that the ~1-min. Se activity found in neutron irradiated Se by Edwards[6] might possibly be the short-lived isomeric state of Se^{83}. It was the purpose of the present work to find evidence for short-lived states of Se^{83} and Ge^{77}, decaying by β^--emission to 2.4-hr. Br^{83} and 40-hr. As^{77}, respectively, and if possible to determine their half-lives and energy characteristics.

2. NEUTRON IRRADIATIONS OF Se

2.1. Irradiations of $SeO_3^=$ Solutions and Br Extractions

Selenium was bombarded in the Argonne heavy water pile, and Br^{83} was looked for as soon as possible after bombardment. Since Br^{83} cannot be formed directly from Se by neutron bombardment, Br^{83} found very soon after bombardment must come either from 25-min. Se^{83}, or a short-lived isomeric state of Se^{83}. The amount of Br^{83} growing from the 25-min. Se^{83} can be determined and corrected for. The remainder then represents the yield of a short-lived state, and demonstrates the existence of this state.

The experiments were carried out in the following manner. A solution of Se in the form of $SeO_3^=$ (pH about 4) was irradiated for two minutes in the pneumatic tube of the pile. To an aliquot of the irradiated solution, 2 ml of standardized BrO_3^- carrier (~10-mg Br/ml) was added, and Br separated by the tested method of Edwards, Gest, and Davies,[7] with slight modifications. The first step is the reduction of BrO_3^- to Br^- with H_2S for two minutes to insure complete exchange between the carrier and radio-Br. The solution is then filtered to remove precipitated Se and sulfides, and poured into a separatory funnel containing 25-ml CCl_4 and an excess of $KMnO_4$ solution in 5N HNO_3 to oxidize the Br^- to Br_2, which is extracted into the CCl_4 layer. The H_2S reduction was begun about one and one-half minutes after the end of the irradiation and the total time elapsed to the completion of the extraction was usually four minutes. Thus the uncertainty in the time of isolation of the Br^{83} from Se is short compared to the half-life of the 25-min. state. The time of Br isolation was somewhat arbitrarily taken to be the end of the H_2S reduction—normally three minutes after the end of irradiation.

In order to show that the conditions under which this procedure was tested for radiochemical exchange held in this system, namely, that BrO_3^- was still present at the time of the H_2S reduction, it seemed important to show that $SeO_3^=$ itself does not reduce BrO_3^- rapidly and completely in the solution of pH 4 used; (it has been shown not to do so in neutral solution[7]). To this end, 2-ml BrO_3^- carrier was added to 5-ml stock $SeO_3^=$ solution, and allowed to stand for five minutes. The solution was then oxidized with $KMnO_4$, as above. Considerable Br_2 appeared, indicating appreciable reduction by $SeO_3^=$. The aqueous solution was then completely reduced with $NaHSO_3$, and reoxidized with $KMnO_4$. Again a large quantity of Br_2 was found, showing that the reduction is not complete in five minutes. Since the BrO_3^- and $SeO_3^=$ solutions are in contact only a few seconds before the H_2S reduction begins, it seems safe to assume complete exchange of radio-Br with BrO_3^- in this procedure.

After discarding the aqueous phase, the CCl_4 layer containing Br_2 is extracted with 20 ml of water containing six drops of 1M $NH_2OH \cdot HCl$. The CCl_4 phase is discarded, and HNO_3 and $KMnO_4$ added to the aqueous phase to reoxidize

[6] R. R. Edwards, unpublished work reported in Clinton Laboratory Memo CL-LEG No. 1, July 25, 1946.

[7] R. R. Edwards, H. Gest, and T. H. Davies, Clinton Laboratory Report CC-3390, July, 1946; Plutonium Project Record Vol. 9B, 3.3.5 (1946).

the Br^- to Br_2, which is extracted with CCl_4. The CCl_4 phase is then treated with 20 ml of water containing six drops of 1M $NaHSO_3$, and discarded. The aqueous phase is acidified with HNO_3, and boiled to remove HSO_3^- ion. The solution is cooled, and $AgNO_3$ solution added to precipitate AgBr. The precipitate is filtered on a weighed filter disk, washed with water, alcohol, and ether, and finally dried, weighed, and mounted.

The counting was done with a standard Eck and Krebs argon-ethanol Geiger-Müller tube and a Columbia-type scaler. The tube had an estimated wall thickness of about 30 mg/cm².

To determine the active Br growing from the 25-min. Se, the following procedure was employed. An aliquot of the irradiated solution was boiled with about 20 ml of 6N HCl to reduce any radio-Se in higher valence states to $SeO_3^=$.[8] Metallic Se was precipitated by passing SO_2 through the cold solution for 70 sec. The Se was collected on a coarse sintered glass funnel. This removed the bulk, but not all, of the Br^{83} activity. A second cycle was therefore necessary, the Se being redissolved in cold, concentrated HNO_3. The solution was boiled down to remove HNO_3 and finally made up to 6N HCl. The Se was again precipitated, filtered, and redissolved, after which the solution was carefully neutralized with NH_4OH. The Se separations were performed at a time sufficiently long after the end of the irradiation to insure complete decay of the short-lived Se^{83}. Any Br now present in the separated Se solution must have grown from the 25-min. Se^{83} present at the time of the second Se isolation. After about two hours' decay of the Se^{83}, BrO_3^- carrier was added and the procedure for Br isolation was performed.

In this procedure both Se precipitations must be quantitative. In practice it proved difficult to ascertain this and also to free the Se completely of Br^{83} even by two precipitations, so that the activity of Br^{83} formed from the 25-min. Se^{83} was determined only approximately. Samples of Se separated long after the end of irradiation yielded Br activity far in excess of that which should have grown from the 25-min. Se as determined from earlier Se separations. This excess Br is probably contamination introduced from the initial solution because of the relatively greater activity of Br in the stock solution compared to that which grows from 25-min. Se samples separated after a few half-lives' decay.

After a number of preliminary experiments, consistent results were obtained in Br extraction studies. Four such experiments are reported in Table I. The Br samples isolated from the irradiated Se stock solution at a time t_{Br} from the end of the irradiation are listed as Br-1, Br-2, etc., whereas the Br samples isolated at a time t_{Br} from the Se samples, previously purified from

TABLE I. Br^{83} activity from neutron-irradiated Se solutions.

Experiment	Sample	t_{Se}	t_{Br}	Activity Br^{83}(c/m) at an arbitrary time (normalized for yield and volume of solution)	A^{∞}_{Se}(c/m)	$A^{\infty}_{Se^*}$(c/m)
1	Se-1 Br	49	176	480	5.78×10^5	—
	Se-2 Br	99	220	208	8.05×10^5	—
	Br-1	—	3	5680	(3×10^5)	2.52×10^6
	Br-2	—	10	6960	(3×10^5)	3.06×10^6
	Br-3	—	18	7680	(3×10^5)	3.35×10^6
	Br-4	—	133	7860	(3×10^5)	3.19×10^6
2	Se-1 Br	61	225	178	2.84×10^5	—
	Se-2 Br	111	234	24.2	1.27×10^5	—
	Se-3 Br	206	320	56.4	2.88×10^5	—
	Br-1	—	3	3650	(2×10^5)	1.64×10^6
	Br-2	—	9	4720	(2×10^5)	2.10×10^6
	Br-3	—	14	4480	(2×10^5)	1.98×10^6
	Br-4	—	185	5320	(2×10^5)	2.19×10^6
3	Se-1 Br	53	216	100	1.59×10^5	—
	Se-2 Br	154	311	46.8	7.55×10^5	—
	Br-1	—	3	2870	(2.1×10^5)	1.59×10^6
	Br-2	—	9	3820	(2.1×10^5)	2.09×10^6
	Br-3	—	15	4010	(2.1×10^5)	2.16×10^6
	Br-4	—	65	4260	(2.1×10^5)	2.18×10^6
	Br-5	—	208	4180	(2.1×10^5)	2.09×10^6
4	Se-1 Br	86	230	170	5.8×10^5	—
	Se-2 Br	126	240	215	1.79×10^6	—
	Br-1	—	172	12580	(6×10^5)	6.26×10^6
	Br-2	—	178	12590	(6×10^5)	6.27×10^6
	Br-3	—	184	12200	(6×10^5)	6.07×10^6

A^{∞}_{Se} = Saturation activity of Br^{83} from 25-min. Se^{83}. Values in parentheses were assumed for $A^{\infty}_{Se^*}$ calculations.

$A^{\infty}_{Se^*}$ = Saturation activity of Br^{83} from short-lived Se^{83} (assuming a half-life short compared to ~30 sec.).

t_{Se} = Time (min.) elapsed from end of irradiation to purification of Se.

t_{Br} = Time (min.) elapsed from end of irradiation to isolation of Br.

[8] C. W. Stanley, Plutonium Project Record Vol. 9B, 3.3.1 (1946).

the Se stock solution at a time t_{Se}, are listed as Se-1 Br, Se-2 Br, etc.

The equation relating the value of A_{Br}, the activity of Br isolated from Se (Se-Br samples) and measured at arbitrary counting time t_c normalized for chemical yield and aliquot volume, to A^{∞}_{Se}, the saturation value of activity of 25-min. Se^{83}, is:

$$A_{Br}=A^{\infty}_{Se}(1-e^{-\lambda_1 T})(\lambda_2/[\lambda_1-\lambda_2]) \times[e^{-\lambda_2(t_{Br}-t_{Se})}-e^{-\lambda_1(t_{Br}-t_{Se})}] \times e^{-\lambda_1 t_{Se}}e^{-\lambda_2(t_c-t_{Br})}, \quad (1)$$

where λ_1 is the decay constant of Se^{83} (0.0277 min.$^{-1}$), λ_2 is the decay constant of Br^{83} (0.00481 min.$^{-1}$), T is the time of irradiation (2 min.), and the end of irradiation is the reference point for the measurement of time of purification of Se (t_{Se}), of time of isolation of Br (t_{Br}), and of counting (t_c). From the trend of values of A^{∞}_{Se} and knowledge of comparisons between the irradiations, the selected values of A^{∞}_{Se}, given in parentheses in Table I, were chosen for the various experiments on gross yield of Br^{83} to aid in the estimation of $A^{\infty}_{Se^*}$, the saturation activity of short-lived Se^{83}, under the assumption that the half-life of this species is less than 30 sec. The values of A'_{Br}, the activity of Br separated from the Se stock solution (Br samples) are given as:

$$A'_{Br}=A^{\infty}_{Se}(1-e^{-\lambda_1 T})(\lambda_2/[\lambda_1-\lambda_2]) \times(e^{-\lambda_2 t_{Br}}-e^{-\lambda_1 t_{Br}})e^{-\lambda_2(t_c-t_{Br})} +A^{\infty}_{Se^*}(1-e^{-\lambda_2 T})e^{-\lambda_2 t_c}. \quad (2)$$

Since the four experiments in Table I were carried out under different bombarding conditions, the saturation activities are expected to be different.

The results of Table I, showing the high activity of 2.4-hr. Br^{83} grown from the short-lived Se^{83} compared to that grown from the 25-min. Se^{83}, establish the existence of a short-lived isomeric state of Se^{83}, which is formed by neutron capture from Se^{82}. The cross section is roughly tenfold higher than that of the 25-min. state, and the nucleus decays by β^--emission to the 2.4-hr. Br. This is evident from the lack of substantial growth of activity in the Br samples separated at varying times from the end of irradiation (Table I).

The values obtained for the saturation activity of the 25-min. Se (A^{∞}_{Se}, Table I) were erratic because of the combination of causes discussed above. However, the uncertainty introduced by this into the much larger cross section of the short-lived state is small. This may easily be seen from the high degree of internal consistency of the Br samples taken after more than five minutes. The differences here are well within an experimental error of ~5 percent.

The first sample, isolated after three minutes, shows a value of $A^{\infty}_{Se^*}$ about 20 percent lower than the average of the later samples in each irradiation where such a sample was taken. This shows that the short-lived nucleus has a half-life which is not negligibly short compared to ~30 seconds as was assumed in the calculations, and in fact after ~3 minutes decay not all of the Br has been formed from the short-lived state. The estimate for the half-life from these extraction experiments is about 1 to 1.5 minutes.

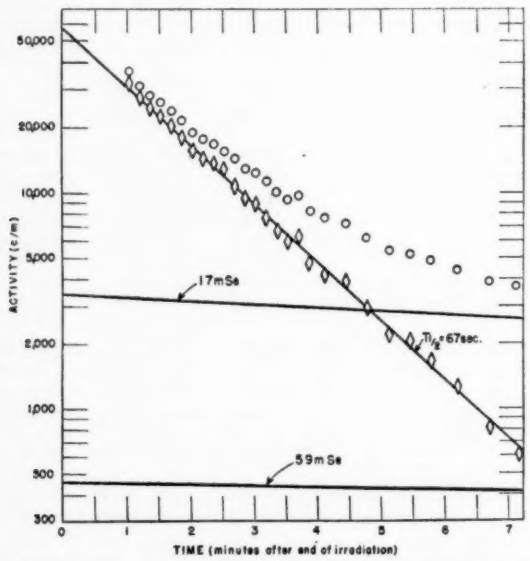

FIG. 1. Decay curve of Se metal irradiated for 20 seconds. Counted through 511-mg Al/cm² added absorber. ○ original points. ◇ subtracted curve, activities of 17-min. Se and 59-min. Se determined from later part of curve.

2.2. Irradiations of Se Metal. Identification of the Short-lived State of Se^{83}

Irradiations of spectroscopically pure Se metal were performed in a search for the short-lived state of Se^{83}. After twenty-second irradiations, Se samples were counted through varying thicknesses of Al absorber and a period of ~1 min.

half-life appeared as the absorber thickness was increased. This activity is probably identical with that found by Edwards[6] in Se irradiation experiments. The activity of the ~1-min. Se increased relative to that of the 17-min. Se^{81} as the absorber thickness increased, an optimum value being reached at ~600 mg Al/cm². The half-life was determined by counting samples through Al of about the optimum absorber thickness; the value so determined was 67±3 sec. A typical decay curve of the 67-sec. Se is given in Fig. 1. The absorption characteristics of the 67-sec. Se were determined by following the decay of irradiated Se samples through varying thicknesses of Al and normalizing the irradiations by the intensity of the 17-min. component and its known absorption characteristics. With a value of 1.5 Mev for the 17-min. Se^{81} β-energy,[1,5] the β-energy of the 67-sec. Se activity was found to be 3.4 Mev by a Feather comparison method[9] in which the range of β-particles of one substance is determined in terms of that of another standard substance by a comparison of the absorption curves. The Al absorption curves of the 17-min. Se^{81} and the 67-sec. Se are given in Fig. 2. The γ-radiation of the 67-sec. Se was observed by measuring the activity through 2.05-g Pb/cm² and comparing with the relative 17-min. Se activity through this absorber. The value of the γ-component in Al in Fig. 2 was assumed to be the same as that found in Pb since corrections for the relative counting efficiencies of the γ-radiation in Al and Pb could not be made without knowledge of the energy of the γ-radiation.

The genetic relation of the 67-sec. Se to the 2.4-hr. Br formed from the short-lived state of Se was not proved by rapid extractions of Br from Se because of the time required for the Br extractions. The activity of the 67-sec. Se was shown, however, to be genetically consistent with the activity of the Br grown from the short-lived Se state when both activities were compared to that of the 17-min. Se^{81}, used as a reference standard. In a 20-sec. irradiation the ratio of the activity at the end of the irradiation of the 67-sec. Se to that of the 17-min. Se was 0.31. The ratio of the saturated activities after

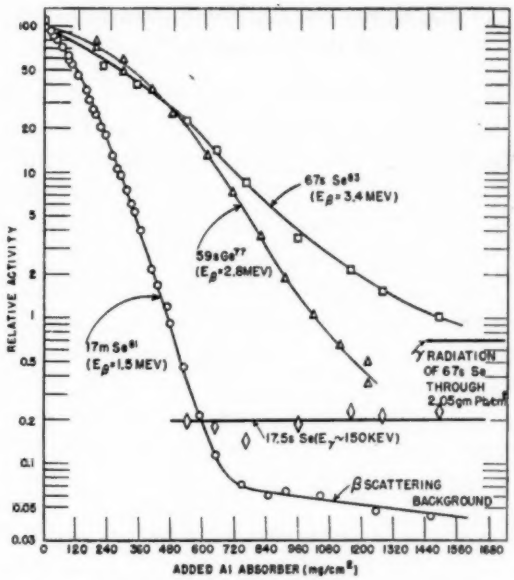

FIG. 2. Aluminum-absorption curves of 17.5-sec. Se, 67-sec. Se^{83}, 17-min. Se^{81}, and 59-sec. Ge^{77}. Absorber thickness at zero added Al estimated at 35 mg/cm². ○ 17-min. Se^{81}. □ 67-sec. Se^{83}. ◇ 17.5-sec. Se. △ 59-sec. Ge^{77}.

correcting for absorption was 0.020. The ratio of the activity of the 2.4-hr. Br grown from the short-lived Se to the 17-min. Se after a 2-min. irradiation was 0.0015, and after correcting for absorption the ratio of the saturated activities was 0.016. The agreement between these two ratios is strong evidence for the identity of the 67-sec. Se and the short-lived Se. Conclusive evidence for the mass assignment of 83 to the 2.4-hr. Br formed from the 67-sec. Se exists in the fact that the half-life and absorption characteristics of this Br activity are identical with those of the 2.4-hr. Br^{83} grown from the 25-min. Se^{83}.

A comparison of the maximum possible decay energy of 3.14 Mev of the 25-min. Se^{83}, obtained by adding the β-energy of 1.5 Mev and the three γ-energies of 0.17, 0.37, and 1.1 Mev,[1,5] with the decay energy of the 67-sec. Se of at least 3.4 Mev, since the γ-energy was not determined, leads to the assignment of the 67-sec. Se as an upper state of the 25-min. Se. The 67-sec. Se^{83} decays by β^--emission to the 2.4-hr. Br^{83} and if isomeric decay occurs to the 25-min. Se, its probability is less than ~10 percent of the disintegrations since the ratio of the two states in neutron irradiation was found to be about 10 to 1.

[9] N. Feather, Proc. Camb. Phil. Soc. **34**, 599 (1938).

2.3. Cross Section for Formation of the 25-min. Se^{83}

The neutron capture cross section of Se for the formation of the 25-min. Se^{83} as found by Seren, Friedlander, and Turkel[10] was determined by measurement of the 2.4-hr. Br^{83} activity. Since it has now been shown that the bulk of the Br activity grows from the 67-sec. Se^{83} and not from the 25-min. Se^{83}, the cross section for formation of the 25-min. Se^{83} is about one-tenth of that reported, or ~ 0.0004 barn relative to a cross section for the 17-min. Se^{81} of 0.25 barn. The cross section for formation of the 67-sec. Se^{83} is 0.0043 barn in agreement with the value found by Seren *et al.* for the 2.4-hr. Br.

2.4. U^{235} Fission Yields of 25-min. Se^{83} and 2.4-hr. Br^{83}

The U^{235} fission yields of 25-min. Se^{83} and 2.4-hr. Br^{83} reported by Glendenin[5] are 0.21 percent and 0.40 percent, respectively. The difference in yield of the 2.4-hr. Br and 25-min. Se of 0.19 percent can now be attributed to the yield of the 67-sec. Se^{83}. The fission yield of the 67-sec. Se relative to that of the 25-min. Se was redetermined by irradiation of UO_2Cl_2 and analysis for Se and total Br. Three Se samples were isolated 35 min., 75 min., and 108 min. after the end of the irradiation. The 2.4-hr. Br was allowed to grow into the Se and was counted. The average value of the saturation activity of 25-min. Se^{83} found was 1.31×10^7 c/m ± 7 percent. Two Br samples were isolated 19 min. and 106 min. after the end of the irradiation and the value of the saturation activity of the 2.4-hr. Br grown from the 67-sec. Se was obtained by correcting for the 2.4-hr. Br grown from the 25-min. Se, and was found to be 1.68×10^7 c/m ± 7 percent. Assuming a fission yield of 0.21 percent for the 25-min. Se, the yield of the 67-sec. Se is 0.27 percent, giving a total yield of 2.4-hr. Br^{83} of 0.48 percent. The discrepancy between the yield of the 67-sec. Se in this experiment and that reported by Glendenin arises from the rapid separation of Br in the earlier experiments before the complete decay of the 67-sec. Se.

[10] L. Seren, H. Friedlander, and S. Turkel, Metallurgical Laboratory Report CP-2081, August 26, 1944.

2.5. Identification and Characteristics of a 17.5-sec. Se

The decay curves of Se irradiated for 20 sec. and measured through Al absorbers of thickness greater than ~ 600 mg/cm^2, revealed another short-lived Se activity whose half-life was found to be 17.5 ± 0.3 sec. This activity appeared in equal yield both in technical-grade and spectroscopically pure Se. A typical decay curve is given in Fig. 3. The absorption curve of the 17.5-sec. Se was determined in the same manner as that of the 67-sec. Se, namely, by comparing the activity of the 17.5-sec. Se with that of the 17-min. Se through various absorbers and normalizing to the Al-absorption curve of the 17-min. Se. As is seen in Fig. 2, the absorption characteristics of the 17.5-sec. Se are those of a γ-ray. The energy of the γ-ray is estimated roughly at ~ 150 Kev from measurements made with absorbers of 1117 mg Al/cm^2 + 209 mg Pb/cm^2 and 2.05 gm Pb/cm^2.

A rough value of the cross section of Se for formation of the 17.5-sec. Se calculated relative to 0.25 barn for formation of the 17-min. Se, and assuming a counting efficiency for the γ-ray of ~ 0.1 percent and no internal conversion, is ~ 0.6 barn.

2.6 Summary of Se-Br Experiments

Extractions of Br from neutron-irradiated $SeO_3^=$ solutions revealed the presence of a short-lived state of Se^{83} decaying by β^--emission to 2.4-hr. Br^{83}. The half-life was estimated to lie between 1 and 1.5 minutes. The cross section for formation of the short-lived state was found to be about ten times greater than for the 25-min. Se^{83}. Direct observations of the radiations from a short-lived Se, effected by measuring the activity of Se irradiated for 20 sec. through Al absorbers, led to a half-life determination of 67 ± 3 sec. and a β-energy of 3.4 Mev. A γ-ray was also observed. There is good reason to believe that a genetic relationship exists between this 67-sec. Se and the 2.4-hr. Br^{83} because of the good agreement found between the cross sections for formation of the 67-sec. Se and the 2.4-hr. Br^{83} formed from the short-lived Se. Energy considerations lead to the assignment of the 67-sec. Se as an upper state of 25-min. Se^{83}.

Experiments were performed on the relative fission yields of the 25-min. Se^{83} and the 67-sec. Se^{83} and a value of 0.27 percent for the 67-sec. Se^{83} was determined, assuming a yield of 0.21 percent for 25-min. Se^{83}. The total fission yield of Br^{83} is, then, 0.48 percent.

A new Se activity of 17.5 ± 0.3 sec. half-life was discovered in the course of this work. It appears to decay by emission of γ-radiation of $\sim$150 Kev. The cross section for formation of this activity is $\sim$0.6 barn.

The presence of the 67-sec. Se^{83} activity decaying by β^--emission to 2.4-hr. Br^{83} resolves the difficulty of the apparently high "independent" yield of Br^{83} in fission.

3. NEUTRON IRRADIATIONS OF Ge

3.1. Irradiations of Ge Solutions and As Extractions

Irradiations of Ge solutions were performed in a manner similar to that used for Se. The experiments were designed to determine whether all of the 40-hr. As^{77} present in solution after irradiation comes from the 12-hr. Ge^{77}, or if a short-lived isomeric state of Ge^{77} is a possible source. Extractions of 40-hr. As^{77} at varying times after the end of the irradiation make it possible to measure the activity of As growing from the 12-hr Ge and from any short-lived Ge^{77} formed from the neutron capture of Ge^{76}.

Liquid $GeCl_4$ was the first compound tried for irradiation because of its high Ge content, an advantageous condition for measurable activities from short irradiations. It was found, however, that tracer As was lost from this solution by adsorption or volatilization at a rate which was sufficiently rapid to obscure the results. A concentrated Ge solution, prepared by dissolving GeS_2 in NH_4OH-NH_4HS solution, was then tried and was shown to be a satisfactory medium for recovery of As tracer.

The procedure for separating Ge and As activities is that of Winsberg[11] with certain modifications. The separation of Ge from As is effected by distilling the Ge as $GeCl_4$ from a conc. HCl solution in the presence of chlorine gas. The pentavalent As is involatile. After the Ge distillation is completed, the residual Cl_2 is displaced by air, Cu_2Cl_2 is added to reduce the As to the trivalent state, and the As is distilled as $AsCl_3$. The detailed procedure used in these experiments follows. A suitable aliquot of the irradiated sulfide solution is placed in an all-glass still with a 50-ml boiler and an arrangement for passing gas through the solution throughout the distillation. The aliquot is washed down with water and 2-ml As carrier (10-mg As/ml) added, followed by 10-ml conc. HCl. Chlorine gas is passed through the still and receiver (40-ml ice water in a 100-ml centrifuge tube, surrounded by an ice-salt mixture); the sulfides of Ge and As, precipitated from the basic sulfide solution by the addition of conc. HCl, dissolve slowly. Some free sulfur remains suspended in the solution. Distillation is begun in a stream of Cl_2 and continued until about 5 ml of solution remains in the still. Under these conditions Ge, but not As, distills. The time of purification of Ge or isolation of As is taken as the midpoint of the first Ge distillation, which lasts about five minutes. Two more distillations are then performed by adding 4-ml Ge carrier (5-mg Ge/ml in 6N HCl) and 6-ml conc. HCl to the residue; each time the distillation is con-

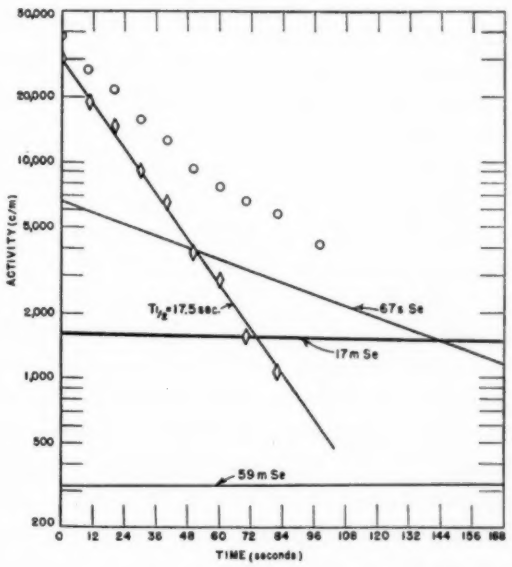

FIG. 3. Decay curve of Se metal irradiated for 20 seconds. Counting started 1 min. after end of irradiation. Counted through 1431-mg Al/cm² added absorber. ○ original points. ◇ subtracted curve, activities of 17-min. Se, 59-min. Se, and 67-sec. Se, determined from later part of curve.

[11] L. Winsberg, Metallurgical Laboratory Memo MUC-NS No. 200, January, 1945; Plutonium Project Record Vol. 9B, 8.2 (1946).

TABLE II. As^{77} activity from neutron-irradiated Ge solutions.

Experiment	Sample	t_{Ge}	t_{As}	Activity As^{77}(c/m) at an arbitrary time. (Normalized for yield and volume of solution)	$A^{\infty}_{Ge^*}$(c/m)	A^{∞}_{Ge}(c/m)
1 (2-hr. irradiation)	As-1	0.28	0.28	5070	4.22×10^5	—
	As-2	4.07	4.07	6340	(4.22×10^5)	4.83×10^5
	As-3	24.93	24.93	8480	(4.22×10^5)	3.10×10^5
	As-4	70.32	70.32	10680	(4.22×10^5)	3.32×10^5
	Ge As-1	2.60	23.35	3310	—	3.71×10^5
	Ge As-2	2.60	69.07	5330	—	3.86×10^5
				Activity As^{77}(c/m) at t_{Ge}	Graphical analysis	
2 (1-hr. irradiation)	As-1	0.23	0.23	10750		
	As-2	2.27	2.27	11320		
	As-3	4.22	4.22	12780		
	As-4	22.40	22.40	12690	5.94×10^5	5.28×10^5
	As-5	26.78	26.78	11610		
	As-6	47.45	47.45	9590		
	As-7	72.73	72.73	6720		
	As-8	76.99	76.99	6526		
	Ge-1 As	0.23	24.23	8160		
	Ge-3 As	4.22	28.22	5700		
	Ge-4 As	22.40	46.40	2160		4.90×10^5
	Ge-5 As	26.78	50.78	1658		
	Ge-6 As	47.45	71.45	487		

A^{∞}_{Ge} = Saturation activity of As^{77} from 12-hr. Ge^{77}.
$A^{\infty}_{Ge^*}$ = Saturation activity of As^{77} from short-lived Ge^{77}. Values in parentheses were used for A^{∞}_{Ge} calculations.
t_{Ge} = Time (hrs.) elapsed from end of irradiation to purification of Ge.
t_{As} = Time (hrs.) elapsed from end of irradiation to separation of As.

tinued until 5 ml remains in the still. The receiver is changed after each distillation. After the completion of the Ge distillations, a new receiver containing 10-ml H_2O is put in place, a stream of air passed through, and 5-ml saturated Cu_2Cl_2 in conc. HCl and 2-ml conc. HCl are added. The solution is distilled until a solid precipitate appears in the still, 5-ml conc. HCl are then added, and the solution is distilled again until solid appears. Both distillates containing As are condensed in the same receiver. The As is precipitated by passing H_2S through the distillate. The precipitate is filtered, dried, and mounted. The factor by which As is freed from Ge contamination in this procedure is about 300, which is quite sufficient for this work.

Samples of Ge activity isolated for As growth from 12-hr. Ge^{77} were obtained from the first Ge distillate. The Ge was precipitated by H_2S, filtered, dried, weighed, and redissolved in NH_4OH-NH_4HS solution. An aliquot of As carrier was added, and the solution allowed to stand for 40-hr. As growth. The As was isolated by the procedure outlined above. The factor by which Ge is freed of As impurity in the first Ge distillation was never measured directly, but a lower limit of 100 can be assigned from the experimental data.

The results of the As-extraction studies are given in Table II. The As samples isolated from the irradiated Ge sulfide solution at a time $t_{Ge}(=t_{As})$ from the end of the irradiation are listed as As-1, As-2, etc., and the As samples isolated at a time t_{As} from the Ge samples, previously purified from the Ge sulfide solution at a time t_{Ge}, are listed as Ge-1 As, Ge-2 As, etc. Calculations of the results of experiment 1 in Table II are made in the same manner as those for Table I, with hours used as the units of time.

The value of the saturation activity of As^{77} from the short-lived $Ge^{77}(A^{\infty}_{Ge^*})$ of experiment 1 of Table II was calculated from the first As sample extracted 0.28 hr. after the end of the irradiation. This value was used in correcting the As activities of later extractions for the As present at the end of irradiation. The saturation activity of As^{77} grown from the 12-hr. Ge (A^{∞}_{Ge}) as determined from the As samples was found to agree favorably with that found from the Ge-As samples. The extraction data of the second experiment were complete enough to be subjected to graphical analysis and again good agreement was found between the two independently determined A^{∞}_{Ge} values. A graphical representation of the Ge-As data of this experiment is given in Fig. 4, in which the genetic relationship of the 40-hr. As^{77} to the 12-hr. Ge^{77} is clearly represented. The ratio of $A^{\infty}_{Ge^*}$ to A^{∞}_{Ge} from these two experiments of 1.1 establishes the existence of a short-lived isomeric state of Ge^{77}, formed by neutron capture of Ge^{76}, which decays by β^--emission to 40-hr. As^{77}. An upper limit of 3 min. to the half-life of the short-lived Ge^{77} was determined by extractions of As performed 8 min. to 40 min. after the end of irradiation from a Ge solution irradiated for 2 min. The variation in activity of the samples isolated in this time interval could be accounted for by growth from the 12-hr. Ge^{77}.

3.2. Irradiations of GeS_2. Identification of the Short-lived State of Ge^{77}

A search for the short-lived state of Ge^{77} was made by irradiations of GeS_2 prepared from $GeCl_4$. Samples of GeS_2 were irradiated for twenty seconds and counted through Al absorbers. An activity decaying with a half-life of 59 ± 2 sec. was observed as the absorber thickness increased, being most pronounced at $\sim$400 mg Al/cm² (Fig. 5). Preparations of GeS_2 of varying purity showed the presence of the 59-sec. activity as well as the low activity from the 89-min. Ge^{75} and the 37-min. Cl^{38} formed from the Cl impurity in the GeS_2. Irradiations of S showed that this was not the source of the 59-sec. activity. The absorption characteristics of the 59-sec. Ge were determined by following the decay of irradiated samples through sets of two Al absorbers differing by about 200-mg Al/cm², the activity through one absorber being used for normalization of the activity through the other. The Al-absorption curve of the 59-sec. Ge is given in Fig. 2; its β-energy is 2.8 Mev as determined by a Feather comparison method[9] with the 17-min. Se^{81}. The low activities of the samples through thick Al absorbers make it improbable that there is hard γ-radiation present in high intensity.

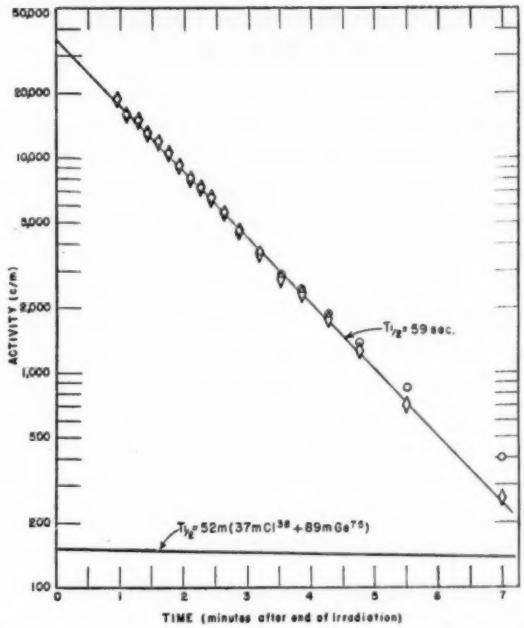

FIG. 5. Decay curve of GeS_2 irradiated for 20 seconds. Counted through 405-mg Al/cm² added absorber. ○ original points. ◇ subtracted curve, activity of 89-min. Ge^{75} and 37-min. Cl^{38} (from Cl impurity) determined from later part of curve.

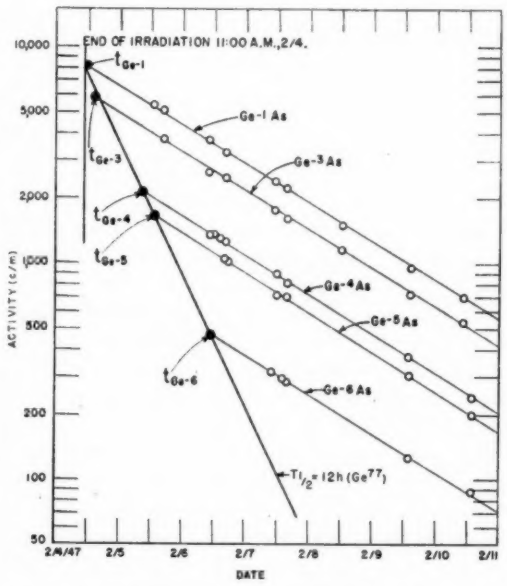

FIG. 4. Decay curves of 40-hr. As^{77} samples extracted from Ge samples separated from Ge solution, showing genetic relationship of 40-hr. As^{77} to 12-hr. Ge^{77} (data of Table II). ○ Measured activity of Ge-As samples. ● Extrapolated activity of Ge-As samples at t_{Ge}.

The activity of the 59-sec. Ge was shown to be genetically consistent with that of the 40-hr. As formed from the short-lived state of Ge by a comparison of these activities with the activity of 89-min. Ge^{75}. The ratio of the 59-sec. Ge activity to the 89-min. Ge^{75} activity at the end of a 20-sec. irradiation was 3.99; the ratio of the saturated activities corrected for absorption, 0.045. The ratio of the 40-hr. As from the short-lived Ge to the 89-min. Ge^{75} at the end of a 2-min. irradiation was 4.32×10^{-4}; the ratio of the saturated activities corrected for absorption, 0.037. It is very probable, from the agreement of the ratios of the saturated activities, that the 59-sec. Ge and the short-lived Ge decaying to 40-hr. As are identical. The 40-hr. As from the 59-sec. Ge was shown to be the same species as the 40-hr. As^{77} from the 12-hr. Ge^{77} by the identity of the half-lives and absorption characteristics.

A definite energy assignment of the 59-sec. Ge^{77} relative to the 12-hr. Ge^{77} cannot be made since the total decay energy of neither nucleus has been determined.

3.3. Cross Section for Formation of the 40-hr. As^{77}

The cross-section of Ge for formation of the 12-hr. Ge^{77} by an (n, γ) process was determined to be 0.0055 barn by Seren, Sturm, and Moyer.[12] Since the 40-hr. As^{77} is formed in two ways, from 12-hr Ge^{77} and 59-sec. Ge^{77}, its formation cross section is the sum of the cross sections of the 12-hr. Ge^{77} and the 59-sec. Ge^{77}, whose cross section was found to be about 10 percent higher than that of 12-hr. Ge^{77} in these experiments, or 0.011 barn. The cross section of 0.0155 barn given by Seren *et al.* for the formation of the 40-hr. Ge^{71} is undoubtedly too high since it contains the contribution of the 40-hr. As^{77} (0.011 barn), an activity which was found after the Ge cross section work was done.

3.4. Summary of Ge-As Experiments

The presence of a short-lived state of Ge^{77} decaying by β^--emission to 40-hr. As^{77} has been shown by As extractions of $GeS_3^=$ solutions irradiated with neutrons. The cross section for formation of the short-lived state was found to be about 10 percent larger than that of the 12-hr. Ge^{77}. A short-lived Ge activity was found by irradiating GeS_2 with neutrons for 20 sec. and measuring the activity through Al absorbers. The half-life was determined to be 59 ± 2 sec. and the β-energy, 2.8 Mev. The agreement between the cross sections for formation of the 59-sec. Ge and the 40-hr. As^{77} from the short-lived Ge^{77} makes it probable that the 59-sec. Ge is genetically related to the 40-hr. As^{77}.

The presence of the 59-sec. Ge^{77} activity decaying by β^--emission to 40-hr. As^{77} resolves the difficulty of the apparently high "independent" yield of As^{77} in fission on the assumption that the excess fission yield of As^{77} is due to 59-sec. Ge^{77}.

This document is based on work performed at the Argonne National Laboratory, Chicago, Illinois, operated by the University of Chicago for the Atomic Energy Commission.

[12] L. Seren, W. Sturm, and W. Moyer, Metallurgical Laboratory Report CP-1389, February 24, 1944.

THE JOURNAL OF CHEMICAL PHYSICS VOLUME 15, NUMBER 10 OCTOBER, 1947

The Mechanism of Processes Initiated by Excited Atoms

III. Photo-Sensitized Hydrocarbon Reactions

KEITH J. LAIDLER
Department of Chemistry, The Catholic University of America, Washington, D. C.

(Received June 9, 1947)

The photo-sensitized reactions of the hydrocarbons are discussed in terms of the following reaction scheme, in which A* indicates the photo-sensitizing atom and MH_2 the hydrocarbon:

$$A^*+MH_2\rightarrow A+MH+H,$$
$$A^*+MH_2\rightarrow A+MH_2^*,$$
$$MH_2^*+MH_2\rightarrow 2MH_2,$$
$$MH_2^*\rightarrow M+H_2,$$
$$MH_2^*\rightarrow MH+H.$$

The first and fifth reactions are followed by polymerizations. Expressions for the quenching rate, the rate of formation of M, and the rate of formation of polymer, are obtained in terms of the original rate constants, and a number of special cases of practical interest are treated. The relative rates of the reactions are discussed with reference to the experimental data, particular regard being paid to the energy relationships, the general kinetic behavior, and the influence of temperature. Evidence is adduced in favor of the following: (1) the strength of the C−H bond in ethylene is about 100 kcal., (2) there is a triplet-excited state of acetylene with an excitational energy of 10–30 kcal., (3) conversion of a large amount of electronic energy into vibrational energy proceeds with difficulty, the process taking place much more readily when some of the energy can be taken up as electronic energy of the colliding molecule.

INTRODUCTION

APPLICATIONS of the theory of chemical change to the elucidation of reaction mechanisms have for the most part followed one of two general paths. The first of these consists of the detailed quantum-mechanical calculation of the rates of simple processes, and the comparison of the results with experiment; the second is the

analysis of reactions, or of groups of homologous reactions, with the aid of the general theory. One class of reactions which are more amenable to analysis in the light of theory, that is, to the second type of treatment, comprises the photo-sensitized reactions of the hydrocarbons. The investigations on these have been recently reviewed by Steacie,[1] in whose laboratory much of the work on them has been done. The quantum-mechanical theory of molecular structure permits the qualitative construction of the potential energy surfaces upon which reaction must take place, and with the aid of these alone it is possible to arrive at a number of significant conclusions regarding the manner in which the reactions occur. Some simplification is provided by the fact that most of the reactions take place with zero activation energy, and that many reaction mechanisms are excluded by the necessity of conservation of spin angular-momentum. Preliminary remarks on these reactions have already been published (Part II),[2] and the object of the present paper is to show that now that much information has accumulated on the reactions of the simpler hydrocarbons, the theoretical analysis is consistent with, and supplements, the conclusions directly derived from experiment.

The experimental work on quenching and photo-sensitization has been done mainly with the metals sodium, zinc, cadmium, and mercury, and in the case of the last three has involved transitions to the ground state ($^1S_0$) from both singlet-excited ($^1P_1$) and triplet-excited ($^3P_1$) states. The details of these transitions are given in Table I, which includes the energy liberated in transition to the normal state (fourth column),

TABLE I. Energies of excitation, and available energies, in electronic transitions.

Metal	Transition	Line (A)	Energy of excitation (kcal.)	Energy of formation of hydride (kcal.)	Total available energy (kcal.)
Sodium	$3^2P-2^2S_{\frac{1}{2}}$	{5890 / 5896}	48.3	51.6	99.9
Zinc	$4^3P_1-4^1S_0$	3076	92.5	23.1	115.6
Zinc	$4^1P_1-4^1S_0$	2139	133.4	23.1	156.5
Cadmium	$5^3P_1-5^1S_0$	3261	87.3	15.5	102.8
Cadmium	$5^1P_1-5^1S_0$	2288	124.4	15.5	139.9
Mercury	$6^3P_1-6^1S_0$	2537	112.2	8.5	120.7
Mercury	$6^1P_1-6^1S_0$	1849	153.9	8.5	162.4

[1] E. W. R. Steacie, *Atomic and Free Radical Reactions* (Reinhold Publishing Corporation, New York, 1946), Chapters IV and VI.
[2] K. J. Laidler, J. Chem. Phys. 10, 43 (1942).

TABLE II. Bond strengths.

Bond	Strength (kcal.)
H−H	103.8
CH_3-H	102
C_2H_5-H	97
$H_2C{:}CH-H$	100[a]
$CH_2{:}CHCH_2-H$	92
$HC{:}C-H$	104
CH_3-CH_3	86
$CH_3-C_2H_5$	84

[a] This value is discussed later.

the heat of formation of the hydride, AH, of the metal A (fifth column), and the sum of these two (last column). The latter figures represent the energy available if, in addition to de-activation to the normal state, the hydride is formed; evidence for the production of the hydrides in these reactions has in some cases been obtained by the detection of their resonance bands. The interactions of most of these excited atoms with hydrogen, ethane, and ethylene, have been studied, and the results interpreted in a general way in terms of the strengths of the bonds which have to be broken.[1] These bond strengths are not known with great certainty, but a set that may be accurate within 1 or 2 kcal. is given in Table II.

Excited sodium (^2P) occupies an exceptional position in that, owing to its comparatively low energy of excitation, it does not in general bring about chemical reaction; it is, however, quenched by hydrogen and the hydrocarbons. Excited zinc, cadmium, and mercury, in both triplet and singlet states, are also quenched by hydrogen which is at the same time dissociated into atoms. With ethane an analogous splitting of the carbon-hydrogen bond takes place, the atom and radical formed bringing about various polymerization reactions. With ethylene and the other unsaturated hydrocarbons the results are much more complicated and show considerable variation according to the excited atom used. It appears that reaction may proceed by two distinct primary mechanisms, one initiated by a carbon-hydrogen bond split and the other by the formation of an excited olefin molecule; however in individual cases one or both of these reaction mechanisms may fail to occur. The facts outlined above have been rather firmly established by experiment, and the evidence for them is

presented in Steacie's book; their interpretation in the light of theory, particularly of the relative rates of the reactions, is the purpose of the present paper.

Previous theoretical discussions of reactions involving excited electronic states in terms of specific potential-energy surfaces[3] have been presented by Magee,[4] who discussed chemi-luminescent reactions, by Magee and Ri,[5] who treated the quenching of sodium by hydrogen, and by the present writer, who treated the quenching of sodium by the inert gases, hydrogen and the halogens (Part I),[6] and the photo-sensitization of hydrogen by excited mercury and cadmium (Part II).[2] The results obtained with hydrogen are of significance in connection with the hydrocarbon reactions, and will therefore be described briefly.

The quenching of excited (^2P) sodium by hydrogen is necessarily a physical process; the over-all reaction may be written as

$$Na(^2P)+H_2(^1\Sigma_g^+)=H_2(^1\Sigma_g^+)^1+Na(^2S), \quad (1)$$

in which $H_2(^1\Sigma_g^+)^1$ denotes hydrogen in its lowest electronic state but containing excess energy which is probably chiefly in the form of vibrational energy. Detailed study of the potential-energy surfaces[5, 6] indicates that the system reaches its final state *via* a polar complex which may be denoted as Na^+H^-H, and that the reaction path may be written as follows:

$$\begin{aligned}Na(^2P)+H_2(^1\Sigma_g^+)&\rightarrow NaH_2(^2\Sigma^+)\rightarrow\\ Na^+H^-H(^2\Sigma^+)&\rightarrow NaH_2(^2\Sigma^+)\rightarrow\\ &Na(^2S)+H_2(^1\Sigma_g^+)^1. \quad (2)\end{aligned}$$

In this scheme the second $NaH_2(^2\Sigma^+)$ state is a lower state than the first, and it has not quite sufficient energy (see Tables I and II) to form NaH and H.

With singlet mercury and cadmium atoms there is sufficient energy to break the H−H bond, and the over-all reaction is:

$$A(^1P)+H_2(^1\Sigma_g^+)\rightarrow A(^1S)+2H(^2S). \quad (3)$$

This process again will proceed *via* a polar state, the steps being:

$$\begin{aligned}A(^1P)+H_2(^1\Sigma^+)&\rightarrow AH_2(^1\Sigma^+)\rightarrow\\ &A^+H^-H(^1\Sigma^+)\rightarrow AH_2(^1\Sigma^+), \quad (4)\end{aligned}$$

the latter AH_2 complex being in a lower state than the former, and decomposing by one of two alternative processes:

$$\begin{aligned}AH_2(^1\Sigma^+)&\rightarrow A(^1S)+H_2(^1\Sigma_g^+)\rightarrow\\ &A(^1S)+2H(^2S), \quad (5)\end{aligned}$$

$$\begin{aligned}AH_2(^1\Sigma^+)&\rightarrow AH(^2\Sigma^+)+H(^2S)\rightarrow\\ &A(^1S)+2H(^2S). \quad (6)\end{aligned}$$

In either case the H_2 or AH produced will have sufficient vibrational energy to decompose at once into the free atoms.

The situation with the triplet atoms is different, owing to the difference in multiplicity between initial and final states. The hydrogen can no longer emerge from the reaction in its lowest electronic state, but only as free atoms. The over-all change is therefore:

$$A(^3P)+H_2(^1\Sigma_g^+)\rightarrow 2H(^2S)+A(^1S), \quad (7)$$

and the detailed mechanism is:

$$\begin{aligned}A(^3P)+H_2(^1\Sigma^+)&\rightarrow AH_2(^3\Pi)\rightarrow\\ &A^+H-H(^3\Sigma^+)\rightarrow AH_2(^3\Sigma^+). \quad (8)\end{aligned}$$

The $AH_2(^3\Sigma^+)$ can now decompose into $AH(^2\Sigma^+)$ and $H(^2S)$ by a process analogous to (6), the AH then splitting into A+H, but the reaction analogous to (5) is now forbidden by the rule of conservation of spin angular-momentum. The reaction can only involve the splitting of the H−H bond.

The mechanisms by which the hydrogen reactions proceed offer important clues as to the mechanisms of the hydrocarbon reactions. The hydrocarbons are, like hydrogen, normally in singlet states,* so that reaction on potential-energy surfaces similar to those designated above is possible. However there is an alternative process which is available to the hydrocarbons; this is the ejection of a hydrogen molecule with the formation of a more unsaturated molecule. This process, which frequently occurs with the olefins, is sometimes restricted for energetic reasons, and sometimes by the necessity for

[3] For a review of the earlier work see S. Glasstone, K. J. Laidler, and H. Eyring, *The Theory of Rate Processes* (McGraw-Hill Book Company, 1941).
[4] J. L. Magee, J. Chem. Phys. **8**, 687 (1940).
[5] J. L. Magee and T. Ri, J. Chem. Phys. **9**, 638 (1941).
[6] K. J. Laidler, J. Chem. Phys. **10**, 34 (1942).

* The evidence for this is to be found in the references quoted later (21–25) in connection with the excited states.

conservation of spin angular-momentum. The conditions under which this reaction can proceed will be discussed in detail later.

REACTION MECHANISMS

The principal reactions that a hydrocarbon can undergo on collision with an excited atom may now be considered. Denoting the excited atom by A* and the hydrocarbon (saturated or unsaturated) by MH_2, the two alternative initial steps are:

$$A^*+MH_2 \xrightarrow{k_1} A+MH+H, \qquad (9)$$

and

$$A^*+MH_2 \xrightarrow{k_1} A+MH_2^*. \qquad (10)$$

Process (9) is the exact analog of processes (4)–(6), and the potential-energy surfaces upon which reaction takes place are similar in multiplicity to those with hydrogen: if A* is singlet-excited, the surfaces will be all singlets, while if it is triplet-excited, they will be triplets. From the probable shape of the potential-energy surfaces it can be inferred that reaction (9) will take place without activation energy, provided that the excitational energy of A* plus the heat of formation of the hydride AH is at least as great as the bond strength HM−H. The reactions will, however, proceed with velocities lower than those calculated using collision theory if there are restrictions to crossings between any of the potential-energy surfaces.

In reaction (10) the product formed may in general have excitational energy in the form of electronic, translational, rotational, and vibrational energy. If there is a change of multiplicity in the process A*→A there must be a compensating change from MH_2 to MH_2^* for conservation of spin angular-momentum; this means, for example that, if A* is in a triplet state and A and MH_2 are in singlet states, MH_2^* must be in a triplet state. It follows that reaction (10) will not occur if there is no sufficiently low electronically-excited state of the right multiplicity, and it seems likely that reaction of this type does not occur between triplet-excited atoms and the saturated hydrocarbons, owing to the lack of a triplet-excited state of sufficiently low energy. When there is no change of multiplicity in the process A*→A, the excited molecule MH_2^* is not required to have electronic excitational energy, and all of its excitational energy can be in the other forms. This situation appears to exist in the reactions of the singlet-excited atoms, but it will be seen that the conversion of a large amount of electronic energy to the other forms proceeds with difficulty.

Reaction (9) is followed by chain processes leading to polymerization; the details will not be discussed here. Reaction (10) may be followed by a number of distinct processes, of which the most important are:

$$MH_2^*+A \xrightarrow{k_{-2}} MH_2+A^*, \qquad (10a)$$

$$MH_2^*+MH_2 \xrightarrow{k_3} MH_2'+MH_2', \qquad (11)$$

$$MH_2^* \xrightarrow{k_4} M+H_2, \qquad (12)$$

$$MH_2^* \xrightarrow{k_5} MH+H. \qquad (13)$$

Of the de-activations (10a) and (11), the former is simply the reverse of (10). It is probable that in most cases this reaction will proceed much more slowly than the remaining reactions, since it virtually has an activation energy. Of the energy transferred to MH_2 during reaction (10) some, at least, will be in the form of translational energy, i.e., of heat, so that the reaction will be exothermic. This translational energy, being rapidly dissipated, will have to be reacquired for process (10a) to take place, and this process will therefore proceed slowly and its rate will be temperature-dependent. It should hence be possible to ignore reaction (10a), at any rate at lower temperatures, since the remaining reactions probably proceed without activation energy; this will be done in the treatment which follows.

Reaction (11) represents de-activation by collision with other hydrocarbon molecules. Translational and rotational energy are rapidly dissipated [and therefore play little part in reactions (12) and (13)], excess vibrational energy survives many collisions, while electronic energy is transferred into other forms even more slowly. To show this persistence of electronic and vibrational energy the molecules produced in reaction (11) are marked with a prime (′) indicating that they still retain some energy.

Reaction (12) represents the formation of a more unsaturated molecule together with a hy-

drogen molecule. With the olefines such products (i.e., acetylenes) have sometimes been obtained, but in other cases the reaction does not occur. This has been explained[2] on the basis of energy considerations, due regard being paid to the necessity for conservation of spin angular-momentum. The detachment of a hydrogen molecule from a normal molecule is endothermic, so that, if the acetylene produced is in its lowest state, the condition for reaction is that the excitational energy given to the olefin is at least as great as the endothermicity. If the acetylene is not in its lowest state, its excitational energy must also be taken into account, and it will be seen later that the kinetic results give some tentative limits for the excitational energy of acetylene.

Reaction (13) gives rise to the same products as (9), and will be followed by polymerization processes. From the kinetic results it is not always possible to distinguish experimentally between the direct formation of MH and H [process (9)] and formation *via* the intermediate formation of the complex MH_2^* [process (10) followed by (13)], because the latter reduces to the former as a special case when the rate of de-activation is not important.

The scheme of reactions (9) to (13) is sufficiently general for the purpose of the arguments which follow, but does not cover every possibility. For example, in the case of 1-butene, one reaction which occurs is isomerization to 2-butene; this process will, however, be regarded as a special case of reaction (11).

The rates of the various over-all processes may now be derived in terms of the individual rate constants. The over-all rates that will be expressed are (1) the rate of quenching, (2) the rate of polymerization, and (3) the rate of formation of the molecule M. These rates will be obtained on the basis of steady-state conditions, which will obtain because $[MH_2^*]$, the concentration of excited molecules, is small, with the result that its rate of change with time is negligible compared with other rates; *viz*:

$$d[MH_2^*]/dt = 0 = k_2[A^*][MH_2] - [MH_2^*](k_3[MH_2]+k_4+k_5), \quad (14)$$

whence

$$[MH_2^*] = k_2[A^*][MH_2]/(k_3[MH_2]+k_4+k_5). \quad (15)$$

The rate of quenching is equal to the combined rates of reactions (9) and (10), i.e., to

$$-k[A^*]/dt = (k_1+k_2)[A^*][MH_2]. \quad (16)$$

This result assumes that a reaction (10a) can be neglected, which has been seen to be usually the case; if reaction (10a) had an appreciable rate, the rate of quenching would be somewhat less than given by Eq. (16).

The rate of formation of the compound M is given by

$$d[M]/dt = k_4[MH_2^*] \quad (17)$$

$$= k_4k_2[A^*][MH_2]/(k_3[MH_2]+k_4+k_5), \quad (18)$$

by use of Eq. (15).

The rate of disappearance of MH_2 to form H and the radical MH, is given by

$$-d[MH_2]_{\text{rad.}}/dt = k_1[A^*][MH_2] + k_5[MH_2^*] \quad (19)$$

$$= k_1[A^*][MH_2] + (k_5k_2[A^*][MH_2]/(k_2[MH_2]+k_4+k_5). \quad (20)$$

If α is the average number of polymer molecules produced by each H atom and MH radical, the rate of polymerization is

$$k[\text{poly.}]/dt = \alpha\{k_1[A^*][MH_2] + (k_5k_2[A^*][MH_2]/(k_3[MH_2]+k_4+k_5))\}. \quad (21)$$

Actually α is not a constant, and may be pressure-dependent, but no important error should arise from treating it as constant in the arguments which follow.

Equations (16), (18), and (21), which give the rates for the three main processes, indicate rather complex kinetic behavior, and it is possible to distinguish a large number of special cases according to the degree to which certain of the rates are negligible. Fortunately each of the reactions which have been studied seems to fall fairly clearly into one of four different cases, so that a considerable simplification in the kinetic equations is possible in individual instances. The main classification depends upon whether either k_1 or k_2 can be neglected compared with the other, and in all of the reactions one of these conditions is realized. A sub-classification depends upon the relative rates of reactions (11), (12), and (13). The important cases will now be

discussed, and mention will be made of reactions which fall into them; the reactions will later be discussed in detail in terms of the kinetic evidence and certain theoretical considerations.

Case I. If $k_1 \gg k_2$ the rate of quenching will be given by

$$-d[A^*]/dt = k_1[A^*][MH_2], \quad (22)$$

the rate of polymerization will be

$$d[\text{poly.}]/dt = \alpha k_1[A^*][MH_2], \quad (23)$$

while the rate of M-formation will be small. This case arises:

(1) in the reactions of the saturated hydrocarbons, when the rate of process (10) is low, owing to the absence of suitably placed electronically-excited states, and

(2) in the reactions of the singlet-excited atoms with ethylene, owing to the lack of a singlet-excited level of ethylene.

Case II. If $k_2 \gg k_1$ the rate of quenching is given by

$$-d[A^*]/dt = k_2[A^*][MH_2], \quad (24)$$

the rate of polymerization by

$$d[\text{poly.}]/dt = \alpha k_5 k_2[A][MH_2]/(k_3[MH_2]+k_4+k_5), \quad (25)$$

and the rate of M-formation by

$$d[M]/dt = k_4 k_2[A^*][MH_2]/(k_3[MH_2]+k_4+k_5). \quad (26)$$

Before this case is sub-divided it may be remarked, in anticipation of some of the arguments of the following section, that the quenching results in general allow a decision to be made between cases I and II. Under conditions where there are no special restrictions to either of the reactions (9) or (10), as with $Hg(^3P_1)$ and C_2H_4, it seems that the ratio k_2/k_1 is of the order of 100, which automatically places the reaction in case II or one of its sub-divisions. However in certain instances, when the molecule has no suitable electronic state, k_2 is very low, and case I arises. It therefore follows that case II will be associated with a high quenching rate, and case I with a low one; the two cases may therefore be distinguished on the basis of the quenching data.

The two important subdivisions of case II are as follows.

Case IIa. If in addition to $k_2 \gg k_1$, $k_4+k_3[MH_2] \gg k_5$, the rate of quenching is still given by Eq. (24), the rate of polymerization will be small, while the rate of M formation is given by

$$d[M]/dt = k_4 k_2[A^*][MH_2]/(k_3[MH_2]+k_4). \quad (27)$$

This case arises in the reactions of ethylene and butadiene sensitized by $Hg(^3P_1)$.

Case IIb. If in addition to $k_2 \gg k_1$, $k_5+k_3[MH_2] \gg k_4$, the rate of quenching is given by Eq. (24) (and is high), the rate of polymerization is given by

$$d[\text{poly.}]/dt = \alpha k_5 k_2[A^*][MH_2]/(k_3[MH_2]+k_5), \quad (28)$$

while the rate of M formation is small. This

TABLE III. Summary of kinetic behavior. MH and H produce on the average α-molecules of polymer.

Case	Conditions	Rate of quenching	Rate of polymerization	Rate of M formation
General	—	$(k_1+k_2)[A^*][MH_2]$	$\alpha\left\{k_1[A^*][MH_2]+\frac{k_3[AH_2]+k_4+k_5}{k_5 k_2[A^*][MH_2]}\right\}$	$\frac{k_4 k_2[A^*][MH_2]}{k_3[MH_2]+k_4+k_5}$
I	$k_1 \gg k_2$	$k_1[A^*][MH_2]$	$\alpha k_1[A^*][MH_2]$	Small
II	$k_2 \gg k_1$	$k_2[A^*][MH_2]$	$\alpha\frac{k_5 k_2[A^*][MH_2]}{k_3[MH_2]+k_4+k_5}$	$\frac{k_4 k_2[A^*][MH_2]}{k_3[MH_2]+k_4+k_5}$
IIa	$\left\{\begin{matrix}k_2 \gg k_1 \\ k_4+k_3[MH_2] \gg k_5\end{matrix}\right\}$	$k_2[A^*][MH_2]$	Small	$\frac{k_3[MH_2]+k_4+k_5}{k_4 k_2[A^*][MH_2]}$
IIb	$\left\{\begin{matrix}k_2 \gg k_1 \\ k_5+k_3[MH_2] \gg k_5\end{matrix}\right\}$	$k_2[A^*][MH_2]$	$\alpha\frac{k_5 k_2[A^*][MH_2]}{k_3[MH_2]+k_4+k_5}$	Small
III	k_1, k_4, and k_5 small	$k_2[A^*][MH_2]$	Small	Small

TABLE IV. Quenching cross sections, and values of I(A) and I(A)$-Ex$.

Quenching gas	Na(^3P) (A^2)	Hg($^3P_1$) (A^2)	Cd($^3P_1$) (A^2)
Inert gases	0	0	0
H_2	7.4[a]	6.01[b]	3.45[e] 0.67[f]
CH_4	0.11[a]	0.059[c]	0.012[e]
C_2H_6	0.17[a]	0.42[c]	0.02[e]
C_2H_4	44.0[a]	48.0[d]	24.9[e]
C_3H_6	52.0[a]	—	29.1[e]
C_2H_2	—	—	22.0[e]
Isobutene (C_4H_8)	—	—	30.6[e]
I(M)$-$(kcal.)	118.0	239.2	206.5
I(M)$-Ex$(kcal.)	69.7	127.2	119.2

[a] R. G. W. Norrish and W. M. Smith, Proc. Roy. Soc. **A176** 295 (1940).
[b] M. H. Zemansky, Phys. Rev. **36**, 919 (1930).
[c] J. R. Bates, Proc. Nat. Acad. Sci. **14**, 849 (1929); J. Am. Chem. Soc. **52**, 3825 (1930); *ibid.* **54**, 569 (1932).
[d] E. W. R. Steacie, Can. J. Research **18**, 44 (1940).
[e] E. W. R. Steacie and D. J. Le Roy, J. Chem. Phys. **11**, 164 (1943).
[f] H. C. Lipson and A. C. G. Mitchell, Phys. Rev. **48**, 625 (1935).

case seems to be realized in the reactions of propylene, isoprene, isobutene, 1-butene and 2-butene photo-sensitized by Hg($^3P_1$). The higher value of k_5 as compared with k_4 is probably due to the presence of weak C$-$H bonds in these molecules.

Case III. If k_1, k_4, and k_5 are all small, the rate of quenching is given by

$$-d[\mathrm{A}^*]/dt = k_2[\mathrm{A}^*][\mathrm{MH}_2], \qquad (29)$$

while the rates of polymerization and M formation will be small. If k_2 had its normal value, this would represent high quenching accompanied by no reaction, all of the excited molecules formed being deactivated. This case occurs in the quenching of sodium by the hydrocarbons, there being insufficient energy for any of the reactions to take place. It also arises in the quenching of Zn($^3P_1$) and Cd($^3P_1$) by ethylene; here k_1 and k_5 have their normal (small) values, there being adequate energy, and k_4 is small on energetic grounds on account of the necessity for the production of triplet-excited states.

The quenching data will now be discussed in more detail, followed by a discussion of the individual chemical reactions. The expressions derived in the present section are summarized in Table III.

THE QUENCHING RESULTS

The importance of the quenching results is that they provide information as to the net rate of the initial reaction steps (9) and (10) [see Eq. (16)] and therefore supplement the information given by the rate of production of products. Unfortunately, owing to experimental difficulties, some of the quenching rates have not been determined. In Table IV the relevant results are given in the form of quenching cross sections, which are the squares of the quenching radii, i.e., the intermolecular separations that have to be assumed on the basis of simple collision theory, and are proportional to the actual rates of the reactions. It has been shown in Part I[6] that the theory of absolute reaction rates gives an identical equation to collision (kinetic) theory for reactions of this kind, and that the quenching radius corresponds to the intermolecular separation at which a transition to the ionic state takes place.

Owing to the complexity of the potential-energy surfaces it is not possible to interpret these figures in an exactly quantitative fashion, but a rough treatment is useful in indicating the main factors upon which the rates depend. It was pointed out by Magee[4] (see Part I) that, if it can be assumed (as is approximately true) that in the region of the potential-energy surfaces under consideration the ionic terms in the polar surface are much more important than the non-ionic, the quenching radius is given very approximately by the expression

$$r_c = 330/\mathrm{I(A)} - E(\mathrm{MH_2}) - Ex \quad \text{Angstrom units,} \qquad (30)$$

where I(A) is the ionization potential of the metal A, $E(\mathrm{MH_2})$ is the electron affinity of the quenching molecule $\mathrm{MH_2}$, and Ex is the energy of excitation of A; these energies are in kcal. The values of I(A)$-Ex$ for the atoms are included in Table IV. If expression (30) were accurate, the cross sections for the three atoms in the table would fall in the order Na$>$Cd$>$Hg, since the values of I(A)$-Ex$ lie in the reverse order. The results for sodium and triplet cadmium are in agreement with this, but mercury falls out of line, indicating that the crude theory is inadequate.

The quenching of triplet cadmium by hydrogen is of special interest since, even if the formation of the hydride is assumed, there is not

quite sufficient energy to break the hydrogen-hydrogen bond. The possibility of physical quenching is excluded by the law of spin angular-momentum, so that the only process that can occur involves an activation energy at least as great as the endothermicity of the process, which is 1.0 kcal. At 300°K such an activation energy brings about a decrease in rate by a factor of 0.17. The fact that the quenching cross section is as high as it is (even accepting the lower value given) shows that the activation energy required is hardly more than the endothermicity. In all the other reactions with triplet mercury and cadmium there is sufficient energy to break a bond, so that zero activation energy is to be expected *a fortiori;* with sodium, as has been seen, quenching proceeds by a purely physical mechanism without the breaking of a bond or electronic excitation, and again there is no evidence of an activation energy.

A striking feature of the results quoted in Table IV is that the unsaturated hydrocarbons have quenching cross sections which are very much larger than those of the paraffins. This result is no doubt to be correlated with the kinetic evidence, already referred to, that the paraffins react at an appreciable rate by only one [reaction (9)] of the two possible mechanisms, while the olefins react by (9) and (10). This implies that there are two alternative ionic surfaces in the case of the olefins, of which one is very low and gives a correspondingly high quenching cross section. The lowness of this surface is probably associated with the high electron affinity of the double bond; consequently reaction (10) may be regarded as an interaction between A* and the double bond, and (9) between A* and a hydrogen atom. A rough indication of the relative rates of the two reactions in ethylene may be derived as follows on the assumption that reaction (9) proceeds in ethylene at the same rate as in ethane: since ethylene quenches triplet mercury about a hundred times more rapidly than ethane, k_2 for ethane is about 100 times as great as k_1 for ethylene. This result has already been seen to allow a distinction between case I and case II, and will find further application in the following sections.

THE REACTIONS OF THE SATURATED HYDROCARBONS

The reactions of ethane,[7] propane,[8] and butane[9] photo-sensitized by triplet mercury and cadmium have been studied extensively, and the kinetic evidence, which is fully discussed by Steacie,[1] suggests that the initial step is the splitting of a carbon-hydrogen bond with the formation of a hydrogen atom and a radical, which react further to form polymers. There is no evidence that de-activation processes take place, and this fact, together with the fairly low quenching rates, indicates that reaction proceeds solely by mechanism (9), and that reaction (10), and therefore (11) to (13), do not take place: this is case I. The only alternative explanation for the lack of de-activation and of olefin formation would be that reaction (10) occurred and was followed exclusively by (13). This would, however, require the existence of a suitable triplet-excited state: as will be seen, the evidence is that the triplet state is too high to play a part in these reactions. In any case the assumption that reaction (10) is followed exclusively by (13) implies a very small life for the excited complex, which is physically equivalent to postulating that reaction proceeds by (9). It therefore seems correct to explain the kinetics as falling in case I.

Work has not been carried out with the singlet metals, but theory predicts that again reaction would proceed entirely by the free radical mechanism. The evidence for this is that there is no electronically-excited singlet state of low enough energy to be excited by collision.

THE REACTIONS OF THE UNSATURATED HYDROCARBONS

Ethylene and Triplet Mercury

The mercury photo-sensitization of ethylene has been studied by Steacie and Le Roy[10] who found different behavior at 25° and at 300°C. At 25°C the main products of the reaction are

[7] E. W. R. Steacie and H. W. F. Phillips, J. Chem. Phys. **6**, 179 (1938); Can. J. Research **B16**, 303 (1938); E. W. R. Steacie and R. Potvin, J. Chem. Phys. **7**, 782 (1939).

[8] E. W. R. Steacie and D. J. Dewar, J. Chem. Phys. **8**, 571 (1940); E. W. R. Steacie, D. J. Le Roy and R. Potvin, J. Chem. Phys. **9**, 306 (1941).

[9] E. W. R. Steacie and R. Potvin, J. Chem. Phys. **7**, 782 (1939).

[10] D. J. Le Roy and E. W. R. Steacie, J. Chem. Phys. **9**, 829 (1941); *ibid.* **10**, 676 (1942).

hydrogen, acetylene, butane, and butene. The pressure rises initially and then falls rapidly, the initial pressure rise at low pressures corresponding exactly to the amounts of hydrogen and acetylene produced; at higher pressures, on the other hand, the initial rate of formation of acetylene is greater than the rate of pressure increase. The most significant feature of the low temperature reaction is that the rate decreases with increasing ethylene concentration, indicating a de-activation to be involved, and Steacie and Le Roy suggest the scheme

$$Hg(^3P_1)+C_2H_4=C_2H_4^*+Hg(^1S_0), \quad (31)$$

$$C_2H_4+C_2H_4^*=2C_2H_4, \quad (32)$$

$$C_2H_4^*=C_2H_2+H_2, \quad (33)$$

reaction (32) becoming relatively more important as compared with reaction (33) as the pressure is increased. This reaction scheme supersedes that of Taylor and Bates[11] who proposed the primary step

$$Hg(^3P_1)+C_2H_4=C_2H_2+H_2+Hg(^1S_0), \quad (34)$$

which explains the initial pressure rise but does not account for the decrease of rate with increase of initial pressure.

The formation of butane and butene can be attributed to various reactions. The hydrogen produced in reaction (33) may be photo-sensitized to atoms which will then react with ethylene to form ethyl radicals two of which may combine to form butane. Alternatively, vinyl radicals may be produced by one of the reactions

$$Hg(^3P_1)+C_2H_4=C_2H_3+H+Hg(^1S_0), \quad (35)$$

and

$$C_2H_4^*=C_2H_3+H, \quad (36)$$

[these correspond to reactions (9) and (13)], and the radicals may react with ethyl radicals to form butene.

As the temperature is increased the rate of the initial pressure rise decreases, becoming zero at 250°C. Moreover, the rate of disappearance of ethylene increases with increase of initial pressure at the higher temperatures, and increases rapidly with increasing temperature. These facts suggested that at the higher temperatures a free radical mechanism plays a more important part, and this was confirmed by the addition of nitric oxide (which has little effect on the low temperature reaction) which reduced the over-all rate and gave an initial pressure rise at 300°C. At the higher temperatures a good deal of propylene and of compounds of higher molecular weight is formed. The quantum yield for the formation of products other than acetylene and hydrogen was from 5 to 10 times greater at 300°C than at 25°C.

These results may be interpreted in terms of the reaction scheme (9)–(13) as follows. At 25°C the small amount of polymerization suggests that $k_2 \gg k_1$ and that $k_3[C_2H_4]+k_4 \gg k_5$; this is therefore an example of case IIa, the rate of acetylene formation being given by

$$d[C_2H_2]/dt = k_4k_2[Hg^*][C_2H_4]/(k_3[C_2H_4]+k_4). \quad (37)$$

A crude estimate of the relative importance of k_1 and k_2 at 25°C is 1:100, given by the quenching data.

The question of the increase in rate of the free radical reactions with rise in temperature, and the decrease in importance of the de-activating processes with temperature, will now be discussed in terms of the reaction scheme proposed above [reactions (9) to (13)]. In the general case the rate of olefin formation is given by (18), and the rate of polymerization by (21). The temperature affects the magnitude of these rates by its influence on the rate constants k_1, k_2, k_3, k_4, and k_5, the temperature coefficients for which will now be considered.

In order to do this a model for the activated complex has to be assumed in each case. In view of the fact that the quenching rates obey the simple collision theory it seems best to assume that the complexes are held together very loosely, the molecules retaining their individual degrees of freedom; there is, moreover, no evidence of an activation energy for any of the reactions (except (10a), the case of which has been discussed, and which will be ignored). The rate constant for reaction (9) may, on this hypothesis, be expressed as

$$k_1=(kT/h)F_AF_{MH}F_H/F_A^*F_{MH_2}, \quad (38)$$

[11] H. S. Taylor and J. R. Bates, J. Am. Chem. Soc. **49**, 2438 (1927).

where the F are the partition functions. Expressing these in terms of their translational, (t), and rotational, (r), parts for each degree of freedom, the equation becomes*

$$k_1=(kT/h)(t^3)_A(t^3r^3)_{MH}(t^3)_H/(t^3)_A^*(t^3r^3)_{MH_2}. \quad (39)$$

Separating out temperature-dependent parts, gives

$$k_1=k_1'T(T^{\frac{3}{2}})_A(T^{\frac{3}{2}}T^{\frac{3}{2}})_{MH}(T^{\frac{3}{2}})_H/(T^{\frac{3}{2}})_A^*(T^{\frac{3}{2}}T^{\frac{3}{2}})_{MH_2}, \quad (40)$$

where k_1' is temperature-independent. The equation reduces to

$$k_1=k_1'T^{5/2}, \quad (41)$$

i.e., the rate constant is proportional to the 5/2 power of the absolute temperature. It is clear from the derivation that this high temperature-dependence is due to the high entropy of the activated state in which an extra species has been formed.

The rate constant for (10) is given by

$$k_2=(kT/h)F_A^*F_{MH_2}/F_AF_{MH_2}^*, \quad (42)$$

so that, since the partition function for the activated state has now the same temperature-dependence as that for the initial state, the rate constant is

$$k_2=k_2'T. \quad (42a)$$

By similar arguments it can be shown that

$$k_3=k_3'T. \quad (43)$$

The dependence of k_4 on temperature is given by

$$k_4=(kT/h)F_MF_{H_2}/F_{MH_2} \quad (44)$$

$$=(kT/h)(t^3r^3)_M(t^3r^2)_{H_2}/(t^3r^3)_{MH_2} \quad (45)$$

$$=k_1'T(T^{\frac{3}{2}}T^{\frac{3}{2}})_M(T^{\frac{3}{2}}T)_{H_2}/(T^{\frac{3}{2}}T^{\frac{3}{2}})_{MH_2} \quad (46)$$

$$=k_1'T^{7/2}. \quad (47)$$

Similarly the dependence of k_5 is

$$k_5=k_5'T^{5/2}. \quad (48)$$

It is thus seen that in spite of there being no activation energy for any of the reactions, some of the rates, namely k_1, k_4, and k_5, show a fairly high temperature-dependence. Since by Eq. (21) the rate of polymerization depends upon k_1 and k_5, it is clear that this rate will increase significantly between 25°C and 300°C, as was actually found. The rate of acetylene formation, according to Eq. (18), will also increase with temperature owing to the increase in k_4, but not to the same extent owing to the effect of k_4 in the denominator. Since, moreover, k_4 increases with temperature relative to $k_3[MH_2]$ the importance of de-activations will diminish as the temperature is raised.

Le Roy and Steacie[10] report that the quantum yield for ethylene disappearance is greater at 300°C than at 25°C by a factor of 5 to 10. According to the scheme of reactions (9) to (13) the rate of ethylene disappearance is given by Eq. (27); the temperature-dependence of the quantum yield therefore depends on those of k_2, k_3, and k_4. Since k_4 varies with the 7/2 power of the absolute temperature it increases by a factor of about 10 from 25° to 300°C; k_2 and k_3 on the other hand increase by only a factor of 1.9. The theory would therefore predict an increase of quantum yield between these two figures, the higher figure being approached the greater is $k_3[MH_2]$ compared with k_4.

Ethylene and Triplet Cadmium

The results for the photo-sensitization of ethylene by triplet cadmium atoms[12] differ significantly from those with triplet mercury in that the quantum yield is much lower, being only about 0.015. The high quenching efficiency, on the other hand, indicates that the reaction [reaction (10)]

$$Cd(^3P_1)+C_2H_4=C_2H_4^*+Cd(^1S_0), \quad (49)$$

proceeds at a normal rate, and it therefore appears that the subsequent reactions to give acetylene take place only slowly. This has been interpreted[2] in terms of the energies involved in the reactions. For conservation of spin angular-momentum the excited ethylene produced in reaction (49) must be in a triplet state, and the acetylene produced by the reaction

$$C_2H_4(^3B_{1u})=C_2H_2(\text{triplet})+H_2(^1\Sigma_g^+), \quad (50)$$

must therefore also be in a triplet state. It is estimated that the heat of the reaction analogous

* As an approximation, the vibrational partition functions are assumed to be temperature-independent, and have been omitted.

[12] E. R. R. Steacie and R. Potvin, Can. J. Research **B16**, 337 (1938).

to (50) in which the molecules are in their normal states is about 85 kcal.; hence, if the excitational energies of C_2H_4(triplet) and C_2H_2(triplet) are x and y kcal., respectively, the heat of reaction (50) will be about $85+y-x$ kcal. Since the energy released by the de-activation of the $Cd(^3P_1)$ atom is 87.3 kcal., the energy other than electronic in the triplet-excited C_2H_4 molecule produced in reaction (50) is $87.3-x$ kcal. If $y>2.3$ kcal., there will be an activation energy, and reaction will be slow. The slow rate with which the reaction actually proceeds suggests that the latter alternative is the correct one. Since the reaction proceeds readily with triplet mercury it can further be concluded that $y<27.7$ kcal., this figure being the difference between the excitational energy for triplet mercury, and 87.3.

On the other hand, there is no reason to believe that reactions (9) and (13), involving a bond split, cannot proceed, since the energy released by the $Cd(^3P_1)$ atom (assuming hydride formation) is 102.8 kcal., which is probably greater than the strength of the C−H bond in ethylene (see below). Such reaction as does occur therefore probably proceeds by the free radical mechanism. It is not so easy to predict whether reaction (13) will proceed rapidly, since some of the energy acquired by the excited ethylene will be in the form of translational energy, which will be dissipated rapidly, and enough energy for reaction (13) may not remain. On the assumption that there is not sufficient energy for reaction (13) to proceed, the rate of polymerization will be given by [see Eq. (21)]

$$d[\text{poly.}]/dt=\alpha k_1[Cd^*][C_2H_4], \qquad (51)$$

which will be small since k_1 is normally small; this is an example of case III. Since the quenching rate is given by [see Eq. (16)]

$$-d[Cd^*]/dt=(k_1+k_2)[Cd^*][C_2H_4], \qquad (52)$$

and since k_2/k_1 is large and probably of the order of 100, it follows that unless α is large the quantum yield should be small. The experimental yield is 0.015, and this, together with the rough value of k_2/k_1, suggests that α is of the order of unity. It is to be noted that the experimental quantum yield is not consistent with the hypothesis that reaction (13) proceeds readily.

In view of the rough numerical agreement this interpretation of the cadmium reaction seems preferable to that of Steacie,[1] who considers that the low rate is to be attributed to the inhibition of reaction by *both* the free radical and the excited molecule mechanisms.

Ethylene and Triplet Zinc

The results with triplet zinc (13) are very similar to those with cadmium; very little reaction occurs with either. The excitational energy of $Zn(^3P_1)$ is 92.5 kcal., and this suggests that y, the excitational energy of triplet acetylene, is greater than 7.5 (=92.5−85) kcal. The results with zinc, therefore, further narrow the limits of the excitational energy of acetylene to 7.5 and 27.7 kcal. The accuracy of these figures is, of course, dependent on the reliability of the figure 85 kcal. for the heat of dissociation of ethylene into acetylene and hydrogen.

Ethylene and Singlet Zinc and Cadmium

The reactions of ethylene photo-sensitized by singlet zinc[13] and cadmium[14] have also been studied. With cadmium, reaction occurs readily with a quantum yield of about unity, the products being olefines together with small amounts of acetylene and hydrogen. These facts suggest that the reaction proceeds mainly by the free radical mechanism and that the excited molecule mechanism takes place to a small extent only. The reason for the low rate of the excited molecule reaction is not immediately clear; it is not to be explained, as it was with triplet cadmium, in terms of insufficient energy for the formation of acetylene, since there is now ample energy (124.4 kcal.), and the acetylene does not have to be excited electronically as there is no change of multiplicity. This suggests strongly that the low rate of production of acetylene is due to the low rate of reaction (10) itself. The excited ethylene formed in reaction (10) must, for conservation of spin angular-momentum, be in a singlet state, and this must be its lowest electronic state since there is no excited singlet state of ethylene with sufficiently low energy. The excitational energy of the

[13] H. Habeeb, D. J. Le Roy, and E. W. R. Steacie, J. Chem. Phys. **10**, 261 (1942).
[14] E. W. R. Steacie and D. J. Le Roy, J. Chem. Phys. 10, 22 (1942).

ethylene must therefore be entirely in the form of non-electronic energy, and most will be vibrational energy. It therefore appears that the transfer of large amounts of electronic energy into vibrational energy proceeds only slowly.

The reaction, therefore, seems to be an example of case I ($k_1 \gg k_2$). The results with singlet zinc are similar to those with cadmium except that the amount of acetylene produced is even smaller. With zinc more electronic energy has to be converted into vibrational energy, and the rate will be even further reduced on this account. The singlet-mercury reaction has not yet been investigated, but as the electronic energy available is still higher than with zinc (153.9 as compared with 133.4 kcal.), it might be anticipated that the rate of the excited-molecule reaction would be still lower.

It is to be noted that this interpretation of the reactions of the singlet atoms, postulating as it does that the primary reaction which forms the excited molecule proceeds slowly, implies that the quenching rates (which have not been determined) would be low. The mechanism of quenching would in fact be similar to that of the saturated hydrocarbons, and it is to be expected that the cross sections would be of the same order as those found with the saturated hydrocarbons.

Ethylene and Sodium (^2P); Strength of the C−H Bond in Ethylene

Ethylene strongly quenches excited sodium (see Table IV) but no reaction occurs; this is presumably because the energy available even with hydride formation (99.9 kcal.) is insufficient to break the carbon-hydrogen bond in ethylene, while the energy that could be given to excite the ethylene (48.3 kcal.) is insufficient for acetylene formation; this is case III. There is considerable doubt about the strength of this C−H bond, and the only directly obtained value, that of 91 kcal. provided by electron-impact data,[15] is almost certainly too small. One piece of evidence for this is derived from the results of J. O. Smith and H. S. Taylor[16] on the reaction between methyl groups and the various hydrocarbons, a C−H group in the hydrocarbon being broken with the formation of methane. Since ethylene reacts much less readily than ethane, with an activation energy of at least 2 kcal. higher, it would appear that the C−H bond in ethylene is stronger than that in ethane (97 kcal.) and that its strength is more probably about 100 kcal. This figure is consistent with the failure of excited sodium (99.9 kcal.) to induce reaction (which the figure 91 kcal. would not be) and is also consistent with the results with Cd($^3P_1$); as already seen, it is probable that Cd($^3P_1$) effects reaction readily by the free radical mechanism, and this would impose an upper limit of 102.8 kcal. on the strength of the bond. The kinetic results therefore indicate that the correct value for the strength of the C−H bond in ethylene is approximately 100 kcal.

Butadiene and Triplet Mercury

Butadiene ($H_2C=CH-CH=CH_2$) is structurally analogous to ethylene in that its C−H groups are all olefinic, and it is therefore to be expected that its photo-sensitized reactions will be similar. That this is so with triplet mercury has been shown by Gunning and Steacie,[17] who found that the initial rate of polymerization decreases with decreasing pressure. The reaction products were principally a dimer, hydrogen, and an acetylenic compound (C_4H_4). The results are consistent with the hypothesis that the main initial step is the formation of an excited butadiene molecule [reaction (10)] which may either dimerize on collision with another butadiene molecule or split off hydrogen to give C_4H_4 [reaction (12)]. As was the case with ethylene, reaction by way of the free radical [reactions (9) and (13)] seems to be negligible. The quantum yield of the reaction was of the order of unity, indicating that when the excited molecule collides with another molecule de-activation takes place to a minor extent compared with dimerization. This reaction is an example of case IIa.

Propylene and Triplet Mercury

Propylene ($H_2C=CH-CH_3$) differs from ethylene and butadiene in having three C−H

[15] D. P. Stevenson, J. Am. Chem. Soc. **64**, 1588 (1942); *ibid.* **65**, 209 (1943).

[16] J. O. Smith and H. S. Taylor, J. Chem. Phys. **7**, 390 (1939); ibid. **8**, 543 (1940).

[17] H. E. Gunning and E. W. R. Steacie, J. Chem. Phys. **12**, 484 (1944); see also D. H. Volman, J. Chem. Phys. **14**, 467 (1946).

bonds which are once removed from a double bond, and since these are believed to be somewhat weaker than C−H bonds which are next to a double bond, it might be expected that there would be a greater tendency for reaction to proceed by a free radical mechanism. The results of Gunning and Steacie[18] show a low quantum yield and a decrease in rate with increasing pressure, suggesting that de-activations are important and that, therefore, the reaction

$$Hg(^3P_1)+C_3H_6=C_3H_6^*+Hg(^1S_0), \quad (53)$$

where $C_3H_6^*$ is triplet-excited, plays an important part. On the other hand, the main products are liquid polymers and hydrogen, indicating that free radicals are produced by the processes

$$C_3H_6^*=C_3H_5+H, \quad (54)$$

and

$$Hg(^3P_1)+C_3H_6=C_3H_5+H+Hg(^1S_0). \quad (55)$$

The rate of decomposition of C_3H_6 into $C_3H_4+H_2$ seems to be small compared with the rates of the above reactions, so that the reaction falls into case IIb ($k_4 \ll k_5+k_3[C_3H_6]$). The greater rates of (54) and (55) as compared with the corresponding ones with ethylene and butadiene are no doubt due to the lower strength of the C−H bond in propylene, evidence for which was given by the free radical investigations of Smith and Taylor.[16]

Isoprene and Triplet Mercury

The results for the polymerization of isoprene ($CH_2=CHC(CH_3)=CH_2$) photo-sensitized by $Hg(^3P_1)$[18] are closely analogous to those of propylene, the quantum yield being low and the rate decreasing with initial pressure.

Isobutene and Triplet Mercury

Isobutene ($H_2C=C=(CH_3)_2$) has six C−H bonds in positions once removed from a double bond, and two which are next to a double bond. The results[19] indicate a quantum yield of 0.59, no initial pressure rise, and, as chief products, propylene, a polymer, acetylene, and propane. The products are believed to be formed from H and the radical C_4H_7, formed by the three processes:

$$Hg(^3P_1)+C_4H_8=C_4H_7+H+Hg(^1S_0), \quad (56)$$

$$Hg(^3P_1)+C_4H_8=C_4H_8^*+Hg(^1S_0), \quad (57)$$

and

$$C_4H_8^*=C_4H_7+H. \quad (58)$$

As with ethylene and triplet cadmium, the $C_4H_8^*$ does not split off a hydrogen molecule, presumably for energetic reasons, but will be deactivated by collisions. The low quantum yield is due to these de-activations. This is an example of case IIb.

Gunning and Steacie offer an alternative explanation of these results, postulating an inefficiency in the primary process and explaining the low quantum yield in terms of physical quenching in which electronic energy is transferred into vibrational and rotational energy only. However this latter suggestion is not to be maintained, owing to the change of multiplicity which would make such a reaction exceedingly inefficient. The isobutene formed in reaction (57) must be in a triplet-excited electronic state, and only the extra energy set free can pass into vibrational and rotational energy. This type of energy transfer can, of course, be described as physical in this instance, in which it does not lead to chemical reaction, but it must be noted that this kind of quenching does frequently lead to reaction and in favorable cases (as with ethylene and triplet mercury) to very rapid reaction with high quantum yield. The reason for the low rate of decomposition of triplet-excited isobutene cannot be interpreted quantitatively since the energies are not known, but it is doubtless associated with the energies of the triplet-excited molecules that have to be formed in subsequent reactions.

1-Butene and Triplet Mercury

The products formed in the mercury-photosensitized reaction of 1-butene ($H_2C=CH-CH_2-CH_3$) are chiefly 2-butene and a polymer.[20] It is found that increasing the pressure increases

[18] H. E. Gunning and E. W. R. Steacie, J. Chem. Phys. **14**, 57)1946).
[19] H. E. Gunning and E. W. R. Steacie, J. Chem. Phys. **14**, 544 (1946).
[20] D. J. Le Roy and E. W. R. Steacie, J. Chem. Phys. **10**, 683 (1942); H. E. Gunning and E. W. R. Steacie, J. Chem. Phys. **14**, 581 (1946).

the rate of isomerization but decreases the rate of polymerization. This indicates that isomerization depends upon collisions between excited 1-butene molecules and normal molecules, and that polymerization involves the splitting-off of a hydrogen atom from an excited 1-butene molecule followed by chain processes. The only plausible mechanism would seem to be that proposed by Gunning and Steacie as follows:

$$Hg(^3P_1)+1-C_4H_8=1-C_4H_8^*+Hg(^1S_0) \quad (59)$$

$$1-C_4H_8^*+1-C_4H_8=2-C_4H_8+1-C_4H_8, \quad (60)$$

$$1-C_4H_8^*=C_4H_7+H. \quad (61)$$

This reaction scheme corresponds to our case IIb. The process is of interest in that it was the first to give concrete evidence that free radicals may be produced through an excited molecule having a finite life. On the basis of their kinetic results, Gunning and Steacie conclude that de-activation without isomerization takes place to an insignificant extent compared with (60).

2-Butene and Triplet Mercury

The reaction between 2-butene ($H_3C-CH=CH-CH_3$) and triplet mercury[20] gives rise mainly to liquid polymer. Except that there is no isomerization the kinetics are similar to those with 1-butene and the scheme

$$Hg(^3P_1)+2-C_4H_8=2-C_4H_8^*+Hg(^1S_0), \quad (62)$$

$$2-C_4H_8^*+2-C_4H_8=2(2-C_4H_8), \quad (63)$$

$$2-C_4H_8^*=C_4H_7+H, \quad (64)$$

is postulated. This falls into case IIb, and we again have positive evidence that free radicals are formed from $C_4H_8^*$.

GENERAL DISCUSSION

In spite of the kinetic complexity of the photosensitized reactions of the hydrocarbons, it has been possible to classify them into four groups. There is naturally some variation within one group, but this seems to be considerably less important than the variations between reactions lying in different groups.

The classification which has been made depends upon the following assumptions which the analysis of the kinetic results seems to make necessary:

1. When there is a suitable electronic state to absorb part of the energy of excitation, the rate of formation of the excited hydrocarbon [reaction (10)] occurs with about one hundred times the velocity with which the C−H bond is broken [reaction (9)]. This is case II.

2. When there is no suitable electronic state of the hydrocarbon molecule, the rate of formation of the excited hydrocarbon, which must have its excitational energy in the form of vibrational and rotational energy, must be very low (case I).

3. When all of the C−H bonds in the hydrocarbon are next to a double bond, the excited hydrocarbon readily splits off a hydrogen molecule (case IIa).

TABLE V. Summary of conclusions.

Hydrocarbon	Sensitizer	Case	Conditions	Remarks
Ethane, Propane, Butane	$Cd(^3P_1)$, $Hg(^3P_1)$	I	$k_1 \gg k_2$	No triplet-excited states
Ethylene	$Zn(^3P_1)$	III	k_1, k_2, k_4, k_5 small	Insufficient energy
Ethylene	$Cd(^3P_1)$	III	k_1, k_2, k_4, k_5 small	Insufficient energy
Ethylene	$Hg(^3P_1)$	IIa	$k_2 \gg k_1,\ k_4+k_3[C_2H_4] \gg k_5$	Triplet-excited state
Ethylene	$Zn(^1P_1)$	I	$k_1 \gg k_2$	No singlet-excited states
Ethylene	$Cd(^1P_1)$	I	$k_1 \gg k_2$	No singlet-excited states
Ethylene	$Na(^2P)$	III	k_1, k_4, k_5 small	Insufficient energy
Butadiene	$Hg(^3P_1)$	IIa	$k_2 \gg k_1,\ k_4+k_3[C_4H_6] \gg k_5$	Triplet-excited state
Propylene	$Hg(^3P_1)$	IIb	$k_2 \gg k_1,\ k_5+k_3[C_2H_6] \gg k_4$	Low energy C−H bonds favoring (5) as compared with (4)
Isoprene	$Hg(^3P_1)$	IIb	$k_2 \gg k_1,\ k_5+k_3[C_2H_6] \gg k_4$	
Isobutene	$Hg(^3P_1)$	IIb	$k_2 \gg k_1,\ k_5+k_3[C_2H_6] \gg k_4$	
1-Butene	$Hg(^3P_1)$	IIb	$k_2 \gg k_1,\ k_5+k_3[C_2H_6] \gg k_4$	
2-Butene	$Hg(^3P_1)$	IIb	$k_2 \gg k_1,\ k_5+k_3[C_2H_6] \gg k_4$	

4. When the molecule has C−H bonds which are next but one to a double bond, and which are consequently weak, the excited molecule may split off a hydrogen atom to the exclusion of a hydrogen molecule (case IIb).

5. Sometimes, when the exciting atom has insufficient energy, the excited molecule produced may be unable to perform any reaction (case III).

The allocation of the reactions to the various groups is summarized in Table V.

Since the arguments of the present paper are concerned with the existence or non-existence of electronically-excited states of the hydrocarbons, consideration will be given to the question of what other and more direct evidence is available.

The simple saturated hydrocarbons do not absorb except at very low wave-lengths, and therefore have no low-lying singlet energy levels. Mulliken[21] estimates the excitational energy of the lowest singlet ($^1T_2$) state of methane to be about 225 kcal. The lowest excited triplet state ($^3T_2$) of methane should be lower, but Mulliken estimates its energy as at least 140 kcal. The excitation energies of both singlet and triplet states are thus too high for the states to be produced in any of the reactions discussed here, and this is consistent with the observed quenching and kinetic data.

The singlet-excited states of the olefins are also very high. Absorption starts with ethylene at about 57,000 cm^{-1} which corresponds to about 160 kcal.[22] In the case of sodium and the singlet atoms there is, therefore, not enough energy for electronic excitation, and the excitational energy must all be taken up as vibrational energy. As has been seen, the evidence suggest that this transfer of energy takes place more readily the smaller the amount of energy that has to be transferred. Thus excited sodium, which has only a small amount of energy (48.3 kcal.), is strongly quenched by the unsaturated hydrocarbons. Unfortunately the quenching rates with the singlet atoms are not known; however, singlet cadmium, which has 124.4 kcal. of energy to transfer, produces only small amounts of acetylene and hydrogen from ethylene, while singlet zinc, with 133.4 kcal. produces even less. It is difficult to see how these results would be explained except on the basis given.

The energy of the triplet state of the olefins has been a matter of considerable discussion. On qualitative grounds a fairly low lying state is to be expected, corresponding to the uncoupling of one of the electron pairs in the double bond (compare oxygen). Magee, Shand, and Eyring[23] have postulated that the excitational energy is about 20 kcal., on the basis of an activation energy of this value for certain isomerizations involving rotation about the double bond. However, Hartmann[24] has calculated the energy to be 70 kcal., in good agreement with the value of 72–74 kcal. obtained by G. N. Lewis and M. Kasha[25] on the basis of their phosphorescence studies. In any case the energy appears to be sufficiently low to allow the formation of a triplet-excited state in the case of all of the reactions with the triplet atoms.

[21] R. S. Mulliken, J. Chem. Phys. **3**, 517 (1935).
[22] W. C. Price and W. T. Tutte, Proc. Roy. Soc. **A174**, 207 (1940).
[23] J. L. Magee, W. Shand, and H. Eyring, J. Am. Chem. Soc. **63**, 2100 (1944).
[24] H. Hartmann, Zeits. physik. Chemie **B53**, 96 (1943).
[25] G. N. Lewis and M. Kasha, J. Am. Chem. Soc. **66**, 2100 (1944).

THE JOURNAL OF CHEMICAL PHYSICS VOLUME 15, NUMBER 10 OCTOBER, 1947

Forces between Tetrahalide Molecules*

J. H. HILDEBRAND
Department of Chemistry, University of California, Berkeley, California

(Received July 1, 1947)

A review of the evidence furnished by melting and boiling points, entropy of fusion and evaporation, crystal structure, ionic-bond character, radii, Raman frequencies, energy of evaporation and differential energy of expansion, polarizability, and solubility relations has led to the following conclusions: (1) Hindrance to rotation is small in liquid CCl_4 and CBr_4 but increases with increasing radius ratio of central atom to halide atom. This indicates that the van der Waals radii of the halide atoms in these liquids are considerably smaller than those assigned by Pauling. (2) In spite of the hindrance to rotation, the solubility relations can be calculated with considerable accuracy by means of equations derived for spherical molecules with radial force fields. (3) Attraction between molecules of different species is not appreciably influenced by the kind of bonding orbitals of the central atom, but is strongly influenced by the ionic character of the bond. (4) The apparent anomaly of the low boiling point and internal pressure of $SiCl_4$ is due to the large increase in molal volume between CCl_4 and $SiCl_4$; the attraction constant increases uniformly with M-X distance in the series of chlorides of C, Si, Ge, Ti, Sn. (5) The attraction constant is closely related to the square of the polarizability, in accordance with the London theory. (6) The two isotropic Raman frequencies for the chlorides of C, Si, Ge, Ti, Sn, Pb decrease uniformly with increasing M-X distance. (7) None of the properties of $SiCl_4$ requires for its explanation the assumption of "double bond resonance."

THE PROBLEM

THE study of the liquid state should obviously begin with liquids composed of simple spherical molecules, of which the inert gases furnish the best and practically only examples, but the cost of most of them and the inconvenient and short temperature range of their liquid forms offer practical obstacles to the gathering of the desirable variety of experimental data. An even stronger reason for turning to polyatomic molecules is the fact that nearly all the solutions in which we are practically interested are composed of polyatomic molecules, so that the elucidation of the behavior of monatomic liquids takes us but a short way towards desired goals. The substances that have appealed to me as the most attractive substitutes for the group 0 elements have been the tetrahalides, and my coworkers and I have for many years been gathering information regarding both the pure substances and their solutions. They possess the next best thing to spherical symmetry, they are obtainable in quantity, and they offer a wide range of intermolecular forces, so different, in the case of $SiCl_4$ and SnI_4, for example, as to give two liquid phases.[1]

Among the more obvious questions that present themselves are the following:

1. To what extent are we justified in treating these tetrahedral molecules as if they had spherical symmetry, due to rotation in the liquid state? Formulas for solubility relationships derived for spherical molecules have proven applicable to a remarkable degree to solutions of polyatomic molecules[2] nevertheless, the evidence shows, as has been pointed out by Halford,[3] that free rotation in tetrahalides is more and more restricted as larger central atoms are chosen.

2. Instead of considering the molecular fields of the tetrahalides as radial from their central atoms, would it be better, in view of the short range of the London forces, to consider the halogen atoms as the main centers of attraction, as I once suggested?[4] The fact that these forces become so weak at a distance of two molecular diameters as to contribute but little to the energy of vaporization has long been evident.[5] It is particularly well illustrated by the fact that such substances as OsO_4, OsF_8, and UF_6 are very volatile despite the many electrons in their central atoms and the extreme non-volatility of the metals themselves.

3. What influence does bond character have upon intermolecular forces?

4. Why do boiling points, internal pressures and solvent powers show $SiCl_4$ apparently out of line, as shown in Table I?

In attempting to answer these questions, it seems best to exclude the halides of the sixth group elements because of instability or lack of

* Presented at the symposium on liquids at Atlantic City, April 17, 1947, under the auspices of the Division of Physical and Inorganic Chemistry.

[1] J. H. Hildebrand and G. R. Negishi, J. Am. Chem. Soc. **59**, 339 (1937).

[2] Cf. R. D. Vold, J. Am. Chem. Soc. **59**, 1515 (1937).

[3] R. S. Halford, J. Chem. Phys. **8**, 496 (1940).

[4] J. H. Hildebrand, Trans. Faraday Soc. **33**, 144 (1937).

[5] Cf. J. H. Hildebrand, *Solubility of Non-Electrolytes* (Reinhold Publishing Corporation, New York), second edition, p. 71.

TABLE I.

	CCl_4	$SiCl_4$	$GeCl_4$	$SnCl_4$
Boiling point, °K	350	332	360	386
Internal pressure, energy of vap. per cc	73.7	56.8	65.5	86.4
Solubility of I_2, mole percent at 25°C	1.15	0.50	—	—

tetrahedral symmetry. Stevenson and Shoemaker[6] have found, for example, that $TeCl_4$ has a bipyramidal structure and Vogt and Biltz[7] found that it is a good conductor of electricity in the liquid state. It has, furthermore, a higher entropy of vaporization than a normal liquid and a low solvent power for iodine.[8]

Any answers given to the questions stated above must be consistent with all of the pertinent physico-chemical properties of these substances, therefore, these properties are reviewed in the paragraphs immediately following.

MELTING POINTS

Melting points in °K, from a resumé kindly furnished by Professor Leo Brewer, are given in Table II and plotted against molal weight in Fig. 1. We see that the points for the halides of silicon, germanium, tin and lead increase with molecular weight about as one might expect from the behavior of the inert gases. Indeed, if the slope of the curve for the rare gases is taken to indicate the effect of increasing molecular weight upon melting and boiling points of symmetrical, non-polar molecules, then the increase in melting point and boiling point for the tetrahalides is largely determined by molecular weight, with the weights of the central atom and the halide atoms counting equally. It is evident, however, that the points for the halides of carbon, vanadium and titanium are distinctly higher than for the others, suggesting that the processes involved in these cases are somewhat different. Divergent melting points for CCl_4 and CBr_4 may be attributed to a different solid lattice, for, unlike the others, they have transition points 24.8° and 43.2°, respectively, below their melting points. The melting process is evidently much the same with the case of the others, as indicated by practically identical entropies of fusion of four chlorides given in Table III reproduced from a paper by Frederick and Hildebrand.[9] In the cases of CCl_4 and CBr_4, sums of the entropies of transition, Δs_t, and of fusion, Δs_f, are less than the entropy of fusion for the other four. Mark[10] found that the lower temperature form of CBr_4 is monoclinic, the higher form tetragonal, and Dickinson[11] reported that SnI_4 has a cubic unit cell of 8 molecules with pyritohedral symmetry. According to Hassell and Kringstad,[12] $TiBr_4$ and TiI_4 have the same crystal structure as SnI_4. Raeder[13] found that the following form mix-crystals in all proportions, indicating indentical crystal structure: $SnCl_4$ and $SnBr_4$; $SnBr_4$ and SnI_4; $TiCl_4$ and $TiBr_4$.

Turkevich, Conner and Smyth[13a] have given definite evidence that the CCl_4 molecules are rotating between the transition point and the melting point, which is in harmony with the fact that they acquire more entropy in the transition than in fusion. CBr_4 must be doing the same thing, although the higher C_p found by Frederick and Hildebrand for the higher solid form, 42.9 cal. compared with 35.0 cal. for the monoclinic form and 36.7 cal. for the liquid, indicates that rotational energy is still being acquired above the transition point. We shall return later to the question of rotation.

TABLE II. Meltings and boiling points, and ratios, °K.

	Chlorides			Bromides			Iodides		
	T_m	T_b	T_b/T_m	T_m	T_b	T_b/T_m	T_m	T_b	T_b/T_m
C	250	350	1.40	363	463	1.28	444	dec.	—
Si	206	330	1.60	278	426	1.57	394	561	1.42
Ge	224	357	1.59	299	462	1.54	419	dec.	
Sn	240	386	1.61	303	480	1.58	418	621	1.48
Pb	258	dec.		—	—		—	—	
V	247	427	1.73	—	—		—	—	
Ti	250	409	1.63	311	503	1.62	423	630	1.49
Zr	710	604	0.85	723	630	0.87	772	704	0.91
Hf	705	590	0.84	693	595	0.86	—	—	
Th	1038	1195	1.14	952	1130	1.19	839	1110	1.32

The higher values for $TiCl_4$ and VCl_4 and the still higher values for $ZrCl_4$, $HfCl_4$ and $ThCl_4$,

[6] D. P. Stevenson and V. S. Shoemaker, J. Am. Chem. Soc. **62**, 1267 (1940).

[7] A. Vogt and W. Biltz, Zeits. f. anorg. allgen, Chemie **133**, 277, 312 (1924); see also J. H. Simons, J. Am. Chem. Soc. **52**, 3483 (1930).

[8] J. H. Hildebrand, J. Phys. Chem. **43**, 109 (1939).

[9] K. J. Frederick and J. H. Hildebrand, J. Am. Chem. Soc. **61**, 1555 (1939).

[10] H. Mark, Ber. d. d. chem. Ges. **57B**, 1820 (1924).

[11] R. G. Dickinson, J. Am. Chem. Soc. **45**, 958 (1923).

[12] O. Hassell and H. Kringstad, Zeits. f. physik. Chemie **B15**, 274 (1932).

[13] M. G. Raeder, Thesis (Trondhjem, 1929).

[13a] A. Turkevich and C. P. Smyth, J. Am. Chem. Soc. **62**, 2468 (1940); W. P. Conner and C. P. Smyth, *ibid.*, **63**, 3424 (1941).

raise the question whether the type of bonding electrons is responsible, *d* and *s* instead of *s* and *p* for the tin group. It seems sufficient, however, to attribute these differences to greater ionic character of their bonds, with greater tendency for higher coordination about the central atom. The ionization potential of Zr is 6.92 electron-volts while that of Sn is much higher, 7.30 electron-volts.[14] The difference in ionic character between ZrI_4 and SnI_4, with melting points of 772°K and 418°K respectively, is strikingly indicated by the absence of color in the former and the orange color in the latter.[15]

BOILING POINTS

Boiling points, also plotted in Fig. 1, are strikingly parallel to melting points for the silicon, germanium, tin and titanium halides, but not so for the others. This is brought out in Table III, which gives the ratios, T_b/T_m. The smaller ratios for CCl_4 and CBr_4, are in the direction to be expected for more nearly symmetrical molecules; this ratio is only 1.04 for argon. The same reason explains the decrease of the ratio in going from the chlorides of Si, Sn and Ti to their iodides.

The sublimation of the solid halides of Zn and Hf must be regarded as further evidence of their salt character.

MOLECULAR DIMENSIONS

The distance between the centers of the central atoms and the halogen atoms, as determined by electron diffraction, are given in Table IV, along with molal volumes at 25°. Let us re-examine the evidence of these figures on the question of restricted rotation. The "Hildebrand rule"[16] ap-

TABLE III. Entropies of transition and fusion.

Substance	$T_{tr.}$	ΔS_t	T_m	ΔS_f	$\Delta S_t+\Delta S_f$
CBr_4	320.0	4.44	363.2	2.61	7.05
CCl_4	225.44	4.79	250.23	2.31	7.10
$TiCl_4$	—	—	250.0	9.00	9.00
$TeCl_4$	—	—	497.2	9.07	9.07
$SiCl_4$	—	—	205.5	9.08	9.08
$SnCl_4$	—	—	239.9	9.11	9.11
SnI_4	—	—	417.6	11.01	11.01

[14] Cf. G. Herzberg, *Atomic Spectra and Atomic Structure* (Prentice-Hall, Inc., New York, 1937).

[15] For a discussion of color as an index of bond character, see K. S. Pitzer and J. H. Hildebrand, J. Am. Chem. Soc. 63, 2472 (1941).

[16] J. H. Hildebrand, J. Chem. Phys. **7**, 233 (1938).

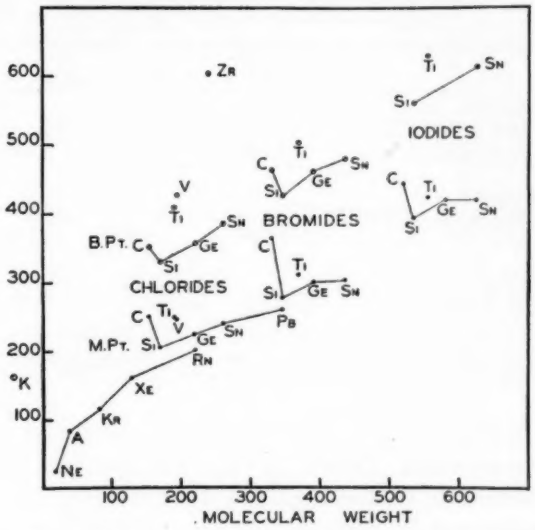

FIG. 1. Melting and boiling points of tetrahalides.

plied to the tetrachlorides of C, Si, and Sn shows the following entropies of vaporization at temperatures where the vapor volume is 49.5 liters, neopentane, "spherical," 20.1 e.u., CCl_4 20.7 e.u., $SiCl_4$ 21.2 e.u., and $SnCl_4$ 21.8 e.u. If the comparison is made at equal ratios of vapor to liquid volume, to correspond with the indications of the theory of corresponding states, as shown by Pitzer,[17] the results would hardly be altered, since these three liquids have nearly identical liquid volumes, indeed the spread between CCl_4 and the other two would be greater. It was concluded, therefore, that as the size of the central atom increases a certain amount of order is forced, which Halford[3] called "restricted rotation." That this must be the case follows from the relation of molecular dimensions to molal volumes. If the molecules are rotating, the volume swept by one is $4/3\pi R^3$, where R is the M-X distance plus the van der Waals radius, and the volume of 6×10^{23} molecules, close packed, divided by 0.74, gives the minimum volume the substance could occupy if its molecules were freely rotating. The maximum value of R that would permit free rotation in liquid CCl_4, calculated in this way, is 3.08A. This corresponds to an intermolecular distance between carbon atoms of 6.16A and between chlorine atoms of 2.64A. The actual C−C distance found by Bray and Gingrich in liquid CCl_4 from x-ray diffraction

[17] K. S. Pitzer, J. Chem. Phys. **7**, 583 (1939).

TABLE IV.

	C	Si	Ge	Sn	Pb	V	Ti	Zr	Th
Chlorides									
Mol. vol., cc. 25°C	97.1	115.4	114.5	117.6	—	105.8	110.5	—	—
M-X dist., A*	1.76[b]	2.00[b]	2.08[b]	2.30[b]	2.43[a]	2.03[c]	2.18[a]	2.33[a]	2.61[a]
Bromides									
Mol. vol., cc. 25°C		126.5	126.0	130.6			2.31[a]		
M-X dist., A	1.94[a]	2.14[a]	2.29[a]	2.44[a]			2.31[a]		
Iodides									
M-X dist., A	2.15[a]	2.43[a]	2.50[a]	2.64[a]					

* *M-X* distances from (a) M. W. Lister and L. E. Sutton, Trans. Faraday Soc. **37**, 393 (1941); (b) L. O. Brockway, Rev. Mod. Phys. **8**, 231 (1936); (c) N. Lipscomb and A. G. Whittaker, J. Am. Chem. Soc. **67**, 2019 (1945).

is 6.4A,[18] so that there is room in the liquid for free-rotation, confirming the evidence found by Turkevich, Conner, and Smyth.[13a] Such rotation would not be possible, however, if the van der Waals radius of Cl were as large as 1.80A, the value assigned by Pauling,[19] which would require a C−C distance of 7.12A. That value for the chlorine radius is evidently too large for liquid CCl_4, which, it should be remembered, is under an internal pressure of 3000 atmospheres. The shortest intermolecular Cl−Cl distance in solid Cl_2[20] is 2.77A, near enough to the distance given above for a close-packed but rotating structure, 2.64A, to permit the rotation for which we have independent evidence. If, now, 1.32A is assumed as the van der Waals radius of Cl, from the intermolecular distance in solid Cl_2, and added to the *M-X* distance in $SnCl_4$, 2.30A, we obtain 3.62A for *R*, much larger than the value, 3.33A, which would be required for free rotation in liquid $SnCl_4$ at 83°C. This is in accord with the evidence furnished by its excess entropy of vaporization.

The molal volume of SnI_4 is 165 cc at 145°C, from which its maximum radius permitting free rotation would be 3.65A. Subtracting the *M-X* distance, 2.64A, leaves only 1.01 for the van der Waals radius of iodine, much too small compared with the value derived from solid iodine,[20a] which is 1.77A. We see why SnI_4 crystallizes to a non-rotating structure. The intermolecular I−I distance in solid SnI_4, according to Dickinson, is 4.21A. All of this is in accord with the evidence from entropy of vaporization given in the preceding section and is to be taken into account in the formulation of intermolecular forces.

RAMAN FREQUENCIES

There are four principal Raman frequencies for regular tetrahedral molecules, one, denoted by ν_1, is attributed to the "breathing" or vibration along the *M-X* bond, a second, ν_2, is for the bending of the bonds, and is influenced by their stiffness and also by interhalogen repulsions, and the third and fourth are anisotropic vibrations, in which the central atom is displaced, along with the halogen atoms, from its rest position. The first two, in which the central atom remains at rest, are not dependent on its mass and therefore offer a clearer means of comparing the different compounds of the same halogen.

Several investigators have analyzed these frequencies on the basis of various bond models, but let us begin by a simple, inductive approach. Haun and Harkins,[21] who determined the Raman frequencies for $GeCl_4$, plotted them with the frequencies for the chlorides of C, Si, and Sn against the period of the several central atoms in the Periodic System, obtaining a decreasing, broken line. Delwaulle and Francois[22] have plotted these frequencies against the atomic weight of the central atom, getting curves with $TiCl_4$ and $TiBr_4$ falling out of line. These irregularities largely disappear if the *M-X* distance is used as the abscissa, as can be seen in Fig. 2, for in the cases of simple vibrations, ν_1 and ν_2, which are

[18] E. E. Bray and N. S. Gingrich, J. Chem. Phys. **61**, 351 (1943).
[19] L. Pauling, *The Nature of the Chemical Bond* (Cornell University Press., 1944), p. 189.
[20] W. H. Keesom and K. W. Tactonis, Proc. Acad. Sci., Amsterdam, **39**, 314 (1936).
[20a] P. M. Harris, E. Mack, Jr., and F. C. Blake, J. Am. Chem. Soc. **50**, 1583 (1928).
[21] R. R. Haun and Wm. D. Harkins, J. Am. Chem. Soc. **54**, 3917 (1932).
[22] L. Delwaulle and F. Francois, J. phys. radium, **7**, 15, 53 (1946).

independent of the mass of the central atom. It should be remembered that the M-X values are mostly subject to an error of about ± 0.02A. The frequencies are from the compilation by Hertzberg,[23] except for $PbCl_4$, the values for which, $\nu_1 = 327$ cm^{-1} and $\nu_2 = 90$ cm^{-1}, have just been obtained by my colleagues, Professor W. Gwinn and Mr. J. T. Neu at my suggestion, to see whether they would conform to this plot. They will publish the details. The frequency along the bond, ν_1, varies linearly with both chlorides and bromides. The bond bending frequency, ν_2, is concave upward, as might be expected from the increased crowding of the halide atoms as the central atom becomes smaller. Table V compares the interhalogen distances and shows where the strain is greatest.

The regularity shown in Fig. 2 gives but scant basis for assuming that any one of these molecules has an exceptional character. It is noteworthy that Urey and Bradley found that only $TiCl_4$ deviated even to a minor extent from the model they used. A similar result was found by Gordy,[24] using a different model. It would be a little greater using Lister and Sutton's value of M-X, 2.18A instead of the older value he used, 2.21A.

Departures of measured M-X distances from the sum of assigned values of covalent radii have been explained by assuming double bond resonance[25] in the cases of $SiCl_4$, $TiCl_4$, and VCl_4. More recently, however, bond shortening has been more generally explained by an empirical correction taking into account differences in electronegativity.[24] If resonance exists in $SiCl_4$ and $TiCl_4$ it seems to have remarkably little effect on

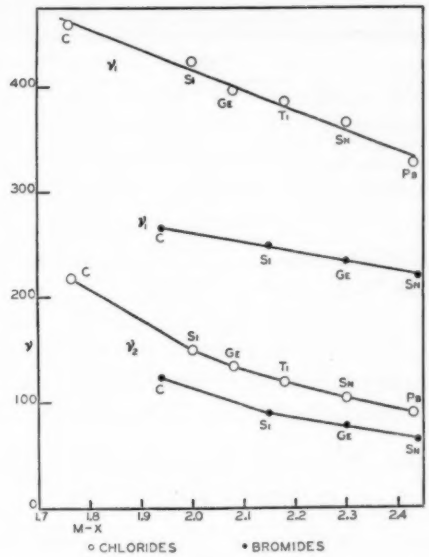

FIG. 2. Isotropic Raman frequencies. Bond stretching, ν_1; bond bending, ν_2.

frequency as correlated in Fig. 2. It has been invoked by Lipscomb and Whittaker to explain the discrepancy between their value for the V—Cl distance, 2.03A, and the value 2.12A reported by Palmer[26] for the same distance in vanadium oxytrichloride. There is, however, another serious discrepancy, that between 2.03A for VCl_4 and 2.18A for $TiCl_4$, a difference too great to accord with the rather close agreement in other properties of VCl_4 and $TiCl_4$ shown in Table VI.

It seems unlikely that the M-X distances in VCl_4, and $TiCl_4$ are seriously affected by different ratios of covalent to ionic binding, since the ionization potentials of V and Ti are nearly identical. Nor is there reason to suppose that the color and paramagnetism of VCl_4 have an appreciable relation to its external field of force.

TABLE V. Interhalogen distances.

	v. d. Waals elements	Tetrahalides C	Si	Ge	Ti	Sn	Zr	Th
Chlorides	2.77[20]	2.89	3.27	3.40	3.57	3.76	3.81	4.27
Bromides	3.30*	3.18	3.53	3.74	3.78	3.99	—	—
Iodides	3.54[20a]	—	3.98	4.09	—	4.32	—	—

* B. Vonnegut and B. E. Warren, J. Am. Chem. Soc. **58**, 2459 (1936).

TABLE VI.

	T_m	T_b	T_b/T_m	Vol., cc., 25°C	M-X, A
VCl_4	251	425	1.69	105.8	2.03
$TiCl_4$	243	410	1.69	110.5	2.18

The apparent association of VCl_4 dissolved in CCl_4, inferred by Simons and Powell[27] from freezing point depression, may be due, instead, to some degree of mutual solubility in the solid

[23] G. Hertzberg, *Infra-Red and Raman Spectra* (D. Van Nostrand Company, Inc., New York, 1945). See also, Kohlrausch, *Ramanspektren* (Becker and Erler, Leipzig, 1943); H. C. Urey and C. A. Bradley, Phys. Rev. **38**, 1969 (1931); J. E. Rosenthall, *ibid* **45**, 538 and 730 (1934), and **49**, 535 (1936).

[24] W. Gordy, J. Chem. Phys. **14**, 305 (1946).

[25] See reference 19, p. 228ff, and reference *c to Table IV.

[26] K. J. Palmer, J. Am. Chem. Soc. **60**, 2360 (1938).

[27] J. H. Simons and M. G. Powell, J. Am. Chem. Soc. **67**, 75 (1945).

TABLE VII. Intermolecular attraction.

	CCl_4	$SiCl_4$	$GeCl_4$	$SnCl_4$	$TiCl_4$	CBr_4	$SiBr_4$	$SnBr_4$	SnI_4
ΔH_{vap} kcal., 298°K	7.83	7.19	8.09	9.55	9.62	—	10.38	—	13.70*
$V\Delta E$ kcal.×liters	7.04	7.62	8.60	10.55	9.98	—	12.40	—	21.65
$V^2(\partial E/\partial V)$ kcal.×liters	7.56	8.23	—	10.95	10.15	—	12.90	15.67	—
aR^3 from $V\Delta E$, relative	221	297	360	532	454		676	—	1860
aR^3 from $V^2(\partial E/\partial V)$	237	321	—	552	462		703	1073	—
$\alpha\times10^{24}$	10.23	11.10	12.12	13.45	14.07	14.06	15.9	18.3	27.8
k/α^2	2.2	2.5	2.5	3.0	2.3		2.7	3.2	2.4

* $T=450$°K.

phase. The situation is evidently one calling for a determination of the electron-diffraction patterns of both substances by the same investigator.

THE STRENGTH OF INTERMOLECULAR ATTRACTION

Hildebrand and Wood[28] derived the formula

$$E_g-E_l=\Delta E_{vap}=\frac{-2\pi N^2}{V}\int W\epsilon r^2dr \qquad (1)$$

for the energy of vaporization of a monatomic liquid of molal volume, V, whose structure is expressed by the radial distribution function, W. N is the Avogadro number, r is the distance from a central molecule and ϵ is the potential energy of a pair of molecules, which is ordinarily expressed by the difference between a repulsive term, oversimplified to j/r^n, where $n\approx9$, and an attractive term, k/r^6, according to the dispersion theory of London, i.e.,

$$\epsilon=j/r^n-k/r^6. \qquad (2)$$

Substituting 2 in 1 gives,

$$E_g-E_l=\Delta E_{vap}$$
$$\frac{-2\pi N^2}{V}\left(j\int\frac{Wdr}{r^{n-2}}-k\int\frac{Wdr}{r^4}\right) \qquad (3)$$

W, and hence the integrals, are not sensitive to small changes in V, so that $V\Delta E_{vap}$ is nearly constant, and we may write

$$V\Delta E_{vap}\approx a\approx V^2(\partial E/\partial V)_T. \qquad (4)$$

The "constant," a, is the familiar van der Waals constant, although it does not necessarily have the same numerical value as the one calculated in the usual way from critical data.

The above formulas are derived for spherical molecules with radial fields of force so that to apply them to the tetrahedral molecules here considered involves a simplification not to be overlooked, but one which is nevertheless enlightening, so we proceed to do it. Westwater, Frantz and Hildebrand[29] and Hildebrand and Carter[30] measured $(\partial p/\partial T)_v$ accurately for a number of tetrahalides, calculated $(\partial E/\partial V)_T$ and showed that $V^2(\partial E/\partial V)_T$ is constant to a high degree over the range studied. Hildebrand[31] compared the two methods of obtaining values of a given in Eq. 4 and found that $V\Delta E_{vap}$ is several percent larger than $V^2(\partial E/\partial V)$, as shown here in Table III. The values of ΔE are based upon the heats of vaporization in the summary by Kelley.[32] This accords with the fact that W is not strictly constant, but is a function of volume. We have no analytical expression for this variation and must be content with a consideration of the qualitative effect. Representing the repulsive and attractive integrals of Eq. 3 by I_r and I_a, respectively, we can write,

$$V^2\left(\frac{\partial E}{\partial V}\right)-V\Delta E_{vap}=2\pi N^2\left[j\frac{\partial I_r}{\partial \ln V}-k\frac{\partial I_a}{\partial \ln V}\right]. \qquad (5)$$

When the liquid is moderately expanded, the attraction is balanced in large part by thermal agitation rather than by repulsion, hence the k-term is larger than the j-term, but $(\partial I_a/\partial \ln V)$ is negative, hence the left hand member of Eq. 5 is positive, in accord with the data in Table VII.

Let us make, next, an approximate evaluation of the attraction constant, k, for certain of these

[28] J. H. Hildebrand and S. E. Wood, J. Chem. Phys. **1**, 12 (1933).

[29] W. Westwater, A. W. Frantz, and J. H. Hildebrand, Phys. Rev. **31**, 135 (1928).

[30] J. H. Hildebrand and J. M. Carter, J. Am. Chem. Soc. **54**, 3592 (1932).

[31] J. H. Hildebrand, Phys. Rev. **34**, 984 (1929).

[32] K. K. Kelley, Bull. U. S. Bur. Mines **383**, (1934).

substances. Let us apply the evidence found by Campbell and Hildebrand[33] that the form of the distribution function, W, depends only on the degree of expansion of the liquid, and should therefore be the same for different liquids if expressed as a function not of r but of $\rho=r/R$, where R is some fixed parameter such as the van der Waals' radius in the case of a spherical molecule. Substituting ρR for r in Eq. 3 and taking $n=9$, a reasonable value, and combining with Eq. 4 gives

$$a=\frac{2\pi N^2 k}{R^3}\int\frac{W d\rho}{\rho^4}-\frac{2\pi N^2 j}{R^6}\int\frac{W d\rho}{\rho^7}. \qquad (6)$$

The integral is assumed to be nearly the same for any pair of liquids and exactly the same under the same degree of expansion, when, accordingly, $k\propto aR^3$, if we neglect the comparatively small repulsive term. For comparable values of R we may use the M-X distances plus the van der Waals halogen radii, given previously from the solid halogens. These values of R are included in Table VII, also aR^3, in arbitrary units, since we are able to obtain only relative values. These values, which are roughly proportional to the attraction constant, k, are plotted against M-X in Fig. 3. The smooth increase justifies the conclusion that the attraction constant for like pairs increases regularly. This would not be the case if the chloride atoms were at the same time the main centers of attraction and in the same electronic state from the standpoint of the London forces. Indeed, if these molecules were freely rotating and their chlorine atoms were equal as centers of attraction, then k should decrease with increasing size due to decreasing average density of chlorine atoms on the surface of the sphere. That the attraction constant increases indicates that the character of each particular bond with the central atom strongly affects the magnitude of the intermolecular force, due either to the bond being more exposed, more ionic, or both.

According to London,[34] the attractive potential between a pair of molecules is

$$\epsilon=-3h\nu_0\alpha^2/4r^6, \qquad (7)$$

where α is the polarizability and $h\nu_0$ the internal zero-point energy, which is approximately given by the ionization potential. We do not know this last for the molecules under consideration, but it is worth noting that our approximate k is roughly proportional to α^2, as shown by the ratios in the last row of Table VII, and by the positions of the crosses in Fig. 3. The connection between polarizability, molecular field strength and bond type was set forth many years ago by Fajans and Joos,[35] who showed that the refraction of Cl^-, and therefore its state, differs in different compounds. In general, the stronger the field of the central atom the tighter the electronic shell of the halide atom. And Fajans,[36] in discussing the difference between AlF_3 and SiF_4, stated that it is due in part to the greater screening of the Si^{+4} but in part, also, to its larger deforming effect upon the F^-, by reason of its small size and greater charge. This deformation is to be regarded as equivalent to the introduction of partially covalent character into the bond.

Figure 3 shows $SiCl_4$ falling in line with the higher chlorides, a fact which, like the Raman frequencies previously cited, argues against the assumption of a double bond resonance peculiar to this molecule. The only members of these series which call for special explanation are CCl_4 and CBr_4. They differ from the others in having less ionic bond character and in the compression of their halide atoms indicated in Table V, but it

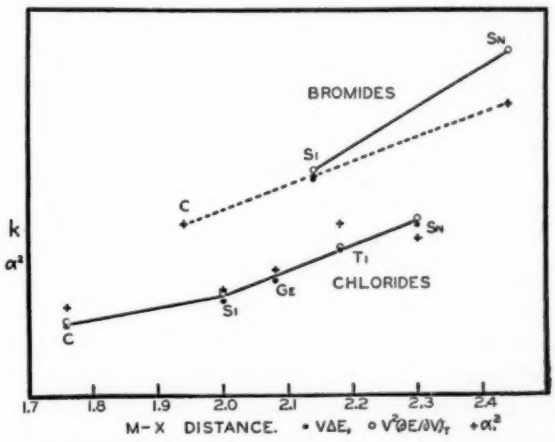

FIG. 3. Variation of intermolecular-attraction constant, k, and polarizability, α (relative scales), with M-X distance.

[33] J. A. Campbell and J. H. Hildebrand, J. Chem. Phys. 11, 334 (1943).
[34] F. London, Trans. Faraday Soc. **338**, (1937).
[35] K. Fajans and G. Joos, Zeits. f. Physik **23**, 27 (1924).
[36] K. Fajans, Zeits. f. Elektrochemie **34**, 443 (1928).

TABLE VIII. Expansion on mixing; percent at 50 mole percent ($t=35°$ for $SnBr_4$ solutions, 25° for all others).

	CCl_4	$SiCl_4$	$TiCl_4$	$SnCl_4$	$SiBr_4$	$SnBr_4$
M-X dist. ÷halide radius	0.97	1.11	1.21	1.28	1.10	1.36
CCl_4	—	0.014	0.083	.408	0.184	0.221
$SnBr_4$		0.111			0.093	

is not clear why either of these factors should increase polarizability and intermolecular potential.

TETRAHALIDE SOLUTIONS

One of the most carefully investigated solutions of a pair of tetrahalides is CCl_4 with $SiCl_4$, whose vapor pressures were measured by Wood[37] and heats of mixing by Vold,[38] both in this laboratory.

The internal pressures of the two components, $\Delta E_{vap}/V$, computed by aid of the careful calculations of heats of vaporization from the vapor pressures, by Vold, are 73.7 cals./cc for CCl_4 and 56.8 cals./cc for $SiCl_4$. The equation derived by Hildebrand and Wood[27] for the partial molal energy of transfer of component 2 from pure liquid to a regular solution—one in which the thermal agitation is able to maintain random mixing—is

$$\bar{E}_2 - E_2^0 = \phi_1^2 V_2 D^2 \qquad (8)$$

where ϕ_1, is the volume fraction of component 1, V_2 the molal volume of component 2, and $D^2=[(\Delta E_1/V_1)^{\frac{1}{2}}-(\Delta E_2/V_2)^{\frac{1}{2}}]^2$. The value of D from the figures given above is 1.05. Vold measured the heat of mixing the components in five mole fractions of $SiCl_4$ ranging from 0.18 to 0.86 and found a mean value of D of 1.12, a most gratifying agreement. The maximum heat of evolved per mole of mixture was 32.3 cals., while the value calculated from the equation and $D=1.05$ is 28.0 cals.

The partial vapor pressures of these solutions, measured by Wood, show small deviations from Raoult's law in the same direction, with a maximum value of the free energy of mixing over that calculated for an ideal solution of 28.3 cals./mole. The measurements deviate among themselves as much as they do from the calculated values. They correspond to a mean value of $D=0.84$, but the difference between this and 1.05 is hardly greater than the experimental error. We may conclude that this system is regular according to the theory and indicates no marked departure in the attraction constant of the unlike molecules from the geometrical mean of the attraction constants of the like molecules; an assumption implicit in Eq. 8. It is gratifying that a treatment based upon spherical symmetry of the molecules applies as well as this to a solution of tetrahedral molecules. The agreement becomes less satisfactory when two species are chosen whose molecules have markedly different shapes.

Boiling point and freezing point curves for the binary solutions of $TiCl_4$ with CCl_4, $SiCl_4$ and $SnCl_4$ were obtained by Nasu.[39] The boiling point curves are hardly precise enough to permit calculating the rather small deviations from Raoult's law, but these are clearly greatest with $SiCl_4$ and least with $SnCl_4$, in accord with the order of internal pressures. The freezing point curve of $TiCl_4$ from $SnCl_4$ shows the separation of solid solutions, and is therefore useless for our purpose. The points for $TiCl_4$ from solutions in CCl_4 fall closely upon the Raoult's law line calculated from Latimer's[40] figure 2235 cal., for its molal heat of fusion, in harmony with the almost identical internal pressures of these components, $\Delta E/V$ is 81.7 cal./cc for $TiCl_4$ and 73.6 cal./cc for CCl_4 at 25°. These values, extrapolated to the low temperatures of the measurements would still be close together.

Nasu's freezing points of $TiCl_4$ from solutions with $SiCl_4$ deviate from the Raoult's law line approximately to the rather small extent demanded by the difference between their internal pressures, but the various uncertainties in the essential data at these low temperatures are sufficient to prevent any significant conclusion being drawn from the minor departures from the simple theory for regular solutions.

The solutions of $SiCl_4$ with SnI_4, investigated by Hildebrand and Negishi[41] accord with the great difference in their internal pressures in giving incompletely miscible liquids. The great difference between the liquid ranges of these two substances requires some extrapolation in order

[37] S. E. Wood, J. Am. Chem. Soc. **59**, 1510 (1937).
[38] R. D. Vold, *ibid.* **59**, 1515 (1937).
[39] N. Nasu, Sci. Rep. Tohoku Imp. Univ., 1st. Ser. **22**, 972 (1933).
[40] W. M. Latimer, J. Am. Chem. Soc. **44**, 90 (1922).
[41] J. H. Hildebrand and G. R. Negishi, J. Am. Chem. Soc. **59**, 339 (1937).

to apply the formula for simple regular solutions based upon Eq. 8, which is

$$4.575T \log(x_2^i/x_2) = \phi_1^2 V_2 D^2, \qquad (9)$$

where x_2 is the mole fraction of component 2, here SnI_4, x_2^i its mole fraction in an ideal solution. At the boiling point of $SiCl_4$, 59°C, its ΔE is 6180 cal. and its V is 122.0, giving $(\Delta E_1/V_1)^{\frac{1}{2}} = 7.12$. From the solubility data cited, $D = 3.68$ at this temperature, and therefore $(\Delta E_2/V_2)^{\frac{1}{2}} = 7.12 + 3.68 = 10.80$ for SnI_4. If the formula of Kelley[32] is used to compute the heat of vaporization of liquid SnI_4 at this temperature, one obtains $\Delta E = 18{,}360$ cal. and since $V_2 = 155.2$ cc, extrapolated for the liquid, $(\Delta E_2/V_2)^{\frac{1}{2}}$ would be 10.88. The close agreement with the above figure from solubility is doubtless fortuitous, in view of the assumptions involved, but it indicates, at least, that the internal pressures as calculated are adequate to account for the solubility relations found, without additional assumptions regarding the nature of the particular species.

Although the assumption of radial force fields involved in the formal treatment of the foregoing solutions appears to be about as adequate as one has any right to expect, it is my belief nevertheless that this is the fortunate result of the similar structures of these molecules, and that it would be theoretically preferable, although practically not worth the effort, to consider the atoms as the centers of the fields of force. The evidence for this comes from the entropy of vaporization of a pair of liquids whose molecules are very different in size but otherwise very similar specifically Cl_2 and CCl_4, and again, C_2H_6 and di-isopropyl.[42] The entropy depends more upon the separation of the peripheral atoms than of the molecular centers.

VOLUME CHANGES ON MIXING

Hildebrand and Carter[30] determined the changes in volume on mixing the tetrahalides shown in Table VIII. These were found, in all cases, to be remarkably small, the largest being only 0.4 percent. It can be seen, also, by aid of the ratios of M-X distance to van der Waals halide radius, that the expansions are roughly parallel to this ratio rather than to M-X distance alone. One may infer that the effect is due mainly to the geometry of the molecules, although influenced, probably, by difference in bond character, internal pressure, and degree of expansion.

[42] J. H. Hildebrand, and T. S. Gilman, J. Chem. Phys. 15, 229 (1947).

CONCLUSIONS

The various lines of evidence surveyed in the foregoing pages seem to justify the following answers to the questions asked at the outset together with several additional inferences.

1. In the case of CCl_4 and CBr_4 the evidence is in favor of a degree of rotational energy sufficient to overcome the barrier of van der Waals repulsion between the halide atoms. This rotation becomes increasingly hindered, however, in passing to the compounds with larger central atoms and rotation must increasingly give way to oscillation. In spite of this restriction, however, the thermodynamic properties of tetrahalide solutions can be calculated with an accuracy sufficient for many purposes by means of equations derived for liquids composed of spherical molecules.

2. These equations, of course, assume that the field of force is central to the molecules, not to the peripheral atoms of polyatomic molecules. Although certain evidence favors the latter assumption, the far more complicated treatment that would be required does not seem ordinarily to be worth while. The halide atoms do not constitute centers of attraction at all uniform, but are greatly dependent upon the character of the central atom.

3. Intermolecular attraction between different species having the same halide atoms does not seem to depend noticeably upon the kind of bonding orbitals of the central atom, for $TiCl_4$ falls in line with $GeCl_4$ and $SnCl_4$ while $HfCl_4$ and $ZrCl_4$ do not. The attraction is strongly influenced by the degree of ionic character of the bond, increasing with the size and electropositive character of the central atom. A large radius ratio of central atom to halide atom permits coordination higher than four and greatly enhanced intermolecular force, as illustrated by comparing SnF_4 with $SnCl_4$. Attractive forces increase in the order chlorides, bromides, iodides, due to the increase in the number and polarizability of the halide electrons.

4. The apparent anomaly of the low boiling point and internal pressure of $SiCl_4$ is due only

to the considerable increase in molal volume between CCl_4 and $SiCl_4$; although the attraction is less, the attraction constant is greater, increasing almost linearly with molecular dimensions in the order CCl_4, $SiCl_4$, $GeCl_4$, $TiCl_4$, $SnCl_4$. None of the properties herein examined, including Raman frequencies, indicates any exceptional character for $SiCl_4$, such as the double-bond resonance that others have assumed to account for the somewhat short M-X distance.

5. The only members of these series that appear to call for any unique explanation are CCl_4 and CBr_4, which have (a) high melting points and low entropies of fusion, which seem to be connected with crystal structure; (b) high boiling points, which require a totally different explanation; (c) slightly high Raman frequencies, which may be ascribed to interhalogen repulsions and covalent bonds; and (d) attraction constants and polarizabilities slightly in excess of the linear relationship to molecular dimensions exhibited by the higher members of the series.

It seems appropriate, in conclusion, to call attention to certain gaps in the experimental data for these important substances which should by all means be filled. They include crystal structures of the solids, densities and expansivities of the solids, heat capacities and heats of fusion, a redetermination of the M-X distance for $TiCl_4$ and VCl_4 by the same investigator; Raman spectrum of VCl_4; additional accurate mutual solubility data; vapor pressures for $SnBr_4$ and nearly every thermodynamic property for the fluorides.

THE JOURNAL OF CHEMICAL PHYSICS VOLUME 15, NUMBER 10 OCTOBER, 1947

Note on a Form of the Secular Equation for Molecular Vibrations

E. BRIGHT WILSON, JR.
Mallinckrodt Chemical Laboratory, Harvard University, Cambridge, Massachusetts

(Received July 21, 1947)

By starting with the Hamiltonian form of the equations of motion, the problem of the small vibrations of a polyatomic molecule can be solved with the aid of a secular equation twice the usual size. This equation, however, is readily adapted to solution by electrical circuits and has the important advantage of having as elements the force constants and inverse kinetic energy coefficients ("G" matrix elements) directly. The force constant matrix elements occupy one off-diagonal corner of the secular equation, the G matrix elements are in the other off-diagonal corner, the circular frequencies ($2\pi\nu$) appear on the principal diagonal, and all other elements are zero.

THE problem of small amplitude vibrations of the atoms of a polyatomic molecule has been extensively treated.[1] Its solution, as is well known, involves some type of determinantal or secular equation, which can assume many forms. It is the purpose of this note to point out the useful properties of one of the lesser known forms.

Consider that a set of "internal" coordinates has been selected, such as $3N-6$ independent interatomic distances and valence angles, where N is the number of atoms. Let R_i be the deviation of the ith coordinate from its equilibrium value. Then the potential energy V of the molecule can be expressed in the form

$$2V=\sum_{ij} F_{ij}R_iR_j, \tag{1}$$

if the zero of energy is properly chosen and if higher order terms (anharmonic terms) are neglected. The constants F_{ij} are the force constants.

The kinetic energy can be expressed in terms of the velocities $\dot{R}_i$ or in terms of the momenta P_i, conjugate to the coordinates R_i. Let the kinetic energy T be written as

$$2T=\sum_{ij} G_{ij}P_iP_j, \tag{2}$$

where the G_{ij} are coefficients involving the masses of the atoms and the geometry of the molecule and are constants to the approximation ordi-

[1] G. Herzberg, *Infrared and Raman Spectra of Polyatomic Molecules* (D. Van Nostrand Company, New York, 1945).

narily used. Simple vectorial rules have been formulated for calculating these coefficients,[2] or they can be tabulated for various types of pairs of internal coordinates.[3]

The equations of motion in Hamiltonian form are

$$\dot{R}_i = \partial H/\partial P_i = \sum_j G_{ij} P_j, \tag{3}$$

and

$$\dot{P}_i = -\partial H/\partial R_i = -\sum_j F_{ij} R_j, \tag{4}$$

since $H = T + V$ for this system.

As a solution of these equations, try

$$R_j = A_j \cos(2\pi\nu t + \epsilon), \tag{5}$$

and

$$P_j = B_j \sin(2\pi\nu t + \epsilon), \tag{6}$$

where ν is the frequency of vibration, t the time, and ϵ an arbitrary phase constant. These expressions lead to the following equations which must be satisfied by the amplitudes A_j and B_j:

$$\begin{aligned} &2\pi\nu A_i + \sum_j G_{ij} B_j = 0, \quad i = 1, 2, \cdots, 3N-6, \\ &\sum_j F_{ij} A_j + 2\pi\nu B_i = 0, \quad i = 1, 2, \cdots, 3N-6. \end{aligned} \tag{7}$$

This set of $2n = 2(3N-6)$ equations for the $2n$ unknown amplitudes A_i and B_i, has solutions differing from zero only if the determinantal or secular equation formed from its coefficients is satisfied; i.e., only if (with $\omega = 2\pi\nu$)

$$\begin{vmatrix} \omega & 0 & 0 & \cdots & G_{11} & G_{12} & G_{13} \\ 0 & \omega & 0 & \cdots & G_{21} & G_{22} & G_{23} \\ 0 & 0 & \omega & \cdots & G_{31} & G_{32} & G_{33} \\ \cdot & \cdot & \cdot & \cdot & \cdot & \cdot & \cdot \\ F_{11} & F_{12} & F_{13} & \cdots & \omega & 0 & 0 \\ F_{21} & F_{22} & F_{23} & \cdots & 0 & \omega & 0 \\ F_{31} & F_{32} & F_{33} & \cdots & 0 & 0 & \omega \end{vmatrix} = 0. \tag{8}$$

This is the form of the secular equation in question. It has certain important properties. *First:* it is twice as large as the usual forms. This is a drawback but not as serious as might be supposed. *Second:* it involves $\omega = 2\pi\nu$ instead of $\lambda = 4\pi^2\nu^2$ as is usual. *Third:* the roots come in pairs, positive and negative; i.e., if $+\omega$ is a root so is $-\omega$. This accounts for the extra n roots required by its double size. *Fourth:* it is unsymmetrical with respect to the principal diagonal. *Fifth:* it has nothing in the principal diagonal except the unknowns ω. *Sixth:* its off-diagonal elements are the force constants F_{ij} and the coefficients G_{ij} directly.

It is the last property which makes this form of the secular equation of interest in molecular vibrational problems. In all other forms of the secular equation it is necessary to carry out some algebraic manipulation on the force constants or the G_{ij}'s before obtaining the elements of the final equation. In this form the Fs and Gs occur directly.

This advantage is particularly profitable when a machine is used to solve the secular equation. For example it is possible to make obvious modifications of the direct-current resistance network computer described by Frost and Tamres[4] for the solution of this type of equation. With this device the coefficients G_{ij} and also the force constants F_{ij} are set directly on dials of the machine so that trial of different force constants, for example, can be carried out by resetting the appropriate dial and determining the new roots.

The double size of the equation is not as objectionable as might be suspected since each row contains only $n+1$ elements because of the $n-1$ zeros. Therefore there are no more resistances required than in Frost and Tamres' general design for n rows. The switching and wiring is somewhat more complicated but not seriously so. In use, it will require more time to find each root because the method of successive approximations increases in difficulty as the number of rows increases.

Unfortunately the form of Eq. (8) precludes the use of the inductance-capacity network type of machine,[5,6] which will not handle unsymmetrical equations.

Naturally, if the molecule has any symmetry, internal symmetry coordinates[1] would be used instead of internal coordinates in setting up the equations, so that one factor of the secular equation at a time would be placed on the machine. This form of the secular equation could be used with other types of coordinates, such as

[2] E. Bright Wilson, Jr., J. Chem. Phys. **9**, 76 (1941).

[3] For example, all the coefficients occurring in substituted methanes and ethanes have been tabulated by J. C. Decius, *Thesis* 1947, Harvard University.

[4] A. A. Frost and M. Tamres, J. Chem. Phys. **15**, 383 (1947).

[5] G. Kron, J. Chem. Phys. **14**, 19 (1946); G. K. Carter and G. Kron, J. Chem. Phys. **14**, 32 (1946).

[6] R. H. Hughes and E. B. Wilson, Jr., Rev. Sci. Inst. **18**, 103 (1947).

Cartesians, but would then probably be inferior to the usual forms in convenience.

The amplitudes A_j of Eq. (5), when properly normalized, provide the coefficients in the transformation from normal coordinates Q_k to internal coordinates R_j. The coefficients B_j of Eq. (6), on the other hand, are related to the coefficients of the inverse transformation from R_js to Q_ks. To see this, let

$$R=LQ \tag{9}$$

in matrix notation, where L is the matrix of the coefficients of the transformation from Q_ks to R_js. Q and R are the appropriate column matrices. Then it has been shown that[2]

$$G=LL', \tag{10}$$

where G is the matrix of the elements G_{ij} and the prime denotes the transpose. Consequently,

$$L^{-1}=L'G^{-1}. \tag{11}$$

But $L=AK$ where A is the matrix $\|A_{jk}\|$ of the amplitudes in Eq. (5), the subscript k labelling the normal mode involved. K is a diagonal matrix which is used to normalize the coefficients. Therefore,

$$L^{-1}=KA'G^{-1}. \tag{12}$$

But from Eq. (7) one sees that

$$-A\omega=GB, \tag{13}$$

where ω is the diagonal matrix with diagonal elements ω_k. Consequently, since $G'=G$,

$$B'=-\omega A'G^{-1}=-\omega K^{-1}L^{-1}, \tag{14}$$

or

$$L^{-1}=-K\omega^{-1}B', \tag{15}$$

so that, except for the normalization factor $(-K\omega^{-1})$, the coefficients B_{jk} provide the elements of L^{-1} as stated above. To determine K, one may use*

$$L'FL=\Lambda=KA'FAK, \tag{16}$$

where F is $\|F_{ij}\|$ and Λ is the diagonal matrix with diagonal elements $4\pi^2\nu_k^2=\omega_k^2$. This equation arises because the normal coordinates, by definition, diagonalize the potential energy.[2] Thus, from Eq. (16),

$$K_k=\omega_k/(\textstyle\sum_{ij} F_{ij}A_{ik}A_{jk})^{\frac{1}{2}}, \tag{17}$$

so that

$$L_{jk}=A_{jk}\omega_k/(\textstyle\sum_{il} F_{il}A_{ik}A_{lk})^{\frac{1}{2}}, \tag{18}$$

and

$$L_{kj}^{-1}=-B_{jk}/(\textstyle\sum_{il} F_{il}A_{ik}A_{lk})^{\frac{1}{2}}. \tag{19}$$

APPENDIX

A simple proof of the equivalence of this form of the secular equation and other more usual forms follows. Consider

$$\begin{vmatrix} \omega E & G \\ F & \omega E \end{vmatrix}=0, \tag{20}$$

which is a symbolic way of writing Eq. (8), F and G here representing the corresponding sets of coefficients. E represents the n-by-n unit matrix. If a given value of ω satisfies this equation, it will also satisfy the equation

$$\begin{vmatrix} \omega E & -G \\ -F & \omega E \end{vmatrix}=0. \tag{21}$$

Multiplication of these two equations by the rule for multiplication of determinants (which is the same as the rule for matrix multiplication) gives

$$\begin{vmatrix} \omega^2E-GF & 0 \\ 0 & \omega^2E-FG \end{vmatrix}=0, \tag{22}$$

or

$$|GF-\omega^2E|=0 \quad \text{or} \quad |FG-\omega^2E|=0. \tag{23}$$

These are two equivalent and previously known[7] forms of the secular equation.

---

* This procedure for normalization was pointed out to me by Dr. R. S. Rasmussen, Shell Development Company, Emeryville, California.

[7] E. B. Wilson, Jr., J. Chem. Phys. **7**, 1047 (1939); also, M. A. Eliashevich, Comptes rendus U.R.S.S. **28**, 604 (1940).

THE JOURNAL OF CHEMICAL PHYSICS VOLUME 15, NUMBER 10 OCTOBER, 1947

Simple Potential Functions for HF and $[F-H\cdot\cdot F]^-$.

MANSEL DAVIES
The Department of Biomolecular Structure, The University, Leeds, England
(Received May 20, 1947)

Calculations based on an electrostatic model have been made of the stabilizing energy in $[F-H\cdot\cdot F]^-$. The terms used have first been tested on the HF molecule and the distortion of the latter in the bifluoride ion is estimated. The calculated value of $-\Delta U$ for $[F-H\cdot\cdot F]^-$ is 47.3 kcal. per g ion, in satisfactory accord with thermochemical estimates.

INTRODUCTION

THE purpose of the present calculations was to provide an acceptable theoretical estimate of the binding energy in the hydrogen bifluoride ion, i.e., $-\Delta U_{gas}$ at 0°K for the reaction $HF+F^-=[F-H\cdots F]^-$. This ion has long been recognized as one of the most stable structures resulting from the phenomenon of "hydrogen bonding." In the numerous discussions of the interaction covered by that term it has frequently been assumed that protonic resonance, arising from the existence of alternative potential minima between the bonded atoms or ions, played an important part. This factor was the more likely to be significant in the case of $[F-H\cdot\cdot F]^-$ owing to its simple, partially ionic structure and the closeness of approach of the two fluorines. X-ray crystal studies[1] give their distance apart as 2.26A: this figure differs from twice the normal H−F distance by less than 25 percent.

However, the infra-red absorption spectra of MHF_2 salts[2] have shown that the contribution of protonic resonance to the interaction energy is of almost negligible proportions. While the analyses of the observed frequencies[2b, 2d] differ greatly, they both agree in assigning a small value to the resonance splitting term. Ketelaar's treatment, which is based on far the more extensive data, gives an observed splitting in the "hydrogen vibration" frequency, $(\nu_3)0\rightarrow1$, of 228 cm^{-1}: Glockler and Evans give 111 cm^{-1} for this term. The former, and larger, value corresponds to a resonance stabilization energy of only 0.04 kcal per g ion in the ground state. While this conclusion agrees with the accumulating evidence on the general physical nature of the "hydrogen bond" interaction,[3] it is important to find whether simple electrostatic forces are sufficient to account for the pronounced stability of the $[F-H\cdot\cdot F]^-$ ion.

As the only structural factor known with certainty for the $[F-H\cdots F]^-$ ion is the 2.26A separation of the fluorines, it seemed advisable to test the mode of calculation in the much better documented case of the HF molecule.

THE HF MOLECULE

The bonding in the hydrogen halides has been treated quantitatively on a number of occasions. A very thorough calculation on a quantum mechanical basis was made by Kirkwood:[4] this provided theoretical estimates of the nuclear separation, dipole moment, dissociation energy, and bond frequency in good agreement with experimental values. The calculation was fully applied only to the case of hydrogen chloride. Born and Heisenberg[5] provided an early electrostatic approach: considering only the charge interaction and the polarizability of the halide ion in the field of the proton, the energy can be written in its simplest form:

$$U=-e^2/r-e^2\cdot\alpha_{eff}/2r^4+\beta e^2/r^n.$$

e = the charge on the atoms: α_{eff} = the effective polarizability of the halide ion: the constant β of the repulsive term is found from the condition $(du/dr)_{r=r_{equilibrium}}=0$. The exponent was

[1] L. Holmholz and M. T. Rogers, J. Am. Chem. Soc. 61, 2590 (1939).
[2] (a) J. A. A. Ketelaar, J. Chem. Phys. 9, 775 (1941); (b) J. A. A. Ketelaar, Rec. trav. chim. des Pays-Bas 60, 523 (1941); (c) A. M. Buswell, R. L. Maycock, and W. H. Rodebush, J. Chem. Phys. 8, 362 (1940); (d) G. Glockler and G. E. Evans, J. Chem. Phys. 10, 607 (1942).
[3] Ann. Reports Chem. Soc. (London) 43 (1946).
[4] J. G. Kirkwood, Physik. Zeits. 33, 259 (1932).
[5] M. Born and W. Heisenberg, Zeits. f. Physik 23, 388 (1924).

TABLE I

	μ in D	ν in cm^{-1}	$U_{(HF\rightarrow H^+ + F^-)}$ kcal./g mole	$U_{(HF\rightarrow H+F)}$ kcal./g mole
Experimental:	1.91	4141	365	153
Born and Heisenberg:	2.03	5180	335*	
Briegleb:	1.98	7000	352	
Present values:	1.91	4141		136

* From their equation (24).

taken by Born and Heisenberg as $n=5$: this is almost certainly too low a value for a single-term approximation, although it is also clear that $n=12$, the figure usually favored for the alkali halide ions will be too high in the present instance. With Briegleb[6] we take $n=7$.

Previous calculations[5,6] have taken $e=\epsilon=$electronic charge$=4.80\times10^{-10}$ e.s.u. As the conditions at equilibrium will depart appreciably from those of an ion-pair,[7] a closer approach to the actual conditions can be attained by taking

$$\mu_{\text{observed}}=er(1-\alpha_{\text{eff}}/r^3)$$

to determine e and using $\mu_{\text{obs}}=1.91D=1.91\times10^{-18}$ e.s.u.[8] and $r=0.92$A.[9] The physical picture involved is thus of electrostatic binding between two particles, the sum of whose effective polarizabilities is α_{eff}.

A further relation is now required to determine α_{eff}. This is provided by $(d^2u/dr^2)=m\times(2\pi\nu)^2$, where ν is the HF vibrational frequency (sec.$^{-1}$) for infinitesimal amplitudes, and m is the molecular reduced mass, i.e., $m_{\text{H}}\cdot m_{\text{F}}/(m_{\text{H}}+m_{\text{F}})$. We take $\nu=4141\times3\times10^{10}$ sec.$^{-1}$.[9] The following values are then evaluated: $e=3.07\times10^{-10}$ e.s.u.: $\alpha_{\text{eff}}=0.247\times10^{-24}$ cc: $\beta=0.138\times10^{-48}$. By definition these figures give the correct values for the observed dipole moment and equilibrium frequency, while the dissociation energy, i.e., $(-U)_{r=r_{\text{equilibrium}}}$ is calculated as 9.49×10^{-12} erg per molecule, i.e., 136 kcal. per g mole. The thermochemical estimate of this factor for HF is 153 kcal. per g mole.[10] This energy is, of course, for the dissociation into (H+F) atoms, as corresponds to the ground state potential curve for HF. It is interesting to note that e/ϵ appears to be 0.64; or writing $\mu_{\text{obs}}=er+\mu_{\text{induced}}=er\times(1-0.321)$. The values quoted[5,6] for α_{F^-} and α_{HF} are near 1.0×10^{-24} and 0.9×10^{-24}, respectively. It is to be expected that α_{eff} should be appreciably less than these figures.

A comparison of the relevant factors deducible in the other cases mentioned is given in Table I. Briegleb's value of α_{eff}, (0.43×10^{-24}) was apparently chosen arbitrarily: he would have obtained significantly better agreement (with the experimental values) in the first and third columns by taking $\alpha_{\text{eff}}=0.44\times10^{-24}$ cc. Notably poorer agreement would be found in the last two rows of the table if an exponent $n=12$ had been used for the repulsive term.*

THE DISTORTION OF F−H IN $[F-H\cdot\cdot F]^-$

Before evaluating the electrostatic energy stabilizing $[F-H\cdot\cdot F]^-$, it is advisable to make an estimate of the distortion both in the internuclear separation and the charge distribution brought about in the F−H molecule by the proximity of the F^- ion. Within the scope of the present treatment the following appears to be a reasonable procedure: we start with a normal F−H molecule and assume an initial net charge distribution corresponding to $\mu_{\text{obs}}=1.91D$: i.e., $e_1=1.91/0.92=2.08\times10^{-10}$ e.s.u. With $d_{F\cdot\cdot F}=2.26$A, and the F−H bond stretched to a total of xA, the F^- ion will induce an additional moment in F−H of value $\mu_{\text{induced}}=\alpha_{\text{eff}}\times\epsilon/(2.26-x/2)^2$. This will give a final charge $e_1=(2.08+\mu_{\text{induced}}/x)\times10^{-10}$ e.s.u. The polarizability of FH in weak external fields is $\alpha_{\text{HF}}=0.9\times10^{-24}$: an effective internal value was deduced above as $\alpha_{\text{eff}}=0.247\times10^{-24}$. For the present circumstances an intermediate value seems most appropriate and $\alpha_{\text{eff}}=0.40\times10^{-24}$ has been used here.

Neglecting the polarization of the F^- ion, the expansive force on F−H may be written as

$$\epsilon e_1[1/(2.26-x)^2+1/(2.26)^2]\times10^{16}.$$

The contractive force leading to equilibrium with this can be taken as consisting of two terms: the first arising from the normal restoring force

[6] G. Briegleb, Zeits. f. physik. Chemie **B51**, 9 (1941).
[7] L. Pauling, J. Am. Chem. Soc. **54**, 998 (1932).
[8] C. P. Smyth and N. B. Hannay, J. Am. Chem. Soc. **68**, 171 (1946)
[9] G. Herzberg, *Molecular Spectra and Molecular Structure* (Prentice-Hall Inc., New York, 1939), Vol. I.
[10] F. R. Bichowsky and F. D. Rossini, *The Thermochemistry of Chemical Substances* (Reinhold, New York, 1936).

* For the present calculations exact agreement with all the tabulated factors, including $U_{\text{equilibrium}}$, is given by a value $n=6.3$.

operative in the F—H vibration, i.e., $k(x-0.92) = 9.59\cdot(x-0.92)\times10^{-3}$ dyne; the second, a repulsive force of the same form as that in F—H itself but acting now between the H and F⁻ centers, i.e., a force $7\beta^1 e_1\epsilon/(2.26-x)^8$. Using the value found below, i.e., $\beta^1=0.830\times10^{-48}$, simple trial quickly shows that these forces are balanced at $x=0.95$A. Some estimate of the uncertainty in this figure can be got from the value $x=1.01$A which is found if $\beta^1=0.138\times10^{-48}$ (see preceding section). The former is considered the better estimate and is used here if only on the ground of consistency, as the lower value of β^1 is not found to be applicable to the interaction in [F—H··F]⁻.

THE ENERGY OF INTERACTION IN [F—H··F]⁻

In continuing the electrostatic calculations to give the energy involved in forming [F—H··F]⁻, it is necessary to make clear the charge distribution assumed. The fluoride ion is assumed to retain its electronic charge: the F—H molecule is taken to behave towards the external field as a dipole of the value $\mu_{obs}=1.91D$, having the polarizability $\alpha_{eff}=0.40\times10^{-24}$. In the field of the F⁻ ion the conditions just evaluated are attained, i.e., charges of $e_1=2.70\times10^{-10}$ e.s.u. on F and H which are now separated by 0.95A.

The energy of interaction between the ion and the F—H dipole (including the moment induced by the former) is thus

$$-\epsilon e_1/r+\epsilon e_1/(r+0.95),$$

where rA = the separation of the hydrogen from the fluoride ion. The moment induced in the latter by the field of the dipole can likewise be written

$$e_1\alpha_F\left[\frac{1}{r^2}-\frac{1}{(r+0.95)^2}\right],$$

and as the interaction energy of two dipoles in line is $-2\mu_1\mu_2/d^3$, where d is the separation of their centers, this term gives an energy

$$-2\mu_1\cdot e_1\cdot\alpha_F\left[\frac{1}{r^2}-\frac{1}{(r+0.95)^2}\right]\Big/(r+0.475)^3.$$

Here $\mu_1=2.70\times0.95\times10^{-18}$ e.s.u. Finally, there is the repulsive energy $+\beta^1 e_1\epsilon/r^7$. Using the equilibrium condition $dU/dr=0$, which occurs at $(r+0.95)=2.26$, i.e., $r=1.31$A, the value of β^1 is 0.830×10^{-48}. The sum of the three energy terms then gives

$$U_{r=1.31}=[-4.160-1.041+1.622]\times10^{-12}\text{ erg/ion}$$
$$=-3.58\times10^{-12}\text{ erg/ion.}$$

To obtain the desired energy of formation of [F—H··F]⁻, this figure must be corrected for the work done in stretching the F—H bond. Using the data already given this item,

$$\int_{x=0.92}^{x=0.95}k(x-0.92)dx+7e_1\epsilon\beta^1\int_{x=0.92}^{x=0.95}\frac{dx}{(2.26-x)^8}$$

is found to total 0.29×10^{-12} erg/ion. The net energy of stabilization is thus 3.29×10^{-12} erg/ion or 47.3 kcal. per g ion.

The available thermochemical data have been used by Ketelaar[2b] to estimate this energy. The result is a value between 30 and 50 kcal. per g ion. The calculated value is thus in good agreement with these experimental indications, and it suffices to show that the electrostatic forces are able to account for the stability of the ion.

Infra-Red Spectrum and Depolarization Factors of the Raman Lines of Spiropentane and the Raman and Infra-Red Spectra of 1,1-Dimethylcyclopropane,[1] 1-Methylcyclobutene, and Methylenecyclobutane

FORREST F. CLEVELAND
Department of Physics, Illinois Institute of Technology, Chicago 16, Illinois

M. J. MURRAY AND W. S. GALLAWAY
Universal Oil Products Company, Chicago, Illinois

(Received May 26, 1947)

The infra-red absorption spectrum in the region 700–4000 cm^{-1}, both for the liquid and for the gas at various pressures, and precise values for the depolarization factors of the Raman lines of spiropentane are reported. Infra-red and Raman frequencies, estimated relative intensities, and qualitative depolarization data are reported also for 1,1-dimethylcyclopropane. Selection rules for the two hydrocarbons are discussed, and it is shown that the observed numbers of Raman frequencies are not inconsistent with the structures D_{2d} and C_{2v} for the spiropentane and 1,1-dimethylcyclopropane, respectively. In addition, Raman and infra-red data are included for the isomers, 1-methylcyclobutene and methylenecyclobutane. Tentative assignments of the fundamentals are made for each of the four hydrocarbons.

INTRODUCTION

MURRAY and Stevenson[2] synthesized a C_5H_8 hydrocarbon by the debromination of pentaerythrityl bromide with zinc dust, using acetamide as a solvent. On the basis of its Raman spectrum, chemical properties, and method of preparation, they assigned to the hydrocarbon the spiropentane structure (symmetry D_{2d}). This structure was later confirmed by an electron-diffraction investigation.[3]

In view of the symmetrical structure of spiropentane it seemed worth while to obtain precise depolarization factors for its Raman lines, to obtain its infra-red spectrum, and to attempt a correlation of these data by use of the group theory selection rules. As a possible aid to this analysis it appeared desirable also to obtain the Raman and infra-red spectra of the similar molecule, 1,1-dimethylcyclopropane. Infra-red and Raman spectra of the isomers, 1-methylcyclobutene and methylenecyclobutane are included.

EXPERIMENTAL PROCEDURE

Raman

The depolarization factors for liquid spiropentane were obtained with a Hilger E-518 spectrograph by use of a previously described method.[4] Calibration marks were placed upon each of the two spectrograms, and corrections were made for real or apparent polarization produced by the spectrograph, reciprocity failure of the plates, and convergence errors. Six independent determinations of the depolarization factor of each line were made; for the four more intense lines, half of these determinations were made from the 2-hr. spectrogram and half from the 5-hr. spectrogram; for the other, weaker lines, all six of the determinations were made from the 5-hr. spectrogram. Intensities were obtained by use of a Gaertner microdensitometer.

1,1-Dimethylcyclopropane

The sample of 1,1-dimethylcyclopropane was prepared by the reduction of $(CH_3)_2C(CH_2Br)_2$ by zinc in acetamide. The method is that described by Whitmore, Popkin, Bernstein, and Wilkins.[5] Because the quantity of the reduction product at hand was too small to permit frac-

[1] The Raman data for the first two compounds were presented at the American Physical Society Meeting, Columbus, Ohio, June 1945; abstract in Phys. Rev. **68**, 98 (1945).

[2] M. J. Murray and E. H. Stevenson, J. Am. Chem. Soc. **66**, 812 (1944).

[3] J. Donohue, G. L. Humphrey, and V. Schomaker, J. Am. Chem. Soc. **67**, 332 (1945).

[4] Forrest F. Cleveland, J. Chem. Phys. **13**, 101 (1945).

[5] F. C. Whitmore, A. H. Popkin, H. I. Bernstein, and J. P. Wilkins, J. Am. Chem. Soc. **63**, 124 (1941).

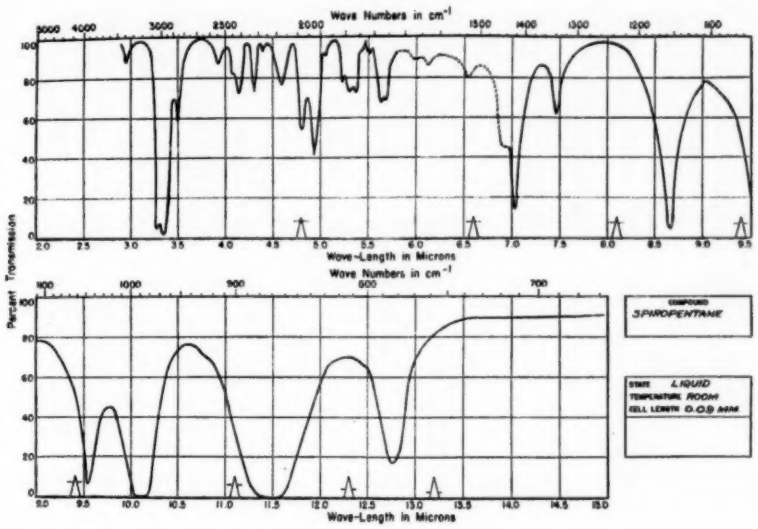

FIG. 1. Infra-red absorption curve for liquid spiropentane.

tionation in the equipment available, the Raman spectrum was obtained with the crude material. Weak Raman lines at 1652 and 3017 cm^{-1} (not included in Table II) are assigned to an olefinic impurity. Before the infra-red spectrum was taken, however, the olefinic contaminant was removed as follows: bromine was added to the crude product at about −40°C until a slight color showed that an excess of the halogen was present. On warming, the 1,1-dimethylcyclopropane vaporized directly into the absorption tube while the dibromides of the olefins remained as residue. Olefinic bands were absent in the spectrum of the sample thus purified.

1-Methylcyclobutene

It was stated by Philipov[6] that the reduction of pentaerythrityl tetrabromide by zinc in alcohol produced methylenecyclobutane and 1-methylcyclobutene. Murray and Stevenson[2] found no spectroscopic (Raman) evidence for the presence of the latter compound, but since its spectrum was not available the conclusion needed verification. A sample of 1-methylcyclobutene was generously furnished by Dr. V. Schomaker. It was prepared as described by Shand, Schomaker, and Fischer.[7]

Even the most prominent unique lines found in

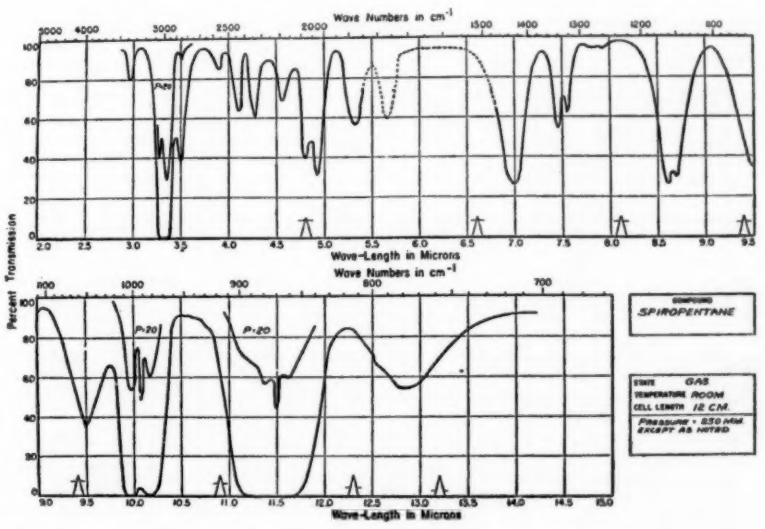

FIG. 2. Infra-red absorption curve for gaseous spiropentane.

[6] O. Philipov, J. prakt. Chem. [2] **93**, 162 (1916).
[7] W. Shand, Jr., V. Schomaker, and J. R. Fischer, J. Am. Chem. Soc. **66**, 636 (1944).

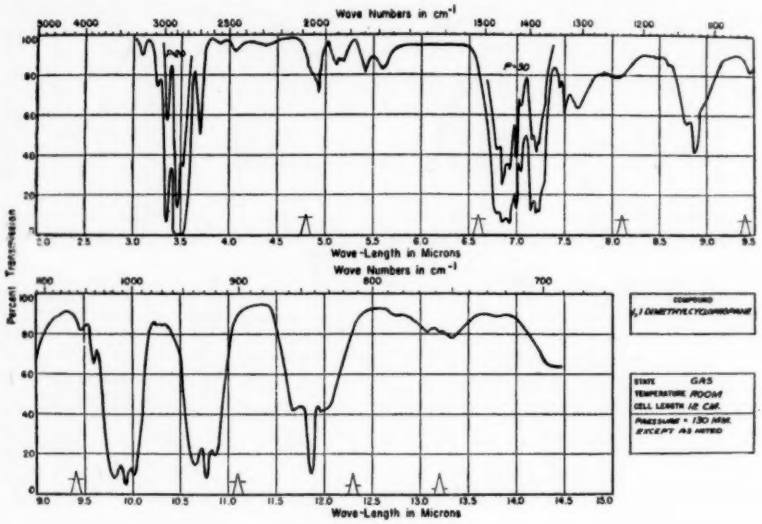

FIG. 3. Infra-red absorption curve for gaseous 1,1-dimethylcyclopropane.

the Raman spectrum of this hydrocarbon are absent from all reduction products of pentaerythrityl bromide so far examined by one of us (M.J.M.), hence it is thought that the concentration of this hydrocarbon in the crude product is probably less than one percent.

The Raman line at 1680 cm^{-1} in the spectrum of the sample of 1-methylcyclobutene is probably due to the presence of a small amount of the isomeric methylenecyclobutane. Likewise the infra-red spectrum of the liquid shows a band at 1670 cm^{-1} which could be assigned to the exocyclic olefin. The infra-red band of the liquid at 1720 cm^{-1} is probably due to carbonyl introduced either accidentally or by atmospheric oxidation. The Raman spectrum when obtained some months earlier with the same sample had no line at this position.

Methylenecyclobutane

The sample of this hydrocarbon was obtained by careful fractionation of the olefins recovered from silver nitrate extraction of the crude reduction products of pentaerythrityl tetrabromide. The sample studied was taken from the middle of the plateau boiling at 41.8°C at 760-mm pressure.

Infra-Red

The infra-red spectra were obtained with a large Littrow spectrometer having a 60° prism of 10×15-cm faces and a collimating mirror of

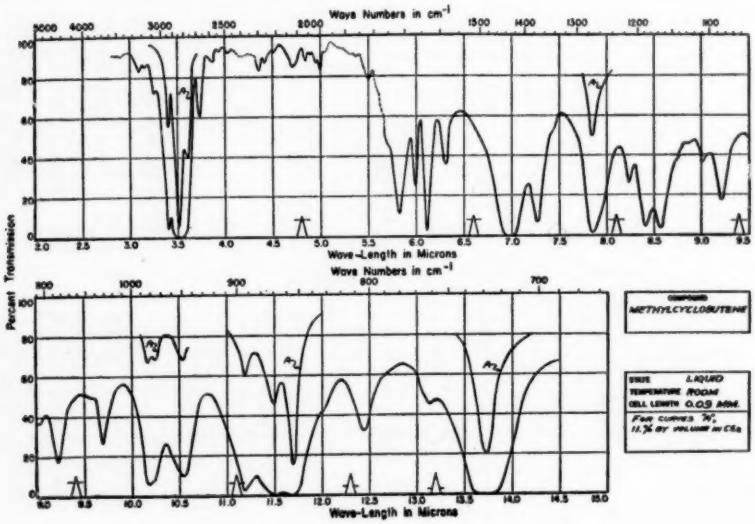

FIG. 4. Infra-red absorption curve for liquid 1-methylcyclobutene.

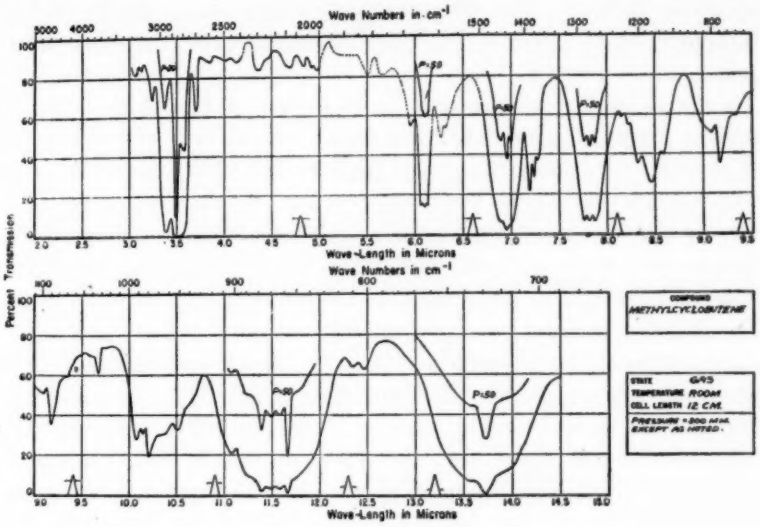

FIG. 5. Infra-red absorption curve for gaseous 1-methylcyclobutene.

100-cm focal length. The spectrometer proper is nearly a duplicate of the instrument described by McAlister, Matheson, and Sweeney.[8] The source used here, however, is a Nernst glower, and the photographic recordings of the thermocouple output are obtained by use of a two-galvanometer amplifier coupled by a conventional split-beam, photo-cell arrangement.

The spectra were recorded using rocksalt cells of the type described by Gildart and Wright[9] and of the thicknesses noted on the spectrograms (Figs. 1–7). The final curve for each compound represents the result obtained by comparing the traces of the thermocouple output when the filled cell is in the beam with that obtained with the evacuated cell.

Good stabilization of all circuits and elimination of sources of erratic disturbances have resulted in records that are reproducible to better than one percent of full-scale response and wave-length measurements to better than 0.01 micron. However, errors introduced in transposing from the records of thermocouple response *versus* dial reading to percent transmission *versus* wave-length may double these figures. To compensate for the variation of the intensity of the radiation emitted by the glower with wave-length, the slits of the spectrometer are manually operated in a

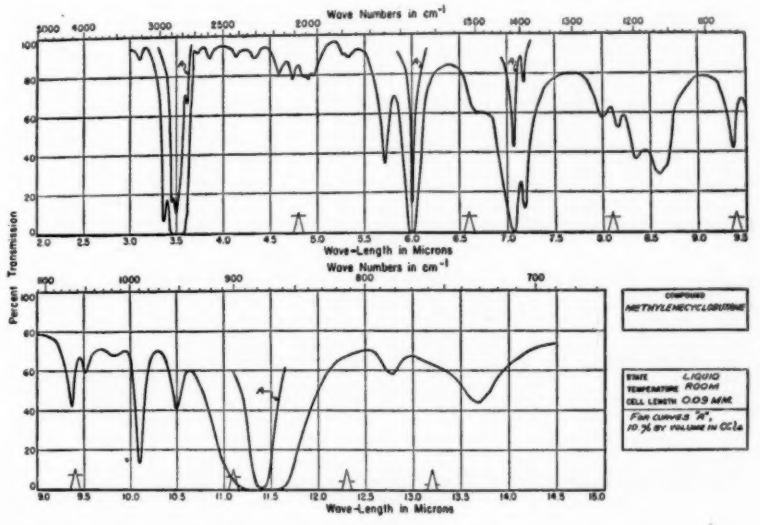

FIG. 6. Infra-red absorption curve for liquid methylenecyclobutane.

[8] E. D. McAlister, G. L. Matheson, and W. J. Sweeney, Rev. Sci. Inst. **12**, 314 (1941).
[9] L. Gildart and N. Wright, Rev. Sci. Inst. **12**, 204 (1941).

stepwise fashion. The effective slit widths are indicated on the curves (Figs. 1–7) at the appropriate wave-lengths.

Careful studies of the spectra of water vapor and of ammonia show that the optics of the instrument are of such sufficiently high quality that the resolving power is determined solely by the size of the slits used. Furthermore, the resolving power obtained is at least equal to or better than that reported by McAlister, Matheson, and Sweeney[8] and by Oetjen, Kao, and Randall,[10] except from 13 to 15 microns where the response of the thermocouple is below par, thus requiring the use of slits somewhat wider than normal. These data also show that the positions of the absorption maxima (as given in the tables) are reliable to 1 cm^{-1} at the longer wave-lengths. Band centers are given to the nearest 5 cm^{-1} for frequencies above 1300 cm^{-1}.

RESULTS

The depolarization data for spiropentane are given at the left in Table I. Depolarization factors were not obtained for the weak lines at 1150, 2836, and 2881 cm^{-1}, and the data for the weak 613- and 779-cm^{-1} lines are less precise than for the stronger lines. The lines at 1033 and 2991 cm^{-1} are strongly polarized, while the ones at 581, 613, and 779 cm^{-1} are only slightly polarized.

The infra-red data for the liquid and gaseous states are given in the central part of Table I, and the corresponding infra-red absorption curves are shown in Figs. 1 and 2. The infra-red spectra of gaseous spiropentane and methylenecyclobutane have also been reported by Cleaves and Sherrick.[11] The data reported by them agree well with those obtained in the present investigation, except for differences in resolving power of the two instruments.

The Raman data obtained for liquid 1,1-dimethylcyclopropane are compared with the Raman data obtained for liquid spiropentane at the left in Table II; the corresponding infra-red data for the two compounds in the gaseous state are compared at the right in Table II. The infra-red absorption curve for the 1,1-dimethylcyclopropane is shown in Fig. 3.

The Raman spectrum of 1-methylcyclobutene and the infra-red spectra for the liquid and gaseous states are compared in Table III. The corresponding infra-red absorption curves are given in Figs. 4 and 5.

The Raman spectrum of methylenecyclobutane and the infra-red spectra for the liquid and gaseous states are compared in Table IV. The corresponding infra-red absorption curves are given in Figs. 6 and 7.

DISCUSSION OF RESULTS

Number of Frequencies Expected for the Bicyclic C_5H_8 Compound

The number of polarized and depolarized Raman lines to be expected in the Raman spec-

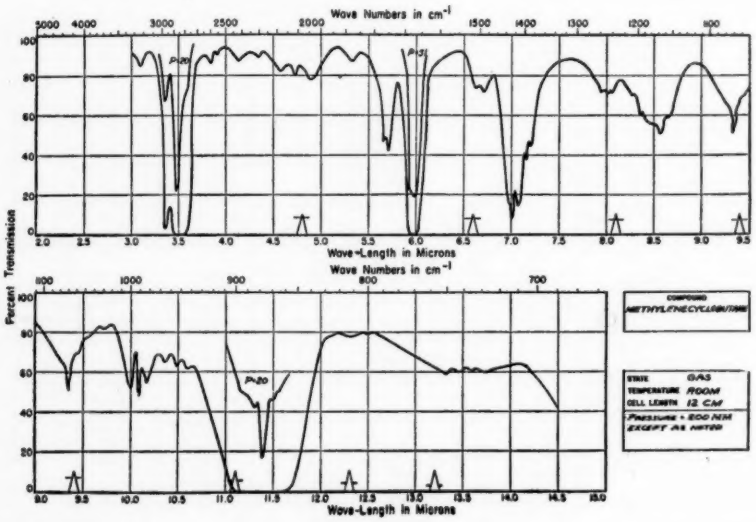

FIG. 7. Infra-red absorption curve for gaseous methylenecyclobutane.

[10] R. A. Oetjen, C. L. Kao, and H. M. Randall, Rev. Sci. Inst. **13**, 515 (1942).
[11] A. P. Cleaves and M. E. Sherrick, N.A.C.A., Tech. Note No. 1160 (1946).

TABLE I. Raman and infra-red data for spiropentane (C_5H_8).*

Raman					Infra-red				
Liquid					Liquid		Gas		Tentative assignment
$\Delta\nu$	I	ρ	a.d.	m.d.	ν_l	I_l	ν_g	I_g	
305	4	0.86	0.03	0.07					Fundamental, E, **305****
581	16	0.69	0.02	0.04					Fundamental, A_1, **581**
613	4	0.71	0.04	0.11					Fundamental, E, **613**
779	4	0.66	0.07	0.12	783	s	778	m	Fundamental, E, **779**
							798	vw	1397−613=**784**, $B_1\times E$
							861	vs	P branch or 1163−305=**858**, (B_2 or E)$\times E$
872	30	0.82	0.01	0.04	871	vs	870	vs	Fundamental, B_2 or E, **870**
							879	vs	R branch
							896	w	305+581=**886**, $A_1\times E$
					(928)	vw	929	vw	3(305)=**915**, E^3
							940	vw	305+613=**918**, $E\times E$
							983	vs	P branch
					990	vs	993	vs	Fundamental, E, **993**
							1003	vs	R branch
1033	50	0.02	0.01	0.03					Fundamental, A_1, **1033**
					1049	s	1053	s	Fundamental, B_2 or E, **1053**
1150	1	—	—	—	1155	s	1151	s	Fundamental, B_2 or E, **1151**
							1163	s	Fundamental, B_2 or E, **1163**
							1260	vw	2(613)=**1226**, E^2
							1280	vw	305+993=**1298**, $E\times E$
							1325	m	Fundamental, B_2 or E, **1325**
					1340	w	1340	m	Fundamental, B_2 or E, **1340**
1397	5	0.81	0.03	0.04					Fundamental, B_1, **1397**
1426	10	0.82	0.02	0.05	1420	s	1430	s	Fundamental, B_2 or E, **1430**
					1445	w			581+870=**1451**, $A_1\times$(B_2 or E)
					1530	w			2(778)=**1556**, E^2
					1630	w			305+1325=**1630**, $E\times$(B_2 or E)
					1675	w			613+1053=**1666**, $E\times$(B_2 or E)
					1760	w			613+1151=**1764**, $E\times$(B_2 or E)
					1775	w	1765	m	613+1163=**1776**, $E\times$(B_2 or E)
					1815	w			1033+778=**1811**, $A_1\times E$
					1825	vw			1053+778=**1831**, $E\times$(B_2 or E)
					1860	vw			870+993=**1863**, $E\times$(B_2 or E)
					1885	vw	1880	m	870+1033=**1903**, $A_1\times$(B_2 or E)
					1915	vw			581+1340=**1921**, $A_1\times$(B_2 or E)
					1985	vw			2(993)=**1986**, E^2
					2025	m	2030	s	993+1033=**2026**, $A_1\times E$
					2085	m	2085	s	1033+1053=**2086**, $A_1\times$(B_2 or E)
					2175	w	2190	m	1033+1151=**2184**, $A_1\times$(B_2 or E)
					2275	w			870+1397=**2267**, $B_1\times$(B_2 or E)
					2320	m	2345	m	993+1340=**2333**, $E\times$(B_2 or E)
					2415	m			993+1430=**2423**, $E\times$(B_2 or E)
					2450	w	2435	m	1053+1397=**2450**, $B_1\times$(B_2 or E)
					2545	w			1151+1397=**2548**, $B_1\times$(B_2 or E)
							2565	w	1163+1397=**2560**, $B_1\times$(B_2 or E)
2836	0.4	—	—	—					Fundamental, A_1 or B_1, **2836**
					2860	m	2850	s	Fundamental, B_2 or E, **2850**
2881	vw	—	—	—					Fundamental, B_1 or A_1, **2881**
					2985	vs	2985	vs	Fundamental, B_2 or E, **2985**
2991	100	0.15	0.03	0.05					Fundamental, A_1, **2991**
					3050	vs	3050	vs	Fundamental, B_2 or E, **3050**
3065	30	0.80	0.02	0.03					Fundamental, B_1, **3065**
							3370	w	305+3065=**3370**, $B_1\times E$
					3400	w			

* $\Delta\nu$ is the Raman displacement in cm^{-1}; I is the relative intensity of the Raman line determined with the microdensitometer; ρ is the mean of the six values of the depolarization factor; a.d. is the average deviation from the mean value of ρ; m.d. is the maximum deviation from the mean value of ρ; ν_l and ν_g are the infra-red frequencies in cm^{-1} for the liquid and gaseous states, respectively; I_l and I_g are the corresponding intensities (vs = very strong, s = strong, m = medium, w = weak, vw = very weak); and the braces enclose branches belonging to one band.

** Assumed value of the fundamental. The type-E fundamentals are doubly degenerate, degeneracy = d = 2, all other fundamentals are non-degenerate, d = 1.

trum was worked out from the group theory formulas[12] for each of the five conceivable structures listed by Murray and Stevenson.[2] This was done both for the entire molecule and for the carbon skeleton alone. The results are given in Table V. The five possible structures given by

[12] See Arnold G. Meister, Forrest F. Cleveland, and M. J. Murray, Am. J. Phys. 11, 239 (1943).

TABLE II. Comparison of the Raman data for the liquid state and the infra-red data for the gaseous state for 1,1-dimethylcyclopropane (C_5H_{10}) and spiropentane (C_5H_8).*

Raman data (liquid)						Infra-red data (gas)			
Spiropentane			1,1-Dimethylcyclopropane			Spiropentane		1,1-Dimethyl-cyclopropane	
$\Delta\nu$	I	ρ	$\Delta\nu$	I_a	ρ_a	ν_0	I_0	ν_0	I_0
305	4	0.86							
			326	1	—				
			356	3	*D*				
			392	1	—				
581	16	0.69							
613	4	0.71							
			658	1	—				
			678	7	*P*				
								724	*w*
								750	*w*
								758	*w*
								766	*w*
779	4	0.66	778	1	—	778	*m*	785	*w*
						798	*vw*		
			836	5	*D*			(830)	*m*
								835	*s*
								842	*vvs*
						861	*vs*	857	*s*
872	30	0.82				870	*vs*		
						879	*vs*		
						896	*w*		
								920	*s*
			928	10	*P*	929	*vw*	928	*vvs*
						940	*vw*	939	*vs*
								(970)	*vvw*
						983	*vs*	(976)	*vvw*
						993	*vs*	999	*vs*
						1003	*vs*	1007	*vvs*
								1019	*vs*
1033	50	0.02						1042	*m*
			1056	5	*P*	1053	*s*	1056	*w*
								(1112)	*m*
			1124	2	—			1127	*m*
								1137	*m*

Murray and Stevenson[2] are shown in the first column, and the observed numbers of lines are listed at the bottom. In determining these observed numbers of lines it was assumed that the carbon skeleton frequencies were those less than 1155 cm^{-1} and that the weak 613- and 779-cm^{-1} lines were depolarized lines. The 581-cm^{-1} line was chosen as a polarized line, rather than the 779 line, because of the greater reliability of the ρ value of the 581 line, because polarized lines are usually more intense in Raman spectra than depolarized lines, and because there is an infra-red band near 779 cm^{-1}. Such a coincidence of Raman and infra-red bands is forbidden for polarized lines by the selection rules if the structure of the hydrocarbon is that indicated by the chemical and electron diffraction evidence.

The 1150-cm^{-1} line could reasonably be expected to correspond to a non-totally-symmetrical vibration involving the *CCC* rings, since the totally-symmetrical frequency involving these rings certainly corresponds to the highly polarized line at 1033 cm^{-1} and since the more unsymmetrical vibration frequently corresponds to a line having a higher frequency than that of the totally-symmetrical vibration; if this is the case, the 1150 line would be a depolarized line.

If these assumptions are made, the observed numbers and those predicted for the spiropentane or D_{2d} structure are in good agreement as far as the skeleton frequencies are concerned; in fact if the 1150 line is actually a depolarized line, as indicated above, the agreement would be perfect. But when the entire molecule is considered, the observed numbers are less than the predicted ones, presumably because of unresolved lines in the region of the carbon-hydrogen frequencies; such unresolved lines are to be expected since

TABLE II.—*Continued.*

Raman data (liquid)						Infra-red data (gas)			
Spiropentane			1,1-Dimethylcyclopropane			Spiropentane		1,1-Dimethyl-cyclopropane	
$\Delta\nu$	I	ρ	$\Delta\nu$	I_e	ρ_c	ν_g	I_g	ν_g	I_g
1150	1	—	1158	1	—	1151	*s*		
						1163	*s*	1163	*w*
								1180	*vw*
								1240	*w*
						1261	*vw*	(1270)	*vw*
						1280	*vw*		
			1319	8	*P*			1310	*m*
						1325	*m*	1335	*m*
						1340	*m*	1340	*w*
			1382	2	—			1380	*m*
								1385	*m*
1397	5	0.81						1395	*m*
1426	10	0.82						1420	*w*
			1433	4*b*	*D*	1430	*s*	1430	*m*
								1445	*s*
			1465	4*b*	*D*			1460	*vs*
								1470	*s*
						1765	*m*	1785	*w*
						1880	*m*	1850	*w*
								1930	*vw*
								1940	*vw*
								1955	*vw*
						2030	*s*	2030	*w*
								(2060)	*vw*
						2085	*s*	(2070)	*vw*
						2190	*m*		
								2285	*w*
						2345	*m*		
						2435	*m*	2460	*w*
						2565	*w*	2560	*w*
								2700	*m*
			2733	3	*P*				
2836	0.4	—						2840	*m*
			2863	6	*P*	2850	*s*		
2881	*vw*	—	2892	5	*P*			2890	*vs*
			2926	7	*P*				
			2950	5	*D*				
2991	100	0.15	2993	10	*P*	2985	*vs*	2985	*m*
						3050	*vs*	3075	*m*
3065	30	0.80	3061	4*b*	*D*			3240	*w*
						3370	*w*		

* I_e = Estimated intensity on the basis of 10 for the strongest line; ρ_e is the qualitative depolarization data, *P* = polarized, *D* = depolarized; *b* = broad; other symbols have the same meaning as in Table I. Data in regard to which there is some uncertainty are enclosed in parentheses.

there should be 15C—H lines all of which involve, however, only one kind of C—H bond. These frequencies would give rise to Raman lines that would undoubtedly fall very close together on the spectrograms and which could well be unresolved.

One can conclude then that the observed Raman data are in reasonably good agreement with the spiropentane or D_{2d} structure. The predictions for the D_{3h} structure are not in as good an agreement with the observed Raman data, even if the 1150 line were considered to be a C—H frequency.

Selection Rules and Assignment of Frequencies for Spiropentane

The selection rules for fundamentals, overtones, and binary combinations[12] for the spiropentane or D_{2d} structure are given in Table VI and a tentative assignment of the frequencies is given at the right in Table I. Twenty-one of the expected 25 bands corresponding to fundamental frequencies were assigned. The fundamentals were selected upon the basis of their intensity, their appearance or non-appearance in the Raman and infra-red spectra, and in consideration of the selection rules for fundamentals, overtones, and

TABLE III. Raman and infra-red data for 1-methylcyclobutene (C_5H_8).*

Raman Liquid		Infra-red Liquid		Infra-red Gas		Tentative assignment
$\Delta\nu$	I_e	ν_l	I_l	ν_g	I_g	
318	4					Fundamental, **318****
390	3					Fundamental, **390**
434	0					729−318=**411** or 1091−651=**440**
520	1					890−390=**500** or 1181−651=**530**
620	1					2(318)=**636**
651	6					Fundamental, **651**
				716	*vs*	1034−318=**716**
723	1	728	*s*	729	*vvs*	Fundamental, **729**
				737	*vs*	1375−651=**724**
762	2	762	*m*			Fundamental, **762**
		804	*s*	802	*w*	1181−390=**791**
		(833)	*w*	810	*w*	1217−390=**827**
860	4	854	*vvs*	858	*vs*	Fundamental, **858**
				864	*vs*	1181−318=**863**
		870	*vs*	870	*vs*	1202−318=**884**
				877	*vs*	1280−390=**890**
890	5	894	*vs*	890	*vs*	Fundamental, **890**
				903	*vs*	1217−318=**899**
957	5	949	*vs*	951	*s*	Fundamental, **951**
		976	*vs*	965	*s*	318+651=**969**
986	6	983	*vs*	979	*s*	Fundamental, **979**
				986	*s*	1375−390=**985**
				993	*s*	1640−651=**989**
				1026	*w*	390+651=**1041**
1037	2	1032	*s*	1034	*m*	Fundamental, **1034**
		(1046)	*vw*	1043	*w*	318+729=**1047**
				1070	*w*	1375−318=**1057**
1091	2	1085	*vs*	1090	*s*	Fundamental, **1090**
		1110	*m*	1100	*w*	1435−318=**1117**
		1130	*vw*			390+729=**1119**
1144	2	1143	*vw*			Fundamental, **1144**
		1167	*vs*	1164	*m*	318+858=**1176**
				1181	*s*	Fundamental, **1181**
1185	1*b*	1189	*vs*	1202	*m*	Fundamental, **1202**
1216	4	1214	*s*	1217	*w*	Fundamental, **1217**
				1227	*w*	390+858=**1248**
				1270	*vs*	318+951=**1269**

binary combinations. Three of the five type-A_1, two of the four type-B_1, and four of the eight type-E fundamentals were definitely assigned. The twelve remaining ones could only be assigned to one or the other of two vibration types, ten as either B_2 or E, two as either A_1 or B_1. Four of the fundamentals, the vibration type of which was at first ambiguous, were assigned to a particular vibration type while accounting for the weak bands as overtones or binary combinations. Only overtones or binary combinations allowed by the selection rules were used in accounting for the weaker bands, and difference bands were used only for the fundamentals below 700 cm^{-1}, for which the corresponding energy states can be expected to be sufficiently well populated to give rise to appreciable intensities. It was not possible to account for the weak infra-red band observed for the liquid state at 3400 cm^{-1}. It could be accounted for as the combination 581+2836 =3417, except for the fact that this combination is forbidden by the selection rules. This weak band may owe its origin to a combination of three, or more, frequencies.

Of the four unassigned lines, three correspond to type-A_2 frequencies that are forbidden in both the Raman and infra-red spectra. These frequencies correspond to C−H vibrations and therefore at least some of them may be expected to fall in the 1400- or 3000-cm^{-1} regions.

For a revision of the present tentative and incomplete assignment, a normal coordinate treatment should be very valuable. Such a treatment should make it possible to remove much or all of the ambiguity inherent in the bands assigned to "B_2 or E" which must be done before reliable

TABLE III.—*Continued.*

Raman Liquid		Infra-red Liquid		Infra-red Gas		Tentative assignment
$\Delta\nu$	I_r	ν_l	I_l	ν_g	I_g	
1278	3	1276	*vs*	1280	*vs*	Fundamental, **1280**
				1290	*vs*	390+890=**1280** or 318+979=**1297** or 2(651)=**1302**
		1345	*w*			390+951=**1341** or 318+1034=**1352**
1378	4	1375	*vs*	1375	*m*	Fundamental, **1375**
				1380	*s*	651+729=**1380**
				1390	*s*	318+1090=**1408**
				1430	*m*	390+1034=**1424**
1430	8*b*	1435	*vvs*	1435	*s*	Fundamental, **1435**
				1450	*m*	2(729)=**1458**
1586	1	1585	*s*	1585	*m*	Fundamental, **1585**
				1595	*m*	318+1280=**1598** or 651+951=**1602**
				1630	*s*	651+979=**1630**
1641	8	1640	*vs*	1640	*s*	Fundamental, **1640**
				1650	*s*	390+**1280**=**1670**
1680	3	1670	*s*	1675	*m*	729+951=**1680** or 651+1034=**1685** or 318+1375=**1693** (or impurity)
		1720	*vs*			2(858)=**1716** or 729+979=**1708** (or impurity)
		1758	*w*			858+890=**1748** or 318+1435=**1753**
				1765	*w*	729+1034=**1763** or 390+1375=**1765**
		1820	*w*	1820	*w*	858+951=**1809** or 729+1090=**1819** or 390+1435=**1825**
				1905	*w*	2(951)=**1902** or 318+1585=**1903** or 729+1181=**1910**
		2000	*w*	2010	*w*	729+1280=**2009** or 979+1034=**2013**
		2020	*w*	2035	*w*	651+1375=**2026** or 390+1640=**2030**
		2045	*vw*			858+1181=**2039** or 951+1090=**2041**
		2065	*vw*	2065	*w*	2(1034)=**2068** or 979+1090=**2069** or 890+1181=**2071**
		2125	*w*	2135	*w*	1034+1090=**2124** or 951+1181=**2132** or 858+1280=**2138**
		2220	*vw*			1034+1181=**2215** or 951+1280=**2231**
		2270	*w*	2235	*w*	858+1375=**2233** or 651+1585=**2236**
		2295	*w*	2290	*w*	651+1640=**2291** or 858+1435=**2293**
		2400	*w*	2420	*w*	1034+1375=**2409** or 979+1435=**2414**
		2480	*w*	2495	*w*	890+1585=**2475** or 1217+1280=**2495** or 858+1640=**2498**
		2540	*vw*			890+1640=**2530** or 951+1585=**2536**
		2585	*w*	2600	*w*	951+1640=**2591** or 1217+1375=**2592**
		2675	*m*			1034+1640=**2674** or 1090+1585=**2675**
2723	2			2700	*m*	Fundamental, **2700**
		2770	*m*	2800	*vs*	Fundamental, **2800**
2851	5*vb*	2850	*vs*	2865	*vvs*	Fundamental, **2865**
2917	10*vb*					Fundamental, **2917**
		2940	*m*	2965	*vs*	Fundamental, **2965**
3044	6					Fundamental, **3044**
		3080	*vw*	3085	*w*	1640+1435=**3075**
		3180	*vw*			2(1585)=**3170** or 318+2865=**3183**
		3240	*vw*	3200	*w*	1640+1585=**3225** or 318+2917=**3235**
				3270	*w*	318+2965=**3283** or 2(1640)=**3280**
		3450	*vw*			651+2800=**3451** or 390+3044=**3434**

* See reference 3, *vb*=very broad; other symbols have the same meaning as in Tables I and II.
** Assumed value of the fundamental. All of the fundamentals are non-degenerate, degeneracy $=d=1$.

values of thermodynamic quantities can be calculated from the spectroscopic data. Then a high resolution investigation, especially in the 3000-cm^{-1} region where the resolution was poorest, might lead to the discovery of the missing A_1 fundamental. A_1 frequencies usually give rise to strong lines in the Raman spectrum, and it seems more likely that the missing A_1 line should be attributed to an unresolved line than to a Raman line so weak that it escaped observation. If the normal coordinate treatment and the high resolution investigation should result in the establishment of the B_2 and E frequencies and in the discovery of the missing A_1 fundamental, the A_2 frequencies might then be located by a comparison of heat capacities calculated from the spectroscopic data with heat capacities experimentally determined.

1,1-Dimethylcyclopropane

The equilibrium configuration of the 1,1-dimethylcyclopropane molecule will depend upon

TABLE IV. Raman and infra-red data for methylenecyclobutane (C_5H_8).*

Raman		Infra-red				
Liquid		Liquid		Gas		Tentative assignment
$\Delta\nu$	I	ν_l	I_l	ν_g	I_g	
354	23					Fundamental, **354****
373	13					Fundamental, **373**
657	20					Fundamental, **657**
		731	*m*	728	*w*	Fundamental, **728**
				736	*w*	354+373=**727**
				743	*w*	2(373)=**746**
				751	*w*	1415−657=**758**
		782	*m*			Fundamental, **782**
				800	*w*	1155−354=**801**
				812	*w*	1167−354=**813**
				825	*w*	1197−373=**824**
				865	*vs*	1197−354=**843**
				870	*vs*	1248−373=**875**
873	14	877	*vvs*	879	*vvs*	Fundamental, **879**
				884	*vs*	1248−354=**894**
907	20			895	*vs*	Fundamental, **895**
				944	*w*	
957	72	952	*m*	954	*w*	Fundamental, A_1, **954**
				966	*w*	
				983	*m*	
		990	*vs*	991	*m*	Fundamental, **991**
				1001	*m*	354+657=**1011**
		1018	*w*	1029	*w*	Fundamental, **1029**
		1051	*m*	1059	*w*	Fundamental, **1059**
		1067	*m*	1070	*m*	Fundamental, **1070**
		1155	*m*	1155	*m*	Fundamental, **1155**
		1164	*s*	1167	*m*	Fundamental, **1167**
				1183	*m*	
1191	11	1198	*s*	1197	*m*	Fundamental, **1197**
				1210	*m*	
		1226	*m*			354+879=**1233**
				1240	*m*	354+895=**1249** or 373+879=**1252**
		1250	*m*	1248	*m*	Fundamental, ($XXC=CH_2$), **1248**
				1260	*m*	373+895=**1268**
				1385	*m*	657+728=**1385**

the orientations of the two methyl groups with respect to rotation about the C−C single bond. A qualitative consideration of the possible interactions between the H and C atoms indicates that only one of two structures, of symmetry C_1 and C_{2v}, is probable.

For the structure C_1 all of the frequencies would be allowed to appear in the Raman spectrum and should all be polarized. For the structure C_{2v} the frequencies allowed in the Raman spectrum are: twelve polarized, type-A_1 frequencies, four of which are frequencies of the carbon skeleton; and 27 depolarized (10 type B_1, 8 type A_2, and 9 type B_2) frequencies, five of which (two type B_2, one type A_2, and two type B_1) are carbon skeleton frequencies. The selection rules allow all of the fundamentals to appear in the Raman spectrum and all except the A_2 fundamentals to appear in the infra-red. All overtones and binary combinations are allowed in the Raman spectrum and all except $A_2{}^n$ (n odd), $A_1\times A_2$, and $B_1\times B_2$ are allowed in the infra-red.

From the qualitative depolarization data given in Table II it does not appear probable that all of the lines are polarized and, consequently, it seems more reasonable to suppose that the structure is C_{2v} rather than C_1. Assuming the C_{2v} structure, a comparison of the expected and observed numbers of lines for the 1,1-dimethylcyclopropane with the corresponding numbers for spiropentane is given in Table VII. Skeleton frequencies were, as for spiropentane, taken as those less than 1155 cm^{-1}; when this is done, the total number of skeleton frequencies observed (10) is one greater than the expected number (9) in this region. The additional frequency could well be a C−H frequency similar to the "rocking frequency" of the methyl group which in dimethyl-

TABLE IV.—*Continued.*

Raman Liquid		Infra-red Liquid		Infra-red Gas		Tentative assignment
$\Delta\nu$	I	ν_l	I_l	ν_g	I_g	
1391	20	1390	*vs*	1395	*s*	Fundamental, ($XXC=CH_2$), **1395**
		1415	*vvs*	1415	*vs*	Fundamental, **1415**
1428	20			1425	*vs*	Fundamental, ($XXC=CH_2$), **1425**
		1485	*m*	1490	*w*	Fundamental, **1490**
				1510	*w*	354+1155=**1509** or 728+782=**1510**
1679	48	1665	*vvs*	1675	*vvs*	Fundamental, ($XXC=CH_2$), **1675**
		1750	*s*	1750	*m*	354+1395=**1749** or 728+1029=**1757** or 2(879)=**1758**
				1770	*m*	373+1395=**1768**
		1880	*w*	1880	*w*	728+1155=**1883**
		1900	*w*			2(954)=**1908**
		2015	*w*			954+1059=**2013**
		2040	*w*	2045	*w*	879+1167=**2046**
		2060	*w*			991+1070=**2061** or 896+1167=**2063**
		2115	*w*	2115	*w*	2(1059)=**2118** or 954+1155=**2109**
		2180	*w*	2185	*w*	782+1395=**2177** or 991+1197=**2188**
		2310	*w*	2305	*w*	879+1425=**2304** or 2(1155)=**2310**
		2420	*w*	2420	*w*	1425+991=**2416**
				2560	*w*	879+1675=**2554**
		2590	*w*	2605	*w*	1197+1395=**2592**
		2690	*w*			1248+1425=**2673**
		2770	*s*	(2785)	*m*	Fundamental, **2770**
2826	4					Fundamental, A_2, **2826**
2861	4	2860	*vvs*	2880	*vvs*	Fundamental, **2860**
2902	60	2900	*s*			Fundamental, **2902**
2921	75					Fundamental, A_2, **2921**
2952	88					Fundamental, A_2, **2952**
2986	100	2980	*s*	2985	*vs*	Fundamental, (ring and $XXC=CH_2$), **2985, 2985**
3072	18					Fundamental, A_2, **3072**
		3225	*w*	3235	*w*	2860+373=**3233**

* See reference 3. For meaning of symbols, see footnotes to Tables I, II, and III.
** Assumed value of the fundamental. All of the fundamentals are non-degenerate, degeneracy $=d=1$.

acetylene[13] appeared at 1029 cm^{-1}. While the observed numbers of frequencies for the carbon skeleton are in fairly good qualitative agreement with the values expected for the C_{2v} structure, definite conclusions cannot be drawn on the basis of the present qualitative depolarization data.

Since all of the fundamentals, overtones, and binary combinations are allowed in the Raman spectrum, whether the structure is C_1 or C_{2v}, and all of them, if the structure is C_1, or most of them, if the structure is C_{2v}, are allowed in the infra-red spectrum, it seemed worth while to attempt a tentative assignment of the frequencies for this molecule. Such an assignment, even if incomplete, is of value to those who may wish to estimate the heat capacity or other thermodynamic quantities, estimates even as far off as 10 percent frequently being of value in work of a practical nature. The tentative assignment finally decided upon is given at the right in Table VIII. The nine fundamental frequencies of the carbon skeleton were assumed to be those at 326, 356, 392, 658, 678, 836, 842, 928, and 1056 cm^{-1}. These are the frequencies that make the greatest contribution to the thermodynamic quantities, and the assignment of these skeleton frequencies is complete. Nineteen other frequencies were chosen as fundamentals (see Table VIII), thus making a total of 28 assigned fundamentals out of the 39 possible ones. The 785-cm^{-1} band was assumed to be a CH_2 deformation frequency, in line with Mecke's results[14] for the isomeric paraffins; he found such a frequency near 750 cm^{-1} for these compounds (at 762 cm^{-1} for *n*-pentane). The intense, polarized Raman lines at 928 and 1056 cm^{-1} correspond to totally symmetrical (A_1) vibrations of the open and closed *CCC* triangles, respectively. For comparison, one may note that the frequency of the open *CCC* triangle in *n*-propane is at 867 cm^{-1}, while the frequency of the *CCC* ring in spiropentane and cyclopropane is 1033 and 1187 cm^{-1}, respectively. The strong, polarized Raman

[13] B. L. Crawford, Jr., J. Chem. Phys. **7**, 555 (1939).

[14] R. Mecke, Zeits. f. physik. Chemie **B36**, 347 (1937).

TABLE V. Comparison of the expected numbers of Raman lines for the five conceivable structures of the bicyclic C_5H_8 hydrocarbon with the experimental results.*

Structure	Symmetry	Number of fundamentals: Molecule P	Molecule D	Molecule T	Skeleton P	Skeleton D	Skeleton T
	C_s	18	15	33	5	4	9
	C_s	19	14	33	6	3	9
	C_s	20	13	33	6	3	9
	D_{3h}	5	11	16	2	3	5
	D_{2d}	5	17	22	2	5	7
	Observed	3	7	13	2	4	7

* P = number of polarized lines, D = number of depolarized lines, T = total number of lines allowed in the Raman spectrum.

line at 678 cm^{-1} also seems certain to correspond to an A_1 fundamental. In the region of the C–H vibrations, where the resolution was poorest, the broad Raman line observed at 3061 cm^{-1} was assumed to correspond to two unresolved fundamentals, one at 3045, the other at 3075 cm^{-1}.

All of the remaining bands observed in the Raman and infra-red spectra were accounted for, in this tentative assignment, as P or R branches, overtones, or binary combinations. Frequencies corresponding to difference bands were calculated only for fundamentals below 700 cm^{-1}, for which the corresponding energy states can be expected to be sufficiently well populated to give rise to appreciable intensities.

TABLE VII. Comparison of the expected and observed numbers of Raman lines for 1,1-dimethylcyclopropane and spiropentane.

Hydrocarbon	Symmetry	Number of frequencies	Molecule P	Molecule D	Molecule T	Skeleton P	Skeleton D	Skeleton T
Spiropentane	D_{2d}	Expected:	5	17	22	2	5	7
		Observed:	3	7	13	2	4	7
1,1-Dimethyl-cyclopropane	C_{2v}	Expected:	12	27	39	4	5	9
		Observed:	9	6	22	3	2	10

Of the eleven unassigned fundamentals, it seems likely that several of them may lie in the 2700–3100-cm^{-1} region and have escaped observation because of insufficient resolution in this region. Fundamentals falling in this region make a relatively small contribution to the thermodynamic quantities. A high resolution investigation in this region, quantitative values for the depolarization factors of the Raman lines, and an experimental measurement of the heat capacity at various temperatures would provide useful data for a revision of the present tentative and incomplete assignment.

1-Methylcyclobutene

Depending upon the orientation of the methyl group, the structure of 1-methylcyclobutene is

TABLE VI. Selection rules for fundamentals, overtones, and binary combinations for the spiropentane or D_{2d} structure.*

Number of fundamentals: Type	Molecule	Skeleton	Number of allowed fundamentals: Molecule i.r.	Molecule R	Skeleton i.r.	Skeleton R	Forbidden overtones: i.r.	Forbidden overtones: R	Forbidden binary combinations: i.r.	Forbidden binary combinations: R
A_1	5	2	0	5 P	0	2 P	All	None	$A_1\times A_1$, $A_1\times A_2$, $A_1\times B_1$	$A_1\times A_2$
A_2	3	0	0	0	0	0	All	A_2^n (n odd)	$A_2\times A_1$, $A_2\times A_2$, $A_2\times B_2$	$A_2\times A_1$
B_1	4	1	0	4 D	0	1 D	All	None	$B_1\times A_1$, $B_1\times B_1$, $B_1\times B_2$	$B_1\times B_2$
B_2	5	2	5 M_z	5 D	2 M_z	2 D	B_2^n (n even)	None	$B_2\times A_2$, $B_2\times B_1$, $B_2\times B_2$	$B_2\times B_1$
E	8	2	8 M_P	8 D	2 M_P	2 D	None	None	None	None

* i.r. = infra-red, R = Raman, P = polarized, D = depolarized, M_z = parallel band, M_P = perpendicular band.

TABLE VIII. Tentative assignment of frequencies for 1,1-dimethylcyclopropane.*

Raman Liquid			Infra-red Gas		Tentative assignment
$\Delta\nu$	I_e	ρ	ν_0	I_0	
326	1	—			Fundamental, **326****
356	3	D			Fundamental, **356**
392	1	—			Fundamental, **392**
658	1	—			Fundamental, **658**
678	7	P			Fundamental, **678**, A_1
			724	w	326+392=**718**
			750	w	356+392=**748**
			758	w	1429−678=**751**
			766	w	1445−678=**767**
778	1	—	785	w	Fundamental, **785**
836	5	D	(830)	m	Fundamental, **836**
			835	s	P branch or 1163−326=**837**
			842	vvs	Fundamental, **842**
			857	s	R branch
			920	s	1310−392=**918** or P branch
928	10	P	928	vvs	Fundamental, **928**, A_1
			939	vs	R branch
			(970)	vvw	1310−356=**954**
			(976)	vvw	326+658=**984** or 3(326)=**978**
			999	vs	P branch or 1380−392=**988**
			1007	vvs	Fundamental, **1007**
			1019	vs	356+658=**1014** or R branch
			1042	m	1430−392=**1038** or 392+658=**1050**
1056	5	P	1056	w	Fundamental, **1056**, A_1
			(1112)	m	326+785=**1111**
1124	2	—	1127	m	Fundamental, **1127**
			1137	m	356+785=**1141** or 1460−326=**1135**
1158	1	—	1163	w	Fundamental, **1163**
			1180	vw	392+785=**1177**
			1240	w	392+842=**1234**
			(1270)	vw	326+928=**1254**

either C_1 or C_s, the only possible symmetry element being a plane of symmetry. If the structure is C_1, with no symmetry, there would be 33 fundamentals, of which nine are vibrations of the carbon skeleton. All of these would be allowed in both the Raman and infra-red spectra, and all of the Raman lines should be polarized.

If the structure is C_s, all of the 33 fundamentals are again allowed in both the Raman and infra-red spectra and, as before, nine of them are frequencies of the carbon skeleton. Of the 33 expected Raman lines, 20 should be polarized and 13 depolarized. Of the nine Raman lines corresponding to frequencies of the carbon skeleton, seven should be polarized and two depolarized. Since some depolarized lines are to be expected for the C_s structure, but not for the C_1 structure, precise values of the depolarization factors of the Raman lines should enable one to decide between these two structures.

Since all of the fundamentals and all of the overtones and combinations (for either structure) are allowed in both the Raman and infra-red spectra, it seemed worth while to attempt an assignment of the fundamentals. The tentative assignments finally decided upon are listed at the right in Table III. The nine fundamental frequencies of the carbon skeleton were assumed to be those at 318, 390, 651, 729, 858, 890, 951, 979, and 1640. These are the frequencies that make the greatest contribution to the thermodynamic quantities and the assignment of these skeleton frequencies is complete. Seventeen other frequencies were chosen as fundamentals (see Table III), thus making a total of 26 assigned fundamentals out of the 33 possible ones. The 762-cm^{-1} band was again, as for 1,1-dimethylcyclopropane, assumed to be a CH_2 deformation frequency. The 1202-cm^{-1} infra-red band, unresolved from the 1181 band in the Raman spectrum, was chosen as a fundamental in order to explain the infra-red band at 870 cm^{-1} as a difference band.

All of the remaining frequencies observed in

TABLE VIII.—*Continued.*

Raman Liquid			Infra-red Gas		Tentative assignment
$\Delta\nu$	I_a	ρ	ν_0	I_a	
1319	8	P	1310	m	Fundamental, **1310**
			1335	m	326+1007=**1333**
			1340	w	658+678=**1336**
1382	2	—	1380	m	Fundamental, **1380**
			1385	m	326+1056=**1382**
			1395	m	392+1007=**1399**
			1420	w	356+1056=**1412**
			1430	m	Fundamental, **1430**
1433	4b	D	1445	s	Fundamental, **1445**
			1460	vs	Fundamental, **1460**
1465	4b	D	1470	s	Fundamental, **1470**
			1785	w	326+1460=**1786** or 785+1007=**1792**
			1850	w	842+1007=**1849**
			1930	vw	928+1007=**1935** or 785+1127=**1912**
			1940	vw	785+1163=**1948**
			1955	vw	836+1127=**1963**
			2030	w	2(1007)=**2014**
			(2060)	vw	678+1380=**2058**
			(2070)	vw	1007+1056=**2063**
			2285	w	842+1445=**2287**
			2460	w	1007+1460=**2467**
			2560	w	1127+1430=**2557**
			2700	m	1310+1380=**2690** or 3045−326=**2719**
2733	3	P			Fundamental, **2733**
			2840	m	Fundamental, **2840**
2863	6	P			Fundamental, **2863**
2892	5	P	2890	vs	Fundamental, **2890**
2926	7	P			Fundamental, **2926**
2950	5	D			Fundamental, **2950**, A_2
2993	10	P	2985	m	Fundamental, **2985**
					Fundamental, **3045**, A_2
***3061	4b	D	3075	m	Fundamental, **3075**
			3240	w	356+2890=**3246**

* For meaning of symbols, see footnotes to Tables I, II, and III.
** Assumed value of the fundamental. All of the fundamentals are non-degenerate, degeneracy $=d=1$.
*** **3061** is assumed to be two unresolved fundamentals, one at 3045, the other at 3075 cm^{-1}.

the Raman and infra-red spectra were accounted for as overtones or binary combinations. Frequencies corresponding to difference bands were again calculated only for the three lowest fundamentals, 318, 390, and 651. While the frequency near 1675 cm^{-1} may be due to the presence of an olefinic impurity, at least part of its intensity may be due to one of the combination bands given in Table III, the intensity of the combination band being enhanced by its nearness to the 1640 fundamental. Likewise, while the 1720 band may be due to an impurity containing a carbonyl group, at least part of its intensity may be accounted for as an overtone or combination.

Of the seven unassigned fundamentals, it seems likely that most of them lie in the 2700–3100-cm^{-1} region and escaped observation because of insufficient resolution, although it is, of course, possible that a few of the bands assigned as overtones or combinations may in reality be fundamentals. A high resolution investigation in the 3000-cm^{-1} region would probably lead to an improved assignment. An experimental measurement of the heat capacity at various temperatures and a quantitative determination of the depolarization factors of the Raman lines would also provide useful data for a revision of the present tentative and incomplete assignment.

Methylenecyclobutane

If the five carbon atoms and the two hydrogen atoms of the methylene group lie in a plane, as seems probable in view of Wilson's analysis of cyclobutane,[15] the symmetry of methylenecyclobutane is C_{2v}. For this structure, there should be eleven type-A_1 frequencies (of which four are

[15] T. P. Wilson, J. Chem. Phys. **11**, 369 (1943).

frequencies of the carbon skeleton), polarized in the Raman spectrum, parallel bands in the infra-red; five type-A_2 frequencies (none of which are carbon skeleton frequencies), depolarized in the Raman spectrum, forbidden in the infra-red; eight type-B_1 frequencies (two of which are carbon skeleton frequencies), depolarized in the Raman spectrum, perpendicular bands in the infra-red; and nine B_2 type frequencies (three of which are carbon skeleton frequencies), depolarized in the Raman spectrum, perpendicular bands in the infra-red. The type-B_2 frequencies are symmetrical with respect to the plane of the ring. There are thus a total of 33 fundamentals, of which 9 are carbon skeleton frequencies and 24 are C—H frequencies.

A tentative assignment of the fundamentals is given at the right in Table IV. Frequencies selected as carbon skeleton fundamentals were those at 354, 373, 657, 728, 879, 895, 954, 991, and 1675 cm^{-1}. The 954-cm^{-1} frequency, because of its great intensity in the Raman spectrum, certainly corresponds to the totally symmetrical, type A_1, "breathing" frequency of the ring. The corresponding frequency for cyclobutane itself appears[15] at 1010 cm^{-1}.

Twenty-one of the C—H frequencies were tentatively assigned; they are the ones at (782), 1029, 1059, 1070, 1155, 1167, 1197, 1248, 1395, 1415, 1425, 1490, (2770), 2826, 2860, 2902, 2921, 2952, 2985, 2985, and 3072 cm^{-1}, the ones in the parentheses being relatively less certain than the others.

Previous results[16] for olefins showed that for molecules containing an $XXC{=}CH_2$ group Raman lines were generally observed near 1300, 1410, 1650, 2980, and 3075 cm^{-1}. Observed frequencies for the methylenecyclobutane that probably correspond to these are the ones at 1248, 1415, 1675, 2985, and 3072 cm^{-1}. The 1675-cm^{-1} frequency is the skeleton frequency associated with the stretching of the carbon-carbon double bond.

The olefinic frequency at 2985 cm^{-1} is believed to be coincident with a ring C—H frequency, for cyclobutane itself has a strong Raman line at 2988 cm^{-1}. Furthermore, for cyclobutane the most intense C—H Raman line is at 2962 cm^{-1}, while for the present compound the strongest Raman line is the one at 2986 cm^{-1}. This change in the relative intensities is understandable if one supposes that the band observed near 2985 cm^{-1} is in reality two unresolved bands, one due to the ring hydrogens, the other to the olefinic hydrogens. This is the basis for assigning two C—H fundamentals with the same frequency at 2985 cm^{-1}.

The five, type-A_2, C—H frequencies are allowed in the Raman spectrum, but are forbidden in the infra-red spectrum. Four of these five type-A_2 frequencies can be ascribed to the four Raman lines observed at 2826, 2921, 2952, and 3072 cm^{-1}. The remaining one could be one of the supposedly coincident lines at 2985 cm^{-1}.

The remaining observed bands can be accounted for as P and R branches, binary combinations, or overtones. While the overtones $A_2{}^n$ (n odd) and the binary combinations $A_1{\times}A_2$ are forbidden in the infra-red, this would not affect any of the overtones or binary combinations used here, since the assigned A_2 fundamentals were all in the 3000-cm^{-1} region. The only other binary combinations forbidden in the infra-red are the $B_1{\times}B_2$ ones, and it is possible that some of the binary combinations used may have involved a type-B_1 and a type-B_2 frequency. In many cases, however, there were several binary combinations that could have been used to account for the observed band, so that the elimination of the $B_1{\times}B_2$ combinations if and when the B_1 and B_2 frequencies are identified would probably not be difficult. All overtones and binary combinations are allowed in the Raman spectrum.

It seems likely that the three unassigned C—H fundamentals exist as unresolved lines, probably in the 3000-cm^{-1} region where the resolution was poorest, although it is of course possible that some of the bands accounted for as overtones or combinations may actually be fundamentals. Precise depolarization factors of the Raman lines and high resolution studies, particularly in the 3000-cm^{-1} region, should provide useful information for a revision of the present tentative and incomplete assignment.

ACKNOWLEDGMENTS

The Hilger, E-518 spectrograph used to secure the polarization spectrograms of spiropentane

[16] Forrest F. Cleveland, J. Chem. Phys. 12, 53 (1944).

was obtained, in part, with a grant to one of us (F.F.C.) from the Permanent Science Fund of the American Academy of Arts and Sciences. The microdensitometer used in the intensity measurements was obtained with a grant (to F.F.C.) from the Penrose Fund of the American Philosophical Society. The optical parts of the two-prism spectrograph used to secure the Raman spectrograms of 1,1-dimethylcyclopropane, 1-methylcyclobutene, and methylenecyclobutane were obtained with a grant (to F.F.C. and M.J.M.) from the Society of the Sigma Xi. The authors are grateful for this assistance.

The authors wish also to thank Dr. Verner Schomaker for supplying the sample of 1-methylcyclobutene.

Letters to the Editor

THIS section will accept reports of new work, provided these are terse and contain few figures, and especially few halftone cuts. The Editorial Board will not hold itself responsible for opinions expressed by the correspondents. Contributions to this section should not exceed 600 words in length and must reach the office of the Managing Editor not later than the 15th of the month preceding that of the issue in which the letter is to appear. No proof will be sent to the authors. The usual publication charge ($4.00 per page) will not be made and no reprints will be furnished free.

Raman Tube Filters

GEORGE GLOCKLER AND JOHN F. HASKIN
Department of Chemistry and Chemical Engineering, State University of Iowa, Iowa City, Iowa
September 4, 1947

SANNIE, Amy, and Paremsky[1] have studied the use of several materials, including nitrobenzene and rhodamine 5G extra in alcohol, for the isolation of the 5358 mercury line as a source of Raman excitation. A modification of this procedure by Edsall and Wilson[2] consisted of 2 percent *p*-nitrotoluene and 1:50000 rhodamine 5 GDN extra (duPont) in alcoholic solution. Crawford and Horwitz[3] replaced the *p*-nitrotoluene by a Wratten 2-A gelatin filter wrapped around the Raman tube.

We have used the Raman apparatus described by Glockler and Tung[4] except that the polaroid has been omitted. One of the Raman tubes was provided with the filter under observation, while the other tube had no filter, and since the exposures were simultaneous, a direct comparison was obtained. The circular arrangement of the twelve General Electric A-H2 mercury vapor lamps made it desirable that we develop cylindrical plastic filters. Various plastic dopes were centrifugally cast on the inside of glass or methacrylate tubing of slightly larger diameter than that of the Raman tube. Methyl methacrylate molding powder dissolved in acetic acid and acetic anhydride, or in chloroform with a small amount of amyl acetate has been found convenient for use with rhodamine 5 GDN extra. After the dye or other absorbing material had been dissolved in the solvent, the molding powder was added. A number of coats of the dope were applied until the desired absorption characteristics were obtained. This procedure was found unsatisfactory when *p*-nitrotoluene was employed because the necessarily high concentration caused it to crystallize out from the polymer. Modifying the procedure used by Shenk, *et al.*[5] for infra-red filters, we found that 15 percent *p*-nitrotoluene solutions could be satisfactorily set. In view of its 90 percent transmission in the region 3800–6200, Beetle 230–8,[6] an unmodified urea-melamine-formaldehyde resin, was selected as the base. To prevent cracking and peeling it was plasticized with Rezyl 330–5,[6] an oxidizing-type phthalic alkyd. A suitable dope consisted of approximately 63 percent Beetle, 20 percent Rezyl, 15 percent *p*-nitrotoluene, 1.5 percent Beckamine accelerator,[7] 0.5 percent Gui-A-Phene[8] antiskinning agent, and the desired amount of rhodamine. Using the latter plastic, we have applied up to 20 coats, and obtained thicknesses of about 1.6 mm for the finished filters. Such filters transmit up to 65 percent of 4358 and less than 10 percent of 4047, with very little continuous background on a benzene spectrum.

In order to reduce the number of reflecting surfaces, we have coated the Raman tube directly with the filter dope. The above techniques were used, except that the Raman tube was dipped or sprayed, and then placed on a slowly rotating spindle until the solvent had evaporated. Heat was applied to the thermo-setting resins by means of an infra-red lamp. 140 hours of direct exposure to a General Electric A-H2 produced no significant change in the transmission of these filters.

In addition, we have satisfactorily removed 4047 by means of a plastic dope furnished by General Aniline and Film Corporation, and also by using an Eastman 2-A gelatin filter. For the removal of continuous background, an Eastman X-3225 gelatin filter produced results similar to those obtained from solutions or plastic filters into which rhodamine 5 GDN extra had been incorporated.

We have found that plastic filters are not only more convenient when applied directly to the Raman tube, but also eliminate some of the extra reflecting surfaces created by several liquid filter jackets or separate solid filters, and they may prove to be more stable than solutions.

[1] C. Sannie, L. Amy, and V. Parmesky, Bull. Soc. Chem. France **3**, 2018 (1936).
[2] J. T. Edsall and E. B. Wilson, Jr., J. Chem. Phys. **6**, 124 (1938).
[3] Byrce L. Crawford, Jr. and William Horwitz, J. Chem. Phys. **15**, 268 (1947).
[4] G. Glockler and Jo-Yun Tung, J. Chem. Phys. **15**, 112 (1947).
[5] John H. Shenk, Edwin S. Hodge, Robert J. Morris, Edward E. Pickett, and Wallace R. Brode, J. Opt. Soc. Am. **36**, 569 (1946).
[6] American Cyanamid and Chemical Corporation.
[7] Reichhold Chemicals, Inc.
[8] Southern Pine Chemical Company.

The Separation of the Isotopes He^3 and He^4 in the Liquid Phase*

J. G. DAUNT, R. E. PROBST, AND H. L. JOHNSTON
The Cryogenic Laboratory, Department of Chemistry and Department of Physics, The Ohio State University, Columbus, Ohio
August 11, 1947

A PARTIAL concentration of the rare isotope He^3 present in atmospheric helium[1] with an abundance ratio[2] of 1.22×10^{-6} has been effected by a method involving the superfluid flow of liquid helium II. We have previously reported[3] that the transference of liquid helium II from one reservoir to another by means of superfluid flow through a supra-surface film effectively filters out the isotope He^3, the superflow through films therefore being a process in which, at the temperature employed, He^3 atoms do not partake, as has been suggested by Franck.[4] Since these experiments[3] were restricted to flow through supra-surface films, it was of interest to observe whether a similar filtration takes place for superfluid flow through narrow channels in the bulk liquid. The results obtained are given below.

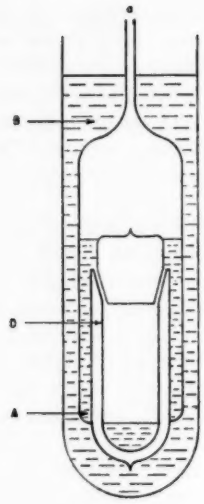

FIG. 1.

The experimental arrangement is illustrated in Fig. 1. The vessel B represents the main helium bath. Immersed in B is the vessel A, of which a small Dewar, D, formed an integral part. The top of D was closed off by an evacuated glass plug ground to fit the Dewar. Atmospheric helium[5] could be condensed in A, via the tube a. It was found that at 4.2°K the flow of helium through the ground joint at the top of D was negligible, even though the level of the liquid in A was well above the ground joint. From estimates of this minute flow, the channel width of the ground joint was assessed at 1 micron.

When the whole arrangement was cooled below the lambda-point, the liquid flowed rapidly from A into D, at 1.5°K the rate being 1.25 cc per minute, until the level in A fell just below the rim of the ground joint. From then on liquid would have flowed into D through the supra-surface film at a rate of approximately 10^{-2} cc per minute. The liquid remaining in A was evaporated at this stage, and subsequently the liquid in D was evaporated and its vapor collected separately.

The abundance ratio of helium isotope He^3 in the vapor collected during two different runs was kindly measured for us by Professor Alfred O. Nier and Mr. L. T. Aldrich[2] to whom we wish to express our appreciation of their cooperation. The He^3/He^4 ratio for A was 1.85×10^{-6} and 1.55×10^{-6} for the two runs, this increase over the normal concentration for atmospheric helium[2] depending on the initial volume condensed. For the vapor from B the average values were 0.37×10^{-6} and 0.35×10^{-6}.

One may conclude that the He^3 was at least partially filtered out by flow through the channel. It was difficult to estimate how complete this filtration might have been since in cooling from 4.2°K some liquid was condensed from the vapor already present in D. Calculation of this effect indicates that the filtration was almost complete, and certainly much more effective than might be concluded from direct calculation from the figures given above. Experiments to determine this effect more exactly are being persued and will be given in detail elsewhere.

The method of filtration of the isotope He^3 by superfluid flow in the liquid phase, whether through supra-surface films[3] or through narrow channels in the bulk liquid, is one which, apart from its theoretical interest,[4,3] may lead to an isolation of the rare isotope in sufficient quantities for many applications. Such work is now in progress.

* This work was assisted by Navy Contract No. N6onr-225.T.O.III between the Office of Naval Research and The Ohio State Research Foundation.

[1] L. W. Alvarez and R. Cornog, Phys. Rev. **56**, 379, 613 (1939).
[2] L. T. Aldrich and A. O. Nier, Phys. Rev. **70**, 983 (1946); see also H. A. Fairbank, C. T. Lane, L. T. Aldrich, and A. O. Nier, Phys. Rev. **71**, 911 (1947).
[3] J. G. Daunt, R. E. Probst, H. L. Johnston, L. T. Aldrich, and A. O. Nier, Phys. Rev. **72**, 502 (1947).
[4] J. Franck, Phys. Rev. **70**, 561 (1946).
[5] We are grateful to Linde Air Products for kindly providing large quantities of atmospheric helium.

The Time Effect in the Fracture of Glass and Other Materials

EDWARD SAIBEL*
Carnegie Institute of Technology, Pittsburgh, Pennsylvania
August 11, 1947

ONE of the important problems in the mechanical properties of glass as well as of other substances is that of the delayed time to fracture. Specimens which do not fail during the time it takes a load to build up to its maximum value may subsequently fracture under the steady application of the load even in the absence of the chemical effects of the atmosphere, which will be the case considered here.

Considerable data have been accumulated and a variety of methods of plotting functions of fracture stress against functions of time have been advanced in the hope that one of them would yield a straight-line relationship and thereby disclose some rational explanation of the phenomenon. Most of the methods of plotting seem to show about equally good approximations to a straight line. This may be because of the experimental errors involved as well as the limited extent of the data.

The author proposes to treat the problem from the point of view of chemical-reaction rate theory in which the breaking of bonds between ions or atoms is the product of the reaction. Although this method has been used before,[1] no account has been taken of either the rate at which the external loads are applied or of the effect of the breaking of bonds upon the remaining ones. The present treatment is an attempt to take both cases into account.

In the usual notation,[2] the net number of jumps of the flow unit per unit time (rate at which bonds are broken) in the presence of a potential gradient is given by:

$$\frac{dN}{dt}=\frac{2kT}{h}e^{-\frac{\Delta F^*}{RT}}\sinh\frac{w}{kT}, \tag{1}$$

where N is the number of bonds broken and w is the work done per flow unit in the process. The latter may be related to the force, f, necessary to break a bond through $w=f(\lambda/2)$, where λ is some distance through which f must act to break the bond.

Equation (1) may be written:

$$dN/dt=A\sinh Bf, \tag{2}$$

where A and B do not depend upon the applied potential gradient.

If the load acts in a steady manner, it may be assumed as a first approximation that the force tending to break a bond increases directly with the number of bonds which have already been broken. Consequently, $f=f_0+cN$, where f_0 is the force tending to break the bond when the load is first applied. Substituting this relation into Eq. (2), integrating, and assuming that when fracture takes place the number of bonds broken is large, there results

$$f_0=D\log\coth Et \tag{3}$$

as the relation between the initially applied stress, f_0, and the time to fracture, t; D and E are constants which may be expressed in terms of A, B, and c. Through A and B the temperature dependence of the process may be studied.

For long times, Eq. (3) may be written:

$$f_0=2De^{-2Et}. \tag{4}$$

For short breaking times, the effect of the rate of loading is predominant, and the additional stresses in the remaining bonds due to the breaking of bonds may be neglected. Assuming that the rate of loading is constant, f may be expressed in the form

$$f=rt. \tag{4}$$

Substituting this into Eq. (2) and integrating leads to

$$t=(1/Br)\cosh^{-1}[(BrN_B/A)+1],$$

N_B being the number of bonds broken to bring about fracture. If the rate of loading is high and the first term in the parentheses large, this becomes approximately

$$t=(0/Br)\log Fr, \tag{5}$$

where F is a constant. This is a relation between the time to fracture, t, and the rate of loading, r. It is interesting to note that Eq. (5) also implies the temperature dependency of the process through the constant B and through F, which in turn depends on A and B. In a paper which the author expects to publish soon, the details and a comparison with experimental data will be given.

* Consultant to Glass Science, Incorporated.

[1] E. S. Machlin and A. S. Nowick, N.A.C.A. Tech. Note No. 1126 (September, 1946).

[2] Glasstone, Laidler, and Eyring, *The Theory of Rate Processes* (McGraw-Hill Book Company, Inc., New York, 1941).

A Formula to Detect Association in Liquids

R. PARSHAD*
Physical Laboratory, Council of Scientific and Industrial Research, Delhi, India

July 28, 1947

THERE are various formulas in literature which distinguish a normal liquid from an abnormal or associated liquid. In the following we present another such theory.

For normal liquids

$$E\chi/V\alpha=T,$$

and for associated liquids,

$$E\chi/V\alpha>T,$$

in which E is cohesive energy in ergs per mole, expressed as the latent heat of vaporization minus RT, and written positive.

χ is the isothermal compressibility in absolute units (barye^{-1}),
V is the molar volume in ccms,
α is the coefficient of cubical expansion, and
T is the absolute temperature.

As an example, we compute the formulas at 20°C = 293°A. (See Table I.) The data for the liquids were mainly taken from International Critical Tables and tables of Landolt-Bornstein. Generally, a direct value of E and χ at 20°C and one atmospheric pressure was not available, and a rough reduction was made simply by guessing. The absence of round figures in most of the E values does not indicate the order of accuracy attained, but that the reduction was made for a value per g and then the value was multiplied

TABLE I. $E\chi/V\alpha$ for liquids.

No.	Liquid	E $\times10^{-7}$ ergs	χ $\times10^{12}$	V	α	$\frac{E\chi}{V\alpha}$
		Class I				
1	Pentane	27000	200	114.9	.001589	295
2	Iso-pentane	25920	225	117.0	.001533	325
3	Hexane	31390	150	130.3	.001445	250
4	Heptane	35000	134	146.3	.00115	279
5	Octane	37620	121	162.4	.001124	249
6	Decane	48280	102	194.3	.000988	256
7	Ether	27010	200	104	.001656	310
8	Acetone	32016	100	73.5	.001487	292
9	Cyclohexane	31080	109	105.4	.00114	282
10	Cyclohexanol	50000	55	105.5	.000804	324
11	Carbon tetrachloride	32953	105	96.5	.001206	297
12	Chloroform	30989	100	80.2	.001254	308
13	Carbon disulphide	28138	75	60.3	.0011823	296
14	Ethylene chloride	33810	80	78.9	.00112	308
15	Ethylene bromide	42255	60	86.1	.000942	312
16	Methyl iodide	39110	56	62.2	.001273	276
17	Methyl acetate	33670	90	79	.00136	281
18	Ethyl bromide	29403	105	74.6	.00141	293
19	Ethyl iodide	31980	95	80.8	.001179	310
20	Ethyl formate	35558	75	80.2	.001378	241
21	Ethyl acetate	34359	113	97.9	.001359	292
22	Ethyl propionate	40800	98	115.0	.001344	264
23	Ethyl *n*-butyrate	46440	95	132.2	.001156	289
24	*n*-Propyl acetate	42840	100	115.1	.001214	306
25	Benzene	33883	92	89	.00124	282
26	Aniline	31080	44	84	.000855	265
27	Nitrobenzene	43970	54.5	105	.0008263	276
28	Chlorobenzene	42750	75	101.7	.0009967	316
29	Bromobenzene	58090	50	105	.00091505	302
30	*O*-Xylene	39220	75	118	.000973	257
31	*m*-Xylene	38160	85	122	.001009	274
32	*p*-Xylene	37600	80	124	.001011	240
33	Toluene	35420	92	106.3	.001099	279
34	*p*-Toluidine	46200	50	112.2	.0008681	259
		Class II				
1	Methyl alcohol	37440	95	140	.001229	735
2	Ethyl alcohol	41860	90	98	.000739	520
3	*n*-Propyl alcohol	42600	90	75	.000956	533
4	*i*-Propyl alcohol	41400	100	75	.001094	493
5	*n*-Butyl alcohol	46620	99	91.4	.000950	488
6	*i*-Butyl alcohol	45880	93	103.6	.0009	458
7	*n*-Amyl alcohol	47520	85	110	.000907	403
8	Allyl alcohol	40600	80	70	.0001241	500
9	Glycol	50840	34	56	.0006375	484
10	Glycerine	924000	22	73	.000505	552
11	Formic acid	28520	55	37.7	.000999	416
12	Acetic acid	27600	98	56	.001065	454
13	*n*-Valeric acid	54129	90	108.8	.0009886	453
14	Mercury	5897934	3.4	14.81	.00018169	745
15	Water	41706	45.5	18.06	.0002097	5010

by the proper molecular weight. The V and α values are comparatively more accurate to the figure described, because density-temperature relations of most of the liquids mentioned are given in the I.C. Tables.

It will be seen that despite the approximations used in computing the data, the liquids bifurcate neatly into two classes. From the variation of $E\chi/V\alpha$ for associated liquids, it can be seen that its magnitude depends not upon the strength of associations (carboxylic acids have much greater strength of association than water), but upon the amount of abnormal behavior of a liquid. It has already been shown that the abnormal behavior of an associated liquid depends not upon the strength of an association, but rather upon its weakness and extensiveness.

Mercury turns out to be an 'associated liquid,' but as it is a metallic liquid it cannot be discussed in the same class as the other organic molecular liquids.

The formula has more than passing interest, and its theoretical implications will be discussed in another paper.

* Present address: Department of Physics, Oregon State College, Corvallis, Oregon.

[1] R. Parshad, J. Chem. Phys. **14**, 348 (1946).

Microwave Spectrum and Structure of Isothiocyanic Acid*

C. I. Beard
Massachusetts Institute of Technology, Cambridge, Massachusetts
and
B. P. Dailey**
Harvard University, Cambridge, Massachusetts
September 12, 1947

To aid in the analysis of the complicated microwave spectrum of methyl isothiocyanate[1] a search for transitions of the simpler molecules HSCN and HNCS was made in the region from 19,000 to 30,000 mc/sec. Stark modulation apparatus[2,3] was used with a 10-foot wave guide absorption path of the acid vapor. Table I gives the absorption lines found for HNCS and its artificially enriched isotopic forms.

Table I. The absorption spectrum of isothiocyanic acid molecules.

Molecule	νmc/sec.
$HNC^{12}S^{32}$	23,464
$DNC^{12}S^{32}$	21,897
$HNC^{13}S^{32}$	23,389
$DNC^{13}S^{32}$	21,839
$HNC^{12}S^{34}$	22,915

The acid was prepared by gentle warming of a mixture of KSCN with H_3PO_4. The $HNC^{13}S$ was prepared from $KSC^{13}N$ obtained by fusing sulfur and $KC^{13}N$ containing 17 percent of C^{13}. The deuterium isotopes were made by the same processes, merely substituting D_3PO_4 for H_3PO_4.

In the preliminary analysis of the spectrum the assumption was made that the NCS group was linear and that, while the HNC angle differed from 180°, the molecule was very nearly a symmetric top. The symmetric Stark pattern of two components gives strong support to this assumption and indicates that the observed spectral lines correspond to transitions from $J=1$ to $J=2$. Using the symmetric top approximation that ν cm$^{-1}=2C(J+1)$, four of the frequencies of the lines of the isotopic molecules enable one to solve for approximate values of the three interatomic distances and the H−N−C angle, neglecting for the moment the effect of the zero-point vibrational energy on these parameters.

The solution for the structure HSCN results in quite unreasonable values of the bond distances and angle. The solution for the structure HNCS, however, yielded: HN = 1.2±0.1A, NC = 1.21±0.01A, CS = 1.57±0.01A, and the angle HNC = 112°±10°.

The NC and CS distances are intermediate between the values for double and triple bonds. The probable resonating structures are H−N=C=S, $H-N^{+}\equiv C-S^{-}$, and $H-N^{-}-C\equiv S^{+}$. The CS distance is the same as in COS and CS_2. The NCS distances for HNCS compare well with those obtained by Goubeau and Gott[4] from Raman spectra of NC = 1.21A and CS = 1.575A. The HNC angle of 112° compares with that of 111° obtained for the HNN angle of N_3H by Eyster.[5] The HN distance is larger than the 1.01A value in N_3H and NH_3 which may indicate partial ionic character of this bond.

The spectral analysis indicated that the vapor is principally isothiocyanic acid; HSCN if it exists in the vapor could not be present by more than 5 percent. Gallais and Voigt,[6] by measuring molecular magnetic rotations, conclude that the acid is isothiocyanic. Goubeau and Gott[4] also conclude that HNCS is the predominant form. The position and intensity of the very weak line at 22,915 mc indicate that it may be the $HNCS^{34}$ line due to the natural 4 percent abundance of S^{34}.

* The research reported in this paper was made possible through support extended Harvard University by the Navy Department (Office of Naval Research) under Office of Naval Research Contract N5ori-76 and Massachusetts Institute of Technology under Joint Service Contract W-36-039sc-32037.
** Present address: Department of Chemistry, Columbia University, New York, New York.
[1] C. I. Beard and B. P. Dailey, paper presented at the Am. Chem. Soc. meeting in New York, September 15, 1947.
[2] R. H. Hughes and E. B. Wilson, Jr., Phys. Rev. **71**, 562 (1947).
[3] B. P. Dailey, Phys. Rev. **72**, 84 (1947).
[4] J. Goubeau and O. Gott, Ber. **73B**, 127 (1940).
[5] E. Eyster, J. Chem. Phys. **8**, 135 (1940).
[6] F. Gallais and D. Voigt, Comptes Rendus **210**, 104 (1940).

Measurement of Na^+ Ion Diffusion by Means of Radiosodium

Arthur W. Adamson
Chemical Laboratories, University of Southern California, Los Angeles 7, California
July 29, 1947

An interesting application of the radioactive tracer technique is to the measurement of the diffusion of ions in solution. This approach was first made by Jehle,[1] who used Na^{24} and Cl^{38} to obtain ionic-diffusion constants in NaCl solutions. Similar work has been done by Schubert and others[2] on the Plutonium Project, and some preliminary studies have been described recently by Robinson

and Drew.[3] Such investigations are potentially of considerable fundamental importance since they constitute one of the few means of studying individual ion behavior.

The equation for the self-diffusion of an ion can be derived from the basic relationship: $\mathfrak{D}=-nw\partial\mu/\partial n$, where n is the moles per cc, w the mobility, and μ the chemical potential of the ion. On expressing mobility in terms of equivalent conductance and introducing the activity coefficient, it follows that for a monovalent ion

$$\mathfrak{D}(\text{cm}^2/\text{sec.})=8.97\times10^{-10}\lambda_+T(1+c\partial\ \ln\gamma_+/\partial c). \quad (1)$$

Using the limiting-law expression, $\log\gamma_+=0.508(c)^{\frac{1}{2}}$ (1) becomes:

$$\mathfrak{D}(\text{cm}^2/\text{day})=0.0231\lambda_+[1-0.583(c)^{\frac{1}{2}}] \text{ at } 25°\text{C}. \quad (2)$$

Equation (2) applies to the diffusion of a tracer in an otherwise uniform solution, and hence is much simpler than that of Onsager and Fuoss.[4] For example, it is not necessary to relate the net movement of the trace ions to that of the oppositely charged ions by the requirement of electro-neutrality, necessary when a bulk concentration gradient exists. Thus, under these circumstances, the differential diffusion coefficient for the ion is obtained, rather than the mean coefficient for the salt.

Another feature of tracer studies is that the measurements may be extended to smaller concentrations than has otherwise been possible (*ca.* 10^{-5}M).

Preliminary investigations have been carried out in this laboratory on the diffusion of Na^+ ion in NaI solutions at 25°C, using Na^{22} (3 yr.) as tracer.[5] The data were obtained by means of McBain-Northrup[6] type, sintered-glass diaphram cells which were calibrated by allowing 0.20 N HCl to diffuse into water. The mean diffusion constant for the HCl was taken to be 2.52 cm²/day, from the data of James and Gordon.[7] Separate tests showed that the tracer sodium was in the same chemical state as the bulk Na^+. For the self-diffusion measurements, both compartments of the cell were filled with NaI solutions, identical except for tracer in the upper cell. The diffusion constant at each bulk NaI concentration was obtained from the amount of tracer present in the lower compartment after a given time. Radio-chemical analyses were made by evaporating aliquots on 1-in. watch glasses and counting by means of a mica-window tube and a scaling circuit.[8]

The results are shown in Fig. 1, where $\mathfrak{D}$ is plotted against $(c)^{\frac{1}{2}}$, and can be represented up to $c=0.01$M by the equation:

$$\mathfrak{D}=\mathfrak{D}_0(1-1.40(c)^{\frac{1}{2}}), \quad \mathfrak{D}_0=1.24 \text{ cm}^2/\text{day}. \quad (3)$$

Where duplicate runs were made, the average deviation was about 1 percent, close to the practical limit set by the various counting errors.

To compare these results with (2), λ_+ must be evaluated as a function of concentration. This was done using the Onsager equation[9] for a 1:1 electrolyte at 25°C.

$$\lambda_+=\lambda_+^0-[0.221\lambda^0+29.9(c)^{\frac{1}{2}}],$$
$$\lambda_+=50.1[1-0.825(c)^{\frac{1}{2}}] \text{ for NaI}. \quad (4)$$

On combining Eqs. (2) and (4), the approximate relationship is obtained:

$$\mathfrak{D}(\text{cm}^2/\text{day})=1.16[1-1.41(c)^{\frac{1}{2}}]. \quad (5)$$

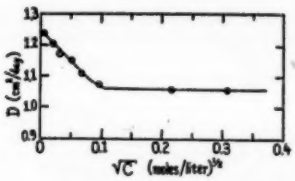

FIG. 1. Diffusion coefficient of Na^+ in NaI solutions at 25°C.

The observed dependence on concentration is in satisfactory agreement with Eq. (5), but $\mathfrak{D}_0$ is about 7 percent greater than the theoretical value. A similar effect is apparent in Jehle's data.

It is planned to present results on I^- diffusion rates in a later paper, together with a more complete discussion.

[1] L. P. Jehle, Ph.D. Thesis (University of California at Berkeley, 1938).
[2] Private communication.
[3] L. B. Robinson and J. B. Drew, J. Chem. Phys. **15**, 417 (1947).
[4] L. Onsager and R. M. Fuoss, J. Phys. Chem. **36**, 2689 (1932).
[5] Supplied by Dr. Clarke at the Massachusetts Institute of Technology.
[6] J. W. McBain and T. H. Liu, J. Am. Chem. Soc. **53**, 59 (1931).
[7] W. A. James and A. R. Gordon, J. Chem. Phys. **7**, 963 (1939).
[8] Some of the counting was done by Miss J. P. Welker.
[9] H. S. Harned and B. B. Owen, *The Physical Chemistry of Electrolytic Solutions* (Reinhold Publishing Corporation, New York), p. 129.

A New Type of Micelle: Soap with Alcohol, Amine, or Other Polar-Nonpolar Molecules*

W. D. HARKINS, R. W. MATTOON, AND R. MITTELMANN
George Herbert Jones Chemical Laboratory, University of Chicago, Chicago 37, Illinois
July 20, 1947

A MEASURE of the thickness of the micelle of a colloidal electrolyte is the spacing d_M' derived from a newly recognized, x-ray diffraction M-band.[1] The unmodified Bragg spacing d_M for potassium caprate (10°C) is 31.7, for the laurate (12°C) 35.3, and for the myristate (14°C) 40.3A. For the corrected micelle thickness these Bragg spacings should be increased by perhaps 10 to 15 percent, but this modification is omitted here for simplicity. An aqueous solution of soap or colloidal electrolyte, when saturated with a hydrocarbon such as benzene, ethyl benzene, or n-heptane, shows a micelle thickness increased by as much as 12A (Table IA), which is presumably the thickness Δd_M of the oil layer. There is no evidence that the oil molecules *penetrate between* the hydrocarbon chains of the soap molecules in the double monolayer, since the area per soap molecule remains at 27A². Thus, hydrocarbons are apparently solubilized in the middle of the micelle between the ends of the hydrocarbon chains of the soap molecules.

The attraction between a hydrocarbon and water is increased if a terminal hydrogen atom is replaced by a hydroxyl group. For example, the energy of adhesion at 20°C between n-heptane and water is 41 ergs/cm² and the

TABLE I. Micelle thickness changes due to "oils" dissolved in aqueous solutions of pure potassium myristate (KC_{14}) and pure sodium lauryl sulfate ($NaC_{12}SO_4$) at 25°C.

	"Oil"	Percent by wt. of soap		Grams "oil" per 100-g soap solution	Simple Bragg spacing $d_M \pm 1$A	M-Spacing change[a] due to "oil" $\Delta d_M \pm 2$A
A.	benzene	7.16	KC_{14}	2.66[b]	52.0	+11.7
	ethyl benzene	8.65	$NaC_{12}SO_4$	2.81[c]	44.0	+ 6.7
	n-heptane	8.65	$NaC_{12}SO_4$	1.46[d]	44.4	+ 7.1
B.	n-heptanol	7.16	KC_{14}	2.4[b]	42.0	+ 1.7
	n-heptanol	9.82	KC_{14}	3.0[d]	41.0	+ 0.7
	n-heptanol	8.65	$NaC_{12}SO_4$	2.98[d]	39.0	+ 1.7
	n-octanol	8.65	$NaC_{12}SO_4$	2.21[d]	39.6	+ 2.3
	n-decanol	8.65	$NaC_{12}SO_4$	2.16[d]	37.5	+ 0.2
	n-decanol	7.16	KC_{14}	1.83[b]	42.5	+ 2.2
	n-decylamine	8.65	$NaC_{12}SO_4$	1.74[d]	36.0	− 1.3
	n-decylamine	8.65	$NaC_{12}SO_4$	1.85[c]	35.3	− 2.0

[a] Without "oil," at any concentration d_M for $NaC_{12}SO_4$ is 37.3 and for KC_{14} is 40.3A.
[b] Just saturated.
[c] The saturation value is slightly less than this figure.
[d] Slightly under-saturated.

total energy of adhesion is 93. For n-heptanol these values increase to 92 and 165, respectively. The attraction of water is not sufficient to allow solubilized hydrocarbon molecules to pass from the interior of a micelle *into* its soap layer and contact the surrounding water. However, the larger attraction of water for the hydroxyl groups of alcohols might enable these molecules to penetrate and become part of the layer of oriented soap molecules.

If a cetyl alcohol monolayer is spread on water and the area adjusted to 25A² per molecule, the film pressure at 20°C is only 1.2 dynes/cm. If the aqueous subphase is made $3(10)^{-6}$ molar sodium cetyl sulfate, and the total film area kept constant, detergent molecules penetrate into the alcohol monolayer until at equilibrium the film pressure increases[2] to 50 dynes/cm—an increase of over 40 times. To squeeze detergent molecules out of this layer would require a lateral film pressure equivalent to 200 atmospheres, and the alcohol monolayer would remain under this pressure.

Considering these relations, it is to be expected that molecules of long-chain alcohols, amines, or similar polar-nonpolar compounds, when dissolved in an aqueous solution of soap or similar colloidal electrolyte, will actually *penetrate* between the soap molecules and produce a larger mixed micelle. Presumably, the polar groups are between the ionic groups of micellar soap molecules, both being in contact with the water. This should reduce the repulsion between the ionic groups and thus make the micelle more stable and larger. These expectations seem to be substantiated by the following experimental results.

The micelle thickness is not appreciably altered, within the experimental error, by dissolved n-alcohols and n-decylamine (Table IB).

By a method of uncertain accuracy developed by Mattoon, the average numbers of soap and "oil" molecules per micelle, n_s and n_0, are calculated from the modified long-spacing x-ray I-band, assuming that it measures the average distance between the nearest micelles. For a 15 percent aqueous solution of potassium laurate, this calculation gives $n_s \approx 76$; when saturated with ethyl benzene, $n_s \approx 150$ and $n_0 \approx 70$; when saturated with n-dodecanol, $n_s \approx 180$ and $n_0 \approx 68$. Although these numbers may not be exact, they indicate larger micelles with either hydrocarbons or alcohols dissolved.

Solubilized hydrocarbons change the critical micelle concentration by a small amount. However, 3 percent of n-butanol decreases[3] the *c.m.c.* of dodecyl ammonium chloride by 67 percent and as little as 0.1 percent of n-heptanol decreases the *c.m.c.* of potassium myristate by 33 percent.

H. Oppenheimer here has found that n-heptanol is more than twice as soluble as n-heptane in aqueous potassium myristate solutions. Also, if s represents the "oil" solubility and c the soap concentration, then $(\partial s/\partial c)_T$ increases with increasing c for hydrocarbons and apparently decreases slightly for n-heptanol.

The contrast in the behavior of hydrocarbons and of long-chain alcohols and amines, cited above, indicates that hydrocarbons *solubilize* in the interior of the micelle, whereas alcohols and amines *penetrate* into the monolayer of soap molecules making up the double-layer micelle.

The total solubility of "oils" in aqueous micellar solutions may be classified as follows:

1. Solubility in water, or in non-micellar solution.
2. Solubility by adsorption on the outer surface of the micelle.
3. *Solubilization* in the middle of the micelle.
4. Solubility by *penetration* into the micellar soap layer.

* This investigation was carried out under the sponsorship of the Reconstruction Finance Corporation, Office of Rubber Reserve, in connection with the Government's synthetic rubber program.

[1] R. W. Mattoon, R. S. Stearns, and W. D. Harkins, J. Chem. Phys. 15, 209 (1947).
[2] W. D. Harkins, L. E. Copeland, and B. Gordon, "Surface chemistry," Pub. 21, Am. Assoc. for the Advancement of Science, p. 79, 1943.
[3] M. L. Corrin and William D. Harkins, J. Chem. Phys. 14, 640 (1946).

An Objective Method for Studying Electron Diffraction by Gases

J. KARLE AND I. LUGOSKI KARLE
Naval Research Laboratory, Washington 20, D. C.

August 21, 1947

THE device described in the previous letter produces a microphotometer trace which may be used for objective study of electron-diffraction negatives. Hitherto these have been interpreted mainly by visual observation. The microphotometer trace as obtained from a standard diffraction negative is limited in usefulness since the molecular portion of the scattered intensity is superimposed on a steeply falling background. The suggestion has been made[1,2] to insert a rotating sector into the diffraction camera which can flatten the background and accentuate the oscillating portion of the diffraction pattern. In practice, this method is rather inconvenient to apply.[3] We have

found it possible to perform the necessary mathematical manipulation directly on the intensities obtained from the linear-response region on the improved microphotometer trace. The procedure could perhaps be further improved by employing in combination with the improved tracing method a simplified sector technique[3] which partially reduces the background effect. The advantage of the simple sector is to extend the range of scattering angle included in the linear-response region of the photographic plate.

The intensity of electron scattering by gases is proportional to

$$\sum_i^N (S_i/s^4)+\sum_i^N (f_i^2/s^4)+\sum_{ij}^N (f_i f_j/s^4)A(r_{ij}, s), \quad (i\neq j). \quad (1)$$

The symbols are explained in a review article by Brockway.[4] A simple sector would multiply this intensity by some convenient power of s. The incoherent term S_i can usually be neglected and the scattering factors of the atoms in the molecule may generally be written as $f_i=f\times Z_i$, where f is a general shape function. In our method the intensities for closely spaced s values are derived from the microphotometer trace and are multiplied by $1/f^2$ and by the required power of s to remove the s^4 from the denominator of (1). Effectively, this process gives

$$\sum_i^N Z_i^2+\sum_{ij}^N Z_i Z_j A(r_{ij}, s), \quad (i\neq j), \quad (2)$$

which is the molecular scattering function superimposed on a level background. The curve obtained in this way may be treated by the correlation procedure as well as the radial-distribution method. Although the factor s^n/f^2 usually applies, it is occasionally necessary to make a correction for the possible variation in the shapes of the scattering factors for small s values and when atoms of very different atomic numbers are present in the molecule.

[1] C. Finbak, Avh. Norsk Vidensk.-Acad., Oslo, M.-N.Kl., No. 13 (1937).
[2] P. P. Debye, Physik. Zeits. **40**, 66, 404 (1939).
[3] C. Finbak, O. Hassel, and B. Ottar, Arch. f. Math. og Nat., Oslo **B44**, No. 13 (1941).
[4] L. O. Brockway, Rev. Mod. Phys. **8**, 231 (1936).

An Improved Microphotometer Trace of Radially Symmetric Patterns

I. Lugoski Karle, D. Hoober, and J. Karle
Naval Research Laboratory, Washington 20, D. C.
August 21, 1947

A DEVICE has been constructed for producing a smooth and accurate microphotometer trace from radially symmetric patterns by minimizing the variations due to the granular character of the emulsion. This device spins the negative while it is being traced. A previous suggestion to this effect has been made by Degard, Pierard, and van der Grinten.[1] The improved trace obtained in this manner makes it possible to use an objective method for analyzing electron-diffraction patterns of gases which consist of oscillations about a steeply falling background.

The spinning attachment shown in Fig. 1 is attached to

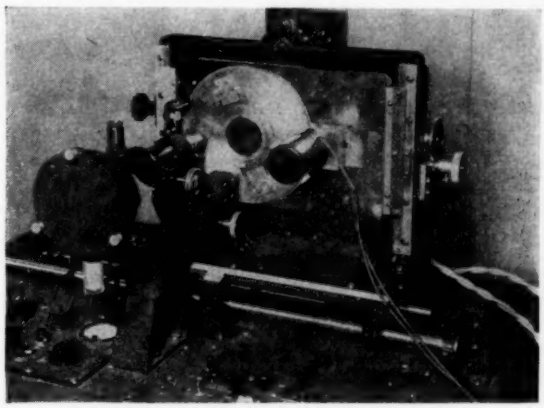

FIG. 1. Photograph of the rotating attachment in place on the Leeds and Northrup microphotometer.

the Leeds and Northrup microphotometer and consists of a geared ring large enough to hold a plate 2 in. by 4 in. The geared ring is mounted into its frame on adjustable ball bearings and is spun by a 0.01-hp alternating current motor whose maximum rated speed is 7000 r.p.m. The gear ratio is 12.5:1, and in practice the motor speed is controlled by an auto-transformer since its maximum speed is not required. The photographic plate is centered by means of cross-hairs on a Lucite disk which is removed for the tracing. The plate is then aligned with respect to the optical system on the microphotometer and is ready to be spun and traced. The improvement of the trace by averaging over the grains of the emulsion is shown in Fig. 2, where A is the

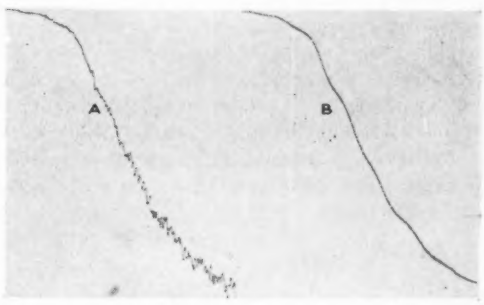

FIG. 2. Microphotometer traces of an electron-diffraction pattern: A, without rotation of the plate, B, with rotation using the same slit system.

trace of the stationary plate and B is the trace of the rotated plate. The microphotometer beam was focused to about 0.02 mm by 0.2 mm on the Eastman commercial plate and was the same for both traces.

[1] C. Degard, J. Pierard, and W. van der Grinten, Nature **136**, 143 (1935).

Influence of Interatomic Forces on Paraffin Properties

HARRY WIENER
Department of Chemistry, Brooklyn College, Brooklyn, New York
July 29, 1947

EMPIRICAL formulas giving excellent agreement with observed molecular refractions, molecular volumes, heats of formation, and boiling points of the paraffin isomers have recently been reported by Platt[1] in this journal. The variables used in these formulas are based on the assumptions of additivity of bond properties and of interaction between different bonds in a molecule. The agreement between observed and calculated values should, however, not be taken as evidence for the influence, additive or constitutive, of bonds upon physical properties; the same basic formula may be derived by a different approach.

The forces acting between two atoms will depend on their kind and distance. Without any assumption as to the nature of these interactions, the sum of the forces acting between n pairs of atoms, of kind x and y, all of which are separated by an equal distance j, will be $k_{xyj}n$. For a paraffin, let n_j be the number of C−C pairs separated by j carbon-carbon bonds, P_{j+1} the number of C−H pairs separated by one carbon-hydrogen and j carbon-carbon bonds, and q_{j+2} the number of H−H pairs separated by two carbon-hydrogen and j carbon-carbon bonds. The sum of all these interactions, or atom-pair contributions to the property G, is

$$G-a_0=\sum_j a_jn_j+\sum_k b_kp_{k+1}+\sum_i c_iq_{i+2}.$$

The structure of paraffins is sufficiently defined by the relations of the carbon atoms, so that the p and q terms may be omitted. If N is the number of carbon atoms, $n_1=N-1$. Platt's coefficients are related to the variables n_j by $\Sigma_\alpha f_\alpha(j-1)=2n_j$. This gives:

$$G=a_0+\sum_j a_jn_j=a_0+a_1(N-1)+\frac{\partial_2}{2}\sum_\alpha f_{\alpha 1}+\frac{\partial_3}{2}\sum_\alpha f_{\alpha 2}+\cdots.$$

This equation is identical, except for the form of the constants, with the equation developed by assuming bond interactions. The difference is essentially one of terminology, but it is believed that the viewpoint presented here is clearer and more firmly founded upon physical experience.

A simple empirical equation, based on the variables defined above, is $G=C_N+(k/N^2)\,\Sigma_j\, j\cdot n_j+b\cdot n_3$, where C_N is a function of N and therefore constant within each group of isomers. C_N may be eliminated by confining the calculations to the differences ΔG between the value of a property for a branched paraffin and its normal isomer. Values of k and b have been evaluated by the method of least squares from the observed data for the paraffins C_5 to C_8, as compiled in the API tables.[2] The average deviations between calculated and observed values for these paraffins are compared for the methods given by Platt,[1] by Taylor, Pignocco, and Rossini,[3] and in this report. (See Table I.)

TABLE I.

	R_D^{20} Molecular refraction ml/mole	V^{20} Molecular volume ml/mole	t^{760mm} Boiling point °C	$\Delta Hf°(gas)$[2] Heat of formation kcal./mole
Empirical constants				
k	−0.45	−14.2	+98	+20.7
b	−0.152	− 2.58	+ 5.5	+ 1.3
Average deviations				
Platt	±0.0106	± 0.22	± 0.67	± 0.19
TPR	±0.013	± 0.16	± 0.55	—
Wiener	±0.013	± 0.23	± 0.53	± 0.33

The accuracy of all three equations is seen to be of the same order of magnitude, except for the heat of formation, where Platt's formula is greatly preferable to the equation discussed here. It should be noted, however, that the latter employs only two empirical parameters, as compared to six and seven in the methods used by Platt and by Taylor, Pignocco, and Rossini, respectively. This gives this equation the advantage of simplicity and ready evaluation; furthermore, the addition of one or two well-chosen structural variables will probably increase its accuracy, while keeping the number of parameters below five.

The calculations for the boiling points have been reported,[4] the symbols used being w for $\Sigma_j\, j\cdot n_j$ and p for n_3. Details of the work on the other properties will be published later.

[1] J. R. Platt, J. Chem. Phys. **15**, 419 (1947).
[2] American Petroleum Institute Research Project 44 at the National Bureau of Standards. *Selected Values of Physical and Thermodynamical Properties of Hydrocarbons.*
[3] W. J. Taylor, J. M. Pignocco, and F. D. Rossini, J. Research Nat. Bur. Stand. **34**, 413 (1945), RP 1651.
[4] H. Wiener, J. Am. Chem. Soc. **69**, 17 (1947).